2017

Physiological mechanisms underlying male Culex quinquefasciatus acoustic mating behaviour

THE DEGREE OF DOCTOR OF PHILOSOPHY (PHD)

ROB INGHAM

To Adam

Abstract

In this thesis, I describe for the first time a stereotypical acoustic behaviour by male mosquitoes in response to female flight tones. This male-specific free-flight behaviour consists of phonotactic flight coincident with an increase in wing-beat frequency (WBF) followed by rapid frequency modulation (RFM) of the WBF, before eventual contact with the sound source. Male RFM behaviour is highly robust and can be elicited without acoustic feedback, from either an artificial sound source, or the physical presence of a female. The auditory Johnston's organ at the base of the male's sound-capturing flagellum detects the WBF of the female. This elaborate nonlinear sound receiver is not acutely tuned to the female WBF *per se* but to the difference between his own WBF and the female's WBF. In this thesis, I propose that the male's own flight tone mixes nonlinearly with the flight tone of a female to generate so-called distortion products (DP) in the antennae, which are detected by the Johnston's organ. The prominent DP in mosquitoes is f2-f1 where f1 represents the WBF of the female and f2, the WBF of the male. This implies that male mosquitoes rely on their own flight tones to locate and orientate towards flying females. To test this distortion product hypothesis I used the temperature dependence of WBF and JO tuning and the ability of a masking tone to interfere and supress the distortion product. Changes in temperature influence the generation of distortion products and impact phonotactic RFM behaviour of males. This thesis is the first to report on the significance of these effects of temperature on both the physiological responses to sound and free-flight behaviour. These findings highlight the importance of matching the temperature in which biological systems operate with the experimental temperature. In addition, the temperature-dependant changes in WBF and JO tuning are closely coupled which suggests that mosquitoes are well adapted to cope with global warming. The RFM of male mosquitoes to acoustic stimulation is also masked most strongly by tones centred on female flight-tones. Masking frequencies above 600 Hz do not suppress RFM behaviour, suggesting that males that fly together in a swarm do not interfere with their ability to detect a female. Masking tones can suppress RFM behaviour by being competitively more attractive than the stimulus tone. Behavioural and electrophysiological measurements reported here indicate that acoustic masking of RFM behaviour is caused through suppression of difference-tone distortion.

TABLE OF CONTENTS

ABSTRACT 2

ABBREVIATIONS 6

PREFACE 7

ACKNOWLEDGEMENTS 8

DECLARATION 9

1 **INTRODUCTION** 10

1.1 THE ANTENNA 10

1.2 FLAGELLUM 10

1.3 PEDICEL 13

1.4 JOHNSTON'S ORGAN 15

1.5 SCOLOPIDIA 15

1.6 MECHANOTRANSDUCTION 19

1.7 SWARMING BEHAVIOUR 24

2 **MATERIALS AND METHODS** 29

2.1 MOSQUITO CARE 29

2.2 ELECTROPHYSIOLOGICAL RECORDINGS 29

2.3 ACOUSTIC STIMULATION & CALIBRATION OF ELECTROPHYSIOLOGICAL RECORDINGS 31

2.4 TEMPERATURE CONTROL FOR ELECTROPHYSIOLOGICAL RECORDINGS 33

2.5 DATA ANALYSIS 34

2.5 BEHAVIOURAL EXPERIMENTS 36

APPENDIX 1.0 SOUND SYSTEM CALIBRATION MANUAL 41

3 **RESULTS**

3.1 **CHAPTER ONE: THE JOHNSTON'S ORGAN OF MALE *CULEX QUINQUEFASCIATUS* IS MIS-TUNED TO THE WING BEAT FREQUENCY OF FEMALE CONSPECIFICS** 46

3.1.1 INTRODUCTION 46

3.1.2 RESULTS 47

FREE-FLIGHT WING BEAT FREQUENCY OF FEMALE AND MALE *CULEX QUINQUEFASCIATUS* 47

FREQUENCY TUNING OF THE JO 48

3.1.3 DISCUSSION 50

3.2 **CHAPTER TWO: FREE-FLIGHT MATING BEHAVIOUR AND PHONOTACTIC TUNING OF MALE MOSQUITOES** 52

3.2.1 INTRODUCTION 52

3.2.2 RESULTS 53

PHONOTACTIC AND AUDITORY-MOTOR BEHAVIOUR OF MALE MOSQUITOES TO A TETHERED FEMALE MOSQUITO. 53

PHONOTACTIC AND AUDITORY-MOTOR BEHAVIOUR OF MALE MOSQUITOES TO PURE TONES 54

FREQUENCY TUNING OF RFM BEHAVIOUR OF MALES 58

PARTICLE VELOCITY LEVEL THRESHOLD TO ELICIT RFM BEHAVIOUR 59

3.2.3 DISCUSSION 62

3.3 **CHAPTER THREE: THE JO OF MALE MOSQUITOES IS TUNED TO AN ACOUSTIC DISTORTION PRODUCT** 66

3.3.1 INTRODUCTION 66

3.3.2 RESULTS 67

THE JO OF MALE MOSQUITOES IS TUNED TO DIFFERENCE TONES GENERATED THROUGH INTERACTION BETWEEN MALE AND FEMALE WBF 67

3.3.3 DISCUSSION 71

3.4 **CHAPTER FOUR: TEMPERATURE AFFECTS WING BEAT FREQUENCY AND FREQUENCY TUNING AND SPONTANEOUS OSCILLATION FREQUENCY OF THE JO OF *CULEX QUINQUEFASCIATUS*.** 73

3.4.1 INTRODUCTION 73

3.4.2 RESULTS 75

TEMPERATURE DEPENDENCE OF WING-BEAT FREQUENCY MEASURED DURING FREE-FLIGHT AND BODY TEMPERATURE DURING FLIGHT. 75

THE FREQUENCY TUNING, UPPER FREQUENCY RANGE AND SPONTANEOUS OSCILLATIONS OF THE JO COMPOUND POTENTIAL ARE POSITIVELY CORRELATED WITH TEMPERATURE 76

THE INFLUENCE OF TEMPERATURE ON THE ACOUSTIC BEHAVIOUR OF FREE FLYING MALE *CULEX QUINQUEFASCIATUS* MOSQUITOES 81

BEHAVIOURAL TUNING 83

3.4.3 DISCUSSION 85

3.5 **CHAPTER FIVE: ACOUSTIC MASKING OF AUDITORY BEHAVIOUR REVEALS MALE MOSQUITOES LISTEN FOR FREQUENCY DIFFERENCES AND NOT FOR FEMALE FLIGHT TONES**.....87

3.5.1 INTRODUCTION..... 87

3.5.2 RESULTS..... 89

3.5.2.1 MALE MOSQUITO RFM CAN BE DISRUPTED THROUGH ACOUSTIC MASKING 89

3.5.2.2 ACOUSTIC MASKING RELATIVE TO JO TUNING..... 91

3.5.2.3 ACOUSTIC MASKING OF DIFFERENCE TONE DISTORTION PRODUCTS RECORDED IN THE COMPOUND JO POTENTIALS IS CENTRED ON THE MOST SENSITIVE FREQUENCY 93

3.5.3 DISCUSSION 97

4 **GENERAL DISCUSSION** 100

4.1 MALE MOSQUITOES USE DISTORTION PRODUCTS TO DETECT FEMALE MOSQUITOES 100

4.2 TEMPERATURE INFLUENCES OF FREE-FLIGHT BEHAVIOUR..... 102

4.3 SUPPRESSION..... 104

4.3 FURTHER EXPERIMENTS..... 105

5 **BIBLIOGRAPHY**..... 108

Abbreviations

JO: Johnston's Organ

WBF: Wing Beat Frequency

DPs: Distortion Products

SO: Spontaneous Oscillations

PVL: Particle Velocity Level

FFT: Fast Fourier Transform

RFM: Rapid Frequency Modulation

SPL: Sound Pressure Level

IR: Infra-Red

Preface

This document includes five results chapters (1-5), each of which contain an Introduction, Results and Discussion. There is a General Introduction at the start of the thesis, and a General Discussion at the end. Materials and Methodology is described in text, but is also summarised in a dedicated Materials and Methods section. Some of the data in Chapters two and three have been published in The Journal of Experimental Biology (Simões et al. 2016) and data in Chapter five submitted for publication in Proceedings of the Royal Society. The behavioural data of this thesis was collected by Patrico Simões.

Acknowledgements

First and foremost, I would like to reserve the biggest thank you to Dr Ben Warren. It is hard to summarise what Ben has done for me over the last 6 years, because the help has been so vast. Ben has been with me through every single step of the journey, from the first lab invitation, to the very last point prior to submission. Going beyond the call of duty as a friend or a supervisor, generously giving up time for me, irrespective of the demands of a successful career and a young family bring. Be it inviting me to visit his German labs, introducing me to influential persons in my field or just dragging me out for hellacious cycles along the Rhine in the middle of winter. I would also like to thank Professor Ian Russell, primarily for welcoming me into the world of research with open arms, but secondly for inspiring and energising my research. Possibly one of the most kind and charismatic persons I have ever had the pleasure to meet. I must also extend a massive thank you to Dr Patricio Simões who, despite joining our lab midway through my studies, has been instrumental to us honing the focus of our research and help designing and collecting the behavioural data of this thesis. Your proactive and intellectual approach has been invaluable.

To my wife Shamima, whom I met one month before coming to university. 10 years later, I am finally bringing my studying to a close. In the meantime, we have been married and have brought a beautiful son into the world, Adam. You have put up with so much, and have been so supportive, especially having to share me with education for so long. Thanks you to James Hartley, who not only single-handedly built all the equipment, but also was always willing to help with repairs and explanations. Your help was always invaluable – get well soon buddy. Thanks to Dr Andrei Lukashkin for helping me understand theoretical science and always taking the time to explain.

I would also like to thank Dr Thomas Weddell and Dr Gareth Jones for your continued support and friendship. Thanks to Dr Mira Buhecha, Joseph Hawthorne and Steve Jones for your company and computer expertise. Thanks to Dr Brian Larsen, whom I met in Plymouth, who has been a great friend and shenanigans adversary (don't finish on a dark!)

Declaration

I declare that the research contained in this thesis, unless otherwise formally indicated within the text, is the original work of the author. The thesis has not been previously submitted to this or any other university for a degree, and does not incorporate any material already submitted to a degree.

Signed

Dated

1.0 Introduction

1.1 The antennae

The antennae of insects are composed of three segments. In mosquitoes, the first segment is the scape, a ring-like structure that attaches the second segment, the bulbous pedicel, to the head of the insect (Figure 1.1). Between the scape and pedicel are two sets of muscles that move the pedicel and third antennal segment, the flagellum, within an angle of 45 degrees. The sound-capturing flagellum is a long segmented appendage comprised of 13 flagellomeres, with mechanosensitive, olfactory and infrared-sensitive sensory neurons (Boo 1980). The flagellum is inserted into the centre of the pedicel and is connected to many thousands of mechanosensitive neurons, which compose the mechanosensory Johnston's Organ (JO). During sound stimulation or airflow during flight, the flagellum pivots about its base within the pedicel and stimulates the mechanosensitive neurons of the JO (Figure 1.2A).

1.2 Flagellum

The flagellum acts as an air particle-capturing appendage, which collects moving air particles during acoustic stimulation or flight. The structure of the flagellum has clear sexual dimorphism, of which the male has ten times the surface area of females, which indicates that the male mosquito are better equipped to detect sound (Clements et al. 1968). The flagellum of both male and female mosquitoes bear numerous appendages, as well as olfactory receptor types, such as deep chambers, sunken pegs, and surface pegs. The large surface pegs, also described as fibrillae, are visible by eye and function to capture moving air particles (inset of Figure 1.2B).

The olfactory sensilla, some of which are sensitive to CO_2 and allow for downstream host detection (Bowen 1991), are present in both males and females but in the males they are restricted to the first two antennal segments called flagellomeres (Boo 1980). On the female flagellum there are a large number of olfactory structures that are innervated, which results in a significantly higher number of axons running from the flagellum and JO of females than in males (765 in males compared to 1717 in females (Boo 1980)). Both

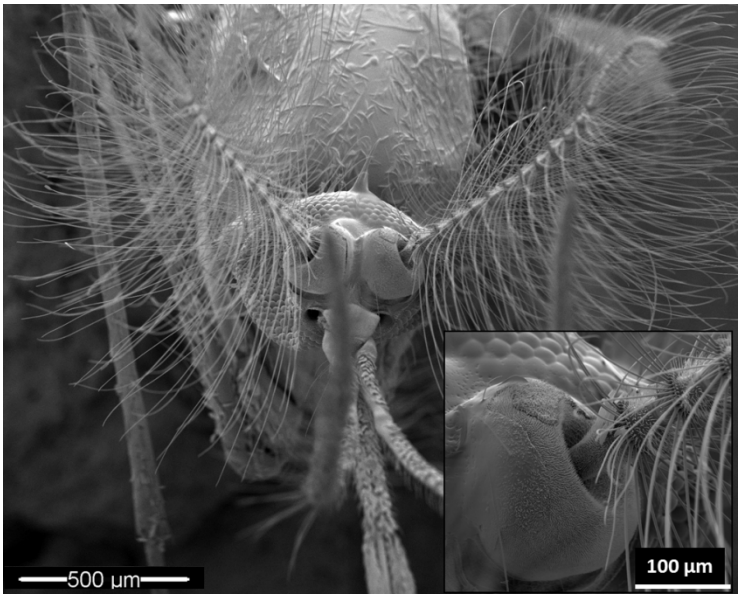

Figure 1.1: SEM image of male *Culex quinquefasciatus*. Image shows two bulbous JO's on the head of the mosquito with the flagellum protruding through the centre. Inset shows a magnified image of the JO and flagellum. Picture courtesy of Tracey Newman and Robbie Girling of the University of Southampton.

males and females have a similar flagellum shaft structure, which are of equal length in females but different length in males (Clements 1999). As a general trend across mosquitoes, the flagellar segments are largest (approximately 410 µm in *An.stephensi*) at the base (13th flagellomere) and decrease in size leading up to the tip (100 µm) (Boo 1980). It was previously believed that the higher surface area of the flagellum was to increase the male JO sensitivity (Belton 1994), but when removing two thirds of the flagellum, there was no change in the behavioural responses to sound (Tischner 1953, Wishart et al. 1962).

Along the shaft of the flagellum there are numerous long fine fibrils termed surface pegs (Boo 1980) which are categorised into two distinct groups; fibrillae and bristles. Fibrillae are the longer and more noticeable structures of the flagellum, in particular for males, which can be seen collectively by the naked eye. These long fibrillae are however absent in some male mosquito species e.g. (*Culiseta inornata, Uranotaenia lowii, Deinocerites cancer,* and *Opifex fuscus* (Clements and Bennett 1968)). These fibrillae form 'whorls' at the base of each of the first 12 flagellar segments (as seen

in Figure 1.2A). The number of fibrillae per whorl greatly depends on the species in question. *Ae.aegypti* have approximately 30 fibrillae per whorl whereas in *Ae.stimulans* there are anything from 60-80 (McIver 1971). One fifth of the fibrillae on the male flagellum are innervated by a single neuron. The non-innervated fibrillae are believed to be purely wind capturing appendages. These fibrillae are inserted into well-developed sockets on two crescent shaped projections of pliable electron dense material on each antennae. The innervated fibrillae are generally located along the flagellar blood vessel, which is suspected to provide the mosquito with relative antennal positioning information (Boo 1980). The second type of surface pegs, the bristle, can be differentiated into two bristle sub-types, which is based on size and innervation. Type-one bristles are innervated and medium in length, and sparsely distributed, predominantly on the 1st and 13th flagellomere. The shorter type two bristles are not innervated, at least not in *An. stephensi*, and confined to the first 12 flagellomeres. It is not certain as to what function these bristles hold, but due to the lack of innervation, they would still increase the surface area, therefore aid sound and wind detection. It has been reported however that in *Ae.aegypti* that the shorter bristles are innervated (Mclver 1982).

The resonant frequency of the flagellum of male and female *Ae.aegypti* is 380 Hz and 230 Hz respectively. However, it has been demonstrated in males that the fibrillae resonate at higher frequencies, between 2600 and 3100 Hz. The stiff coupling of the fibrillae to the flagellum allows for the efficient transmission of sound induced deflections, which results in an increased acoustic sensitivity (Tischner 1953, Gopfert et al. 1999). All haemophilic swarming mosquitoes have permanently erect fibrillae, apart from *An.gambiae* (Mclver 1982, Pennetier et al. 2010). *An.gambiae* fibrillae will remain in a recumbent position for the majority of the 24 hour period, but become erect during periods of swarming. *An.gambaie* adopt a mechanism that allows the fibrillae to move from a resting to an erect position under direct neural control (Nijhout et al. 1979). The resonant properties of the antennae of *Anopheles* are dependent on the fibrillae position. The flagellum is tuned to ~200 Hz when the fibrillae are erect, yet when the fibrillae are recumbent, the flagellum is broadly tuned between 100 and 550 Hz (Pennetier, Warren et al. 2010). The fibrillae found

on each flagellomere (Figure 1.2), are attached to a donut shaped annulus. The annulus is a ringed shaped structure, which lies in between the shaft of the flagellum and the fibrillae. The annulus remains tightly curled during the recumbent phase of the fibrillae, however during erection, becomes swollen causing the fibrillae to extend into an almost perpendicular position. Nijhout (1979) demonstrated that the relative hair position was heavily influenced by pH at the annulus, with low pH's leaving the fibrillae recumbent. Altering the pH towards a more neutral state the annulus becomes swollen causing the fibrillae to become erect, until residing in its maximal erect position (PH 8) (Nijhout and Sheffield 1979).

1.3 Pedicel

The pedicel that houses the JO is attached to the scape. The scape resembles a ring-shaped structure, which allows the flagellum to move in a cone of 45^{o}. There are three muscles that control the movement of the flagellum, two attaching to the scape, one on the base and one on the side, while the third muscle attaches to the base of the pedicel. The flagellum is anchored to the centre of the pedicel, out of a vase shaped pit called the apical pit (Clements 1999). Within the apical pit, the flagellum is fixed to a thick disc of cuticle called the basal plate (Figure 1.2a). The basal plate and the flagellum are tightly mechanically coupled to allow faithful transmission of flagella displacements to the base, and together operate as a simple forced damped harmonic oscillator (Göpfert, Briegel et al. 1999). The basal plate is thicker round the centre where it is attached to the flagellar shaft, and is slightly tapered at the edge (Figure 1.2A) (Risler 1953). Beyond the edge of the basal plate, cuticular projections arise to form the prongs and septa (Figure 1.2a). The prongs and septa are important in conducting the vibrations from the flagellar shaft to the mechanically sensitive sensory cells, called scolopidia.

In *Ae.aegypti* there are on average 58 prongs which extend from the basal plate (Boo et al. 1975). The distal end of the scolopidia connect to the prongs via a cuticular cap (in scolopidial types A and B) or a cap cell (in scolopidial types C and D) (Figure 1.3). The septum is a complex network of cuticular filaments that connect the inside wall of the pedicel with the distal tips of the scolopidia and prongs. These septum

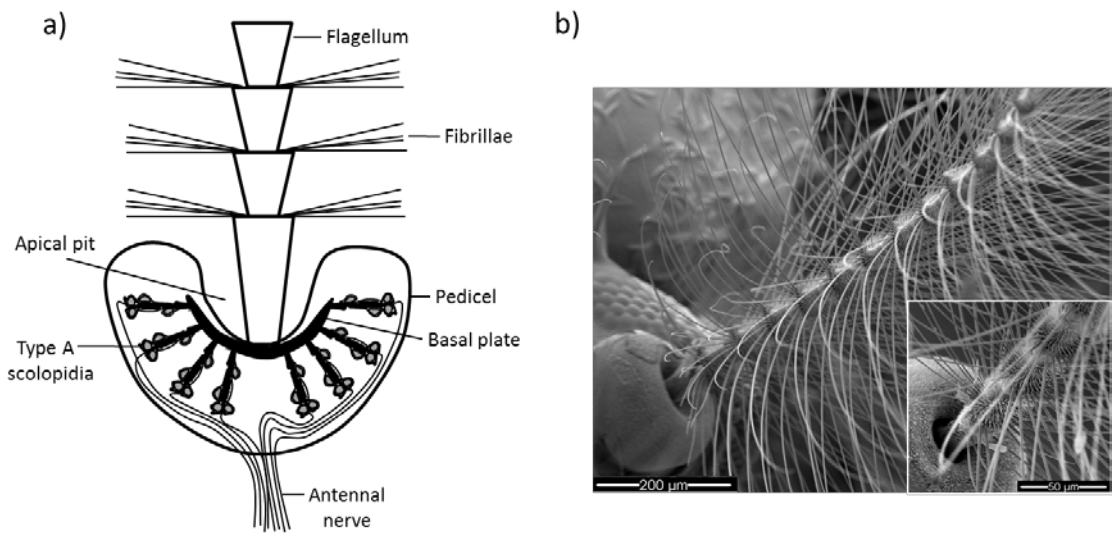

Figure 1.2: Graphical representations of JO and antennae. A) Schematic of JO and Flagellum, illustrating how the mechanical elements are coupled to the scolopidia (Sensory units). Flagellum and basal plate tightly coupled, so upon stimulation, the basal plate rocks, stretching the scolopidia inducing receptor potentials. Components not to scale. B) SEM image of pedicel containing JO with flagellum protruding from the apical pit (scale bar – 200 µm). Inset magnified view of base of flagellum, showing in detail the arrangement of long and short fibrils (scale 50 µm).

connections are referred to as the outer scolopale rods (Belton 1989). The inner scolopale rods are the actin-based cytoskeleton and terminate just above an inflamed section of the cilium, called the ciliary dilation (Schmidt 1967). The ciliary dilation is a feature shared amongst *Drosophila* and other insects, as an electron-dense inclusion within the axoneme, at about two thirds the length of the cilium. The ciliary becomes modified at the dilation, with a clear connection between each mictrotubule doublet and the ciliary membrane. When the axoneme is not expanded as the cilium, the membrane is pulled in to make contact with the axoneme, creating a lobed or ribbed effect (Moran 1977). At the basal plate, the septum is H or Λ shaped per section, but at the scolopidia, the septa become X-shaped and smaller. This X formation facilitates a four-point attachment, with the two inner points of the septa fixing to the cuticle of the pedicel and the two outer points providing a secondary

attachment of the distal part of the scolopidia along with the prong. All these cuticular components contribute to the overall resonance of the system. The force applied to the flagellum during stimulation is relatively proportional to the toque on the basal plate. This force is subsequently resisted by the opposite torque of the basal plate suspension, and upon JO activation, the compound JO potential generated is relative to the rocking of the basal plate.

1.4 Johnston's organ

Based on its morphology, Christopher Johnston speculated as early as 1855, that the JO at the base of male mosquito antennae was important for the acoustic detection and localisation of female conspecifics. It has now been confirmed that the JO is a mechanosensitive chordotonal organ with ~16,000 mechanosensitive neurons (in males) and detects nanometer movements of the flagellum (Göpfert et al. 1999). In addition to the detection of sound, the JO is shown in Drosophila to also serve the role of gravity sensation (Kamikouchi et al. 2009) and the detection of air currents essential for flight (Bowen 1991).

The prongs are an extension of the flagellum and curve up inside the pedicel and they look like the spokes of an upturned umbrella where the flagellum is the umbrella's shaft (Figure 1.2a). The higher number of mechanosensory neurons in the JO of male mosquitoes (16,000 in males; 7500 in females) is thought to be due to the increased selection pressure for the acoustic detection of females with mating swarms. The scolopidia are composed for four distinct types (Carvalho et al. 2014) based on their distribution within the pedicel.

1.5 Scolopidia

The stretch-sensitive neurons of the JO are embedded in supporting cells that together act as a functional unit known as a scolopidium. The mechanosensory neurons themselves are monodendritic (type-one) with a ciliated ending that attaches to a distal attachment cell or filamentous cap. Upon movement of the distal end, the cilium becomes strained, which results in the mechanical opening of a

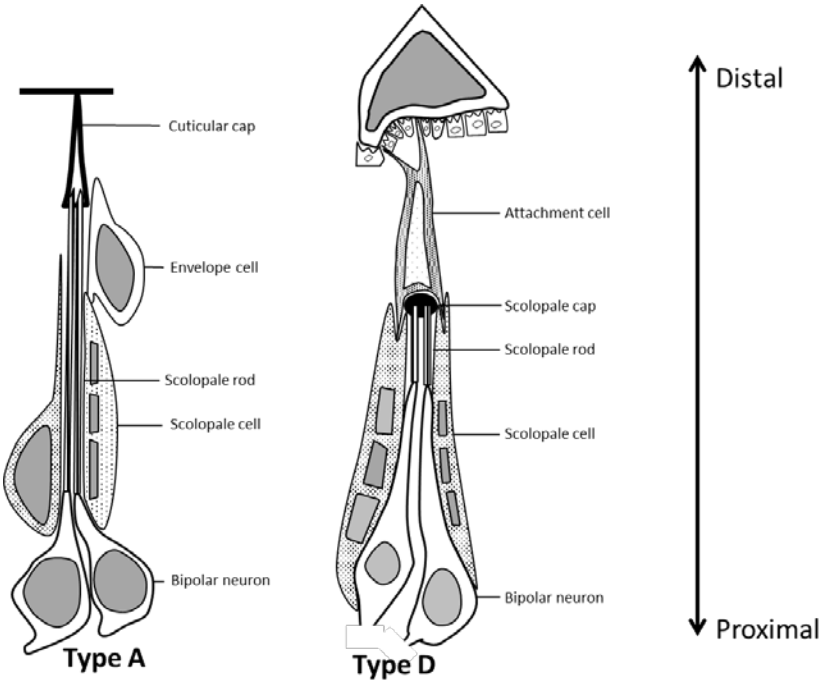

Figure 1.3: Longitudinal schematic of type A (amphinematic) and type D (mononematic) scolopidia of *Aedes aegypti.* (Copied and adapted from Boo 1981).

dedicated ion channels within its membrane. This causes a change in membrane potential upon the influx of potassium ions, resulting in a depolarising potential. The existence of a chordotonal organ is common in leg joints of insects but the JO of the mosquito remains the largest documented example (Kernan 2007).

A cilium is a highly conserved specialised ending, which can have motile and/or sensory functions. A cilium is a common appendage in biology and can be found in motile forms, such as the rotating flagella of a bacteria, or in non-motile sensory forms, as found in most animal cells (Wiederhold 1976). The cilium here is anchored at its base at the apical end of the dendrite and is inserted into a cuticular cap or an attachement cell (Figure 1.3), and thought to be the site of mechanotransduction (Yack 2004). The cilium contains an axoneme, which makes the cytoskeletal structure of the cilium. At the proximal base region of the cilium (the basal body), the microtubule cytoskeleton is attached to the plasma membrane by Y-shaped fibrils, and attached to a scolopale by desmosome-like junctions. This creates an indirect attachment of the cilium to the scolopale (McIver 1985). This scolopale is thought to

provide a rigid channel found around the cilium, such that when physical forces are imposed, there is an effective transfer of mechanical energy to the cilium (Wiederhold 1976, Wolfrum 1990, Wolfrum 1991, Wolfrum 1997). The scolopale can be found within the scolopale cell, which encompasses the distal two thirds of the cilium, and is situated on the proximal side of the scolopidial unit. At the basal body, the cilium has a cylindrical triplet microtubule arrangement, but lacking a central tubule (9x3+0). This constitutes the ciliary root. The ciliary root takes on a fused cylindrical shape and then subdivides into 9 ciliary rootlets, which extends up the length of the dendrite, soma, or even the axon (Moulins 1976). Further up the cilium the microtubule arrangement changes into a doublet formation (9x2+0), which is believed to be the crucial structure in mechanotransduction. There is a slight discontinuity where the two formations meet. This discontinuity has thought to be functionally significant, and that under mechanical stress the area becomes bent (Boo 1981). This hypothesis is however contested by Field and Matheson (1998) whom believed it to be purely an imaging artefact, shown in EM images in Moran et al. (1977).

The cilium has a dilation two thirds up its length, and the electron dense material within is critical for mechanotransduction (Gray 1959, Moulins 1976, Eberl and Kernan 2000). At the dilation, the dynein arms that bridge between the microtubule doublets are absent, which results in a direct attachment to the ciliary membrane. In the subgenual organ of the cockroach, this direct attachment causes the membrane to be pulled inwards towards the tubules creating almost a ‘ribbed’ effect (Moran et al. 1975). The mechanism of mechanotransduction has been likened to campaniform receptors and hair mechanosensilla detecting lateral compression (Thurm et al. 1983). In scolopidia, tightly packed microtubules, described as micro-tubule integrating cones (MICs), interconnect to the electron-dense material, which is consistent with the insertion in campaniform receptors (Thurm, Erler et al. 1983).

Four different scolopidial types can be differentiated into two distinct groups; scolopidia which terminate with a filamentous cuticular cap are named amphinematic, and scolopidia that terminate with a cap cell, are mononematic (Graber 1882) (figure 1.3). There are four different types of scolopidial units in male

mosquito (types A-D), and three in females (Types A-C) (Boo and Richards 1975). The bipolar neurons contained within scolopidia are type one neurons with a soma, an axon and a single dendrite, which are encompassed by a scolopale cell and an envelope cell (figure 1.3).

Type A scolopidia, an amphinematic unit, consist of two bipolar neurons, a scolopale cell, which contains a primary inner scolopale and a secondary outer scolopale, an envelope cell and a long filamentous cap (figure 1.3). The cilium within Type A scolopidia differs in length depending on the sex of the mosquito, with female mosquitoes have a short cilium and long cap cell in comparison to males. The cilium inserts into the long tube-shaped filamentous cap, which encloses 25% of the apical part of the dendrite (Figure 1.3), with the dendrite closely associated with the inner wall. One of the dendrites becomes visibly swollen (Boo and Richards 1975), which is believed to provide anchor support for the cilium into the cap. The cap attaches to the cilium by hemidesmosome junctions, with fine cuticular rods attached to the external parts of the cap (Risler 1955). Each cuticular prong in male *Ae.aegypti* attaches 120 Type A scolopidia. The prongs in female JOs are much shorter and have only-50 Type A scolopida attached (Boo and Richards 1975).

Type B scolopidia (also amphinematic) are structurally very similar to Type A. Type B scolopidia make up the anterior series (group of cells on the anterior plane of the JO), and similarly attach to the prongs (4-5 in both males and females, per prong). Type B scolopidia have three neurons (compared to two in Type A), two of which have only the tips (1-2 um) of their cilia embedded in the filamentous cap. The tips are similar in their organisation to Type A neurons but only extend a short way into the cap, while the third neuron has a cilium which is found deep into the cell body. The third neuron is unlike the others as it lacks a ciliary dilation and has a short axoneme, but the cilium can be found almost to the tip of the cap (Boo 1980).

Type C scolopidia are mononematic, because the distal part of the cilium attach via an attachment cell. Each JO only contains two Type C cells, which are morphologically identical in both males and females found on the posterior plane of the JO (Risler 1955). There are no notable structural variances between the sexes. One of these scolopidia is positioned laterally on the side of the pedicel towards the insects'

midline, with the other positioned ventrally (Risler 1955). The cap cell attaches to the epidermis with finger-like projections via desmosome-like connections, but does not attach to the basal plate directly. The cilium resembles that of the Type A scolopidia, but terminate into a small pouch of electron dense material in the cap (Figure 1.3). The basal part of the cilium is condensed in one neuron and branched in the other, with the cell body of the neuron surrounded by a glial cell. This glial cell makes intimate contact with a *blood vessel* which has been suggested to be an important factor in proprioception (Boo and Richards 1975). Proximity to this blood vessel could provide relative antennal position information (Risler 1955)

Type D mononematic scolopidia are absent in females, are morphologically similar to Type C, however there is no glial cell present and no reported association with *blood vessels*. There is only the sole Type D scolopidium per JO and it has been suggested to play an important role in hearing as females lack this Type D scolopidia (Boo and Richards 1975) and the common belief that females lack any functional hearing (Belton 1979). This is supported by a lack of JO organisation in comparison to males and the reduced surface area of the female flagellum (Göpfert, Briegel et al. 1999).

1.6 Mechanotransduction

Mechanotransduction in the JO is accomplished by the conversion of mechanical energy into an electrochemical signal by specialised mechanosensory neurons. In the initial step of mechanotransduction, the flagellum captures moving air particles; the displacement forces conveys onto the sensory neurons within the pedicel via the cuticular prongs. The second stage of mechanotransduction is thought to occur within the specialised ciliated ending of the sensory neurons through mechanosensitive ion channels which open in response to mechanical force, and lead to an influx of cations and depolarisation of the cilium. The third stage, is the encoding of ciliary depolarisation into action potentials. Coupling and transduction will be discussed in detail here.

Sub-nanometre displacements are efficiently transmitted across the cuticular structures within the organ through the flagellum, fibrillae, prongs and the scolopdial

attachments (French 1988, Gopfert, Briegel et al. 1999). The higher number of scolopidia and prongs in the male JO result in an increased mechanical stiffness, although this is to some degree countered by the increase surface area of the flagellum (McVean 1991), thus providing more force on the JO. In contrast, the reduced surface area of the female flagellum is believed to be a hallmark of the females comparatively weak capacity for hearing, however the lower level of stiffness in the female JO allows for double the rotation under the same mechanical stimulation (McVean 1991). The resonant frequency of the male flagellum is 350 Hz (Tischner 1955, Belton 1994) and is a known particle velocity receiver (Tischner 1955, Belton 1994). The flagellum does not experience a full range of sensation, as the scolopidia do not radiate 360^{o}, and there is a 15^{o} range where a back and forth motion does not cause excitation in the sensory neurons. This is referred to the cone of silence (Wishart, van Sickle et al. 1962).

Upon acoustic stimulation, the cuticular structures attached to the flagellum become mechanically active, this causes the cilium of the sensory neuron to become deformed. This action causes a depolarising current, of which the summated depolarisations can be measured by inserting an electrode into the extracellular space. The compound JO potential can be measured by insertion of the electrode into the compound eye (Tischner 1953), which indicates the tissues of the mosquito are highly conductive (Wishart, van Sickle et al. 1962).

The JO compound potential has a frequency of twice that of the stimulus frequency, known as frequency doubling. Generally, the amplitude of the alternating depolarisations are of a different size. It is also possible to change the phase of the large/small depolarisations by 180^{o} when recordings gross JO potentials by moving the position of the point source stimulation, laterally (Wishart, van Sickle et al. 1962, Belton 1974). The nature of these doubled recordings has been explained by two possible theories. The original and simplest explanation to frequency doubling is that during the stimulation of one sine wave period, one group of scolopidia in the plane of the acoustic stimulation are stimulated by the compression phase of the stimulus, and then by the rarefaction phase (Wishart, van Sickle et al. 1962). The second theory

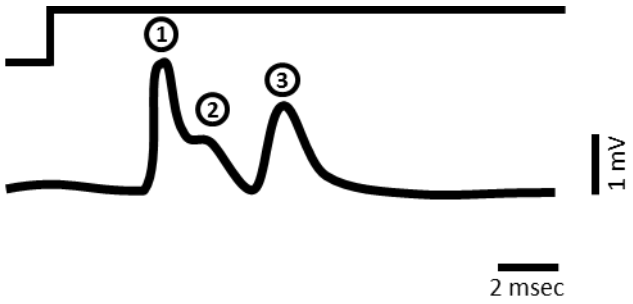

Figure 1.4: Gross potentials of the JO when stimulated using a step stimulus. Upon a mechancal step of the flagellum, the JO produces a large response with a 3.4 ms latency ① which is thought to be the sum of receptor and spike potentials. Another 3.4 ms later, a smaller response occurs ③, the resonant stretch, which is a stretching of the same cells one full cycle later. This would equate to the resonant frequency of the antennae (300 Hz). A small hump ② on the downward phase of the first response, is suggested to be the response by a group of cells on the opposite side of the JO. Focal recordings were made using glass electrodes. Copied and adapted from Belton 1974.

is attributed to the complex physiology of the JO. If you were to slice across the sagittal plane of the JO, it would reveal there is a distribution of Type A scolopidia that are arranged in a radial array and can be distinguished as proximal or distal in respect to the basal plate. When stimulating from a point source speaker, deflecting the antennae in one direction causes a tilting of the basal plate and thus a stimulation of one set of scolopidia, and tilting back to stimulate the opposing set (Tischner 1953, Wishart, van Sickle et al. 1962). The principle differences between the two theories is; one requires activation of one population of scolopidia, and the other requires activation of opposing populations of scolopidia. Metal electrodes detect larger JO compound potentials because of their lower impedance (Tischner 1955), but sharp glass electrodes provide focal recordings, thus indicating which populations are activated locally (Gomes et al. 1996). Focal recordings reveal there is a measured response with a latency of 3.4 ms from the onset of the step/mechanical stimulus, with a smaller second response being seen a further 3.4 ms later (Figure 1.4). It is proposed that this smaller second response is caused by a smaller stretch of the same

cells, sometimes referred to the resonant stretch (Belton 1974). A small hump on the downward phase of the first spike can be seen (Figure 1.4), which is proposed to represent the activity of a distal group of cells responding 180^{o} out of phase of the responses recorded with the sensory cells local to the electrode. It is hypothesised that individual scolopidia either respond to a push or a pull, but not both, where there are pronounced differences between the latency of a push or a pull (pull latency = 1.7 ms) (Belton 1974).

Mechanoelectrical transduction occurs on millisecond timescales, too short for second messengers common in other sensory modalities (Albert et al. 2007). Thus, mechanotransduction ion channels are thought to be directly mechanically activated by stretch of the membrane or a mechanical tether that attaches to the ion channel (Walker et al. 2000, Albert et al. 2007). The identity of the mechanical components that make up the mechanotranducer has been an argument which has raged on for numerous years. Two of the most attractive molecular candidates found in the JO of *Drosophila melanogaster*, for the mechanotransduction ion channel, are NompC (=TRPN1) and Nan/Iav (TRPV) (Figure 1.5). Both are localised to the cilium where transduction is postulated to take place, with NompC expressed in between the tip of the cilium and the ciliary dilation, and Nan/Iav just below the cliliary dilation (Gong et al. 2004). There is evidence that supports the premise that the mechanosensory channel should be near the tip of the cilium, in intimate proximity to the dendritic cap, which contains linker proteins [NompA] (Liedtke 2005). The knockout of either leads to a reduction in the transduction current (Lehnert et al. 2013) and both form ion channels when expressed in heterologous cells (Lee et al. 2010, Gong et al. 2013).

The knockout of *nompC* leads to a reduction of JO compounds by half that of NompC rescue flies, which suggests NompC is dispensable for auditory transduction (Walker, Willingham et al. 2000). It was later shown that the remaining compound potential of NompC knockouts were from gravity-sensing JO neurons (Kamikouchi, Inagaki et al. 2009). Kamikouchi (2009) identified five functional groups of neurons. Subtypes AB detect sound induced vibrations and subtypes CE provide gravity sensation. *nompC* is expressed solely in type AB neurons and absent in the type CE neurons whereas both sound sensing and gravity sensing neurons contains Nan/Iav. This

provides a potential explanation as to how the sensory cells are able to transmit sound induced information to the brain despite the NompC knockout. In *Drosophila*, type AB neurons are connected to the antennal lobe via the giant fibre neuron, whereas type CE neurons are not (Lehnert, Baker et al. 2013).

The active knockout Nan/Iav results in almost complete abolishment of mechanotransduction in the JO under acoustic stimulation (Kim et al. 2003, Gong, Son et al. 2004). A strong conflicting argument against Nan/Iav as the sole mechanotransducer is attributed to the location of expression in the sensory cell, some microns away from the proposed transduction site (Ernstrom et al. 2002, Sukharev et al. 2004) (Figure 1.4). The significant distance from the distal end of the cilium does rule out the likelihood of the channel being directly gated, however it is possible the gates can become mechanically activated via a bending or a 'pulling' of the cilium, as evidenced in the grasshopper. In addition, Göpfert et al (2006) revealed that Nan/Iav not only has an important role in feedback, but is intimately coupled with NompC in overall mechanosensitive performance. Knocking out *nanchung* results in a decrease in mechanosensory current as well as the generation of spontaneous mechanical oscillations. It is speculated that Nan/Iav functions as an amplifier, amplifying sub-threshold signals from the transducer complex (Lehnert, Baker et al. 2013). Eberl (2007) described the function of Nan/Iav in *Drosophila* as a component which controls the activity of NompC-mediated amplificatory feedback. To summarise, Nan/Iav provides a suppressive/controlling feature, with NompC an amplificatory function, therefore the two ion channels operating in opposite roles in regulation. The neurons of the JO spontaneously fires action potentials, which is abolished by Nan/Iav knockouts. Originally it was suggested that Nan/Iav is responsible for amplifying the transduction signal, from the gating of NompC, but Lehnart et al (2013) suggests that this is unlikely, because of the latency and the level of amplification required, especially given the weak voltage dependence of Nan/Iav. From this, Lehnart et al (2013) conclude that Nan/Iav must be acting as the transducer complex itself. If not acting directly as the transducer, then at least managing another unknown channel. It is also suggested that transduction actually

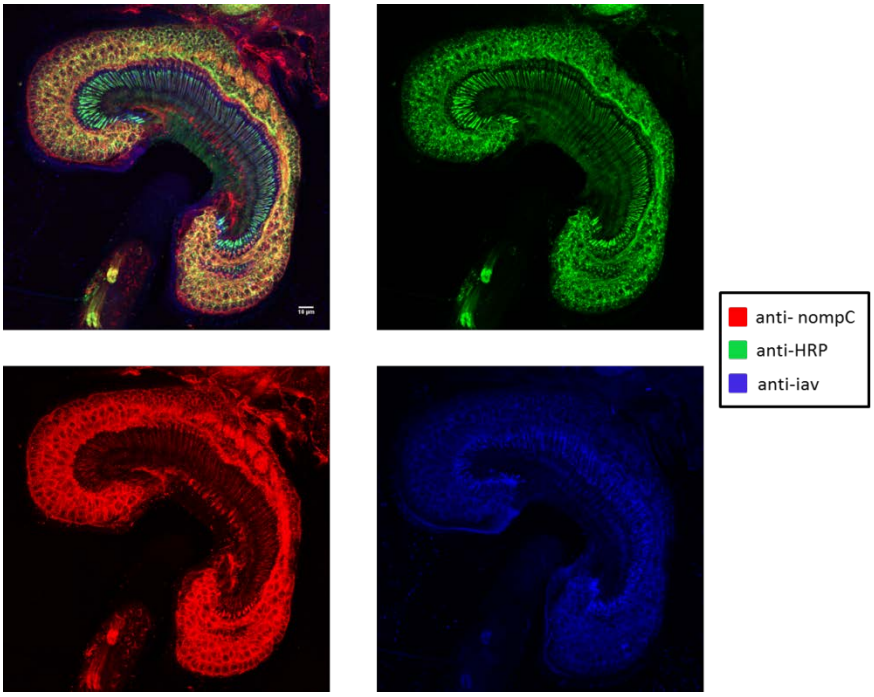

Figure 1.5: Immunostaining of mosquito JO. Staining localises NompC near the distal part of the cilium whereas inactive localises at the ciliary dilation. Images courtesy of Marta Andes, Göttingen University (see Figure 1.2a for JO schematic).

inhibits active amplification of the flagellum, as the flagellum of Nan/Iav mutants oscillates liberally (Göpfert et al. 2006).

1.7 Swarming Behaviour

The majority of male mosquito species form stationary swarms above landmarks of low-high contrast, and is a behaviour used specifically for the purposes of mating (Roth 1948). The swarm of Diptera is described as a *'flight station at an assembly point dictated by a landmark'* (Downes 1961). The physical attributes of a swarming marker generally have contrasting light-dark margins, such as tree-tops, roads, ponds, and even livestock (Knab 1906). The swarms remain stationary over the marker (Gibson 1985), but if the marker is vast in size (for example a lake or pond) individuals can transfer within swarms, and swarms can also migrate (figure 1.6). Swarming is heavily influenced by wind speed and temperature, but is independent

of the physical swarm marker itself (Knab 1906, Nielsen et al. 1950). Most genera of mosquitoes form crepuscular swarms, including the species studied in this thesis.

Males continually swarm above a swarm marker, with females only ever visiting a swarm maybe once or twice in their lifetime (Clements 1963). When unmated males and females are released into a room, both sexes constitute the swarm, but after successful mating, females leave the swarm and do not re-join (Gibson 1945). Post-mating, female's key priorities are to find a host for a blood feed, to locate an ovipositional site to lay eggs and to mature the ovum (Clements 1963). In contrast, *Culex fatigans* form separate swarms in the same area, where a female will leave the female swarm, to join the male swarm in order to locate a mate (Howard et al. 1917), while *Aedes aegypti* form bi-sexual swarms (McClelland 1959). There are also numerous examples where swarms experience cross-speciation, and even engage in cross speciated sexual interactions between species (Downes 1958).

The cues used by mosquitoes to discriminate between sex and species have been debated for decades, however there is significant evidence which supports hearing as an integral component of mate selection and species segregation. However, because of how some species have overlapping frequencies (Todi et al. 2004, Diabaté et al. 2009), it raises some contention. Contact chemosensation and tactile sense could also play an important part (Downes 1958). The antennae on the head of the mosquito is responsible for audition and localisation (Mayer 1874), and the JO used to detect females as they enter the swarm (Roth 1948). However, it is also shown that amputation of the flagellum has no impact on the males ability localise a female, and has little impact on mating success (Tischner 1953, Wishart, van Sickle et al. 1962). Wishart (1962) did report that removing two thirds of the antennae lowered the resonant frequency, but this could be due to a loss in fluid post-amputation, which may in some circumstances result in a change in resonant properties (Keppler 1958).

Visual cues attract mosquitoes to swarming sites (Diabaté, Dao et al. 2009), as both male and females possess visual systems sufficient to detect such locations (Downes 1968). Male mosquitoes have a highly specialised upper part of the eye, suggesting that males could localise females from below, however the mosquito

does possess poor temporal resolution so locating and identifying other mosquitoes during flight seems highly unlikely (Autrum 1949, Downes 1968). Mosquitoes with a highly developed lower eye interact predominantly close to the ground (Downes 1968). A copula is formed on the wing and the genitals are engaged within a few seconds, well before they fall to the ground (Clements 1963). Males can respond to the sound of females' wing beat frequency (WBF) shortly after emerging from pupae, although the sexual organs are not matured, and the fibrillae are not erect, which results in a loss of acoustic sensitivity. Males can still detect the sound of a female in this recumbent state, but the sound must be higher than the amplitude of the wing beat of a flying female. Some genera of mosquito exhibit a narrow range of hearing which would allow them to discriminate between genera, however male *Aedes aegypti* can respond to female WBF of *Culex, Anopheles* and *Aedes vexans* (Roth 1948, Wishart et al. 1959). Across most genera, male mosquitoes respond to sounds between 200 to 450 Hz which encompasses the WBF of a flying female, but not as high as 800 Hz which represents the mean male WBF (Roth 1948). During the life cycle of the mosquito, the females will mate, host-seek, and blood feed before performing ovipositioning (Eckhoff 2011), however male and female mosquitoes have different larval and sexual maturation periods that provide ample opportunity for the adults to disperse from the emergence site before copulation (Hartberg 1971). Females are refractory from insemination for 48-72 hours post emergence, and males require 15-24 hours to rotate their genetalia. Statistical assays show that in *Aedes aegypti,* most mating takes place near the host (Hartberg 1971).

It is believed that different species of *Anopheles* are able to discriminate between one another solely through differences in the WBF (Brogdon 1998). This is called the '*Wingbeat hypotheses'*. The Wingbeat Hypotheses was used to describe the segregation between the recently identified the *Anopheles gambiae sub*-species (Todi, Sharma et al. 2004). However, the findings in lab based behavioural studies did not correlate with field based studies with each sub-species demonstrating a frequency overlap, rendering frequency discrimination unlikely. The large overlap of WBFs suggests that here, *Anopheles gambiae* do not use WBF as a diagnostic tool

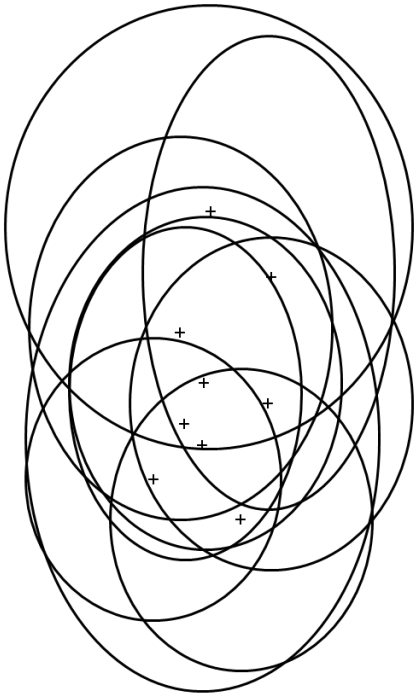

Figure 1.6 Schematic demonstrating swarming dynamics. Three male mosquitoes over three 4-second intervals without sound (scale bar represents 10 cm). Each circle represents the range of swarming of each individual, with a cross indicating the mean position. Copied and adapted from Gibson 1985).

for recognition (Wekesa et al. 1998). Both forms of *Anopheles* (M and S forms) coexist within the same geographical area, and there is little genetic differentiation, however there is still less than 1% of natural hybridisation reported (Gentile et al. 2001, Mukabayire et al. 2001, Torre et al. 2001, Wondji et al. 2005).

Observations of both M form and S form *Anopheles* gambiae in the same area, revealed that they were able to swarm independently of one another, and hybrid swarms were rare occurrences (one mixed swarm in 21 swarms [Diabaté 2009]). S form mosquitoes were collected over bare ground, whereas M form swarms were collected over markers consisting of light/dark contrasting barriers (footpath, small structures, a wall against a light background etc.). This indicates that the *Anopheles* mosquito's sub-species utilise different visual cues for creating swarms, thus

promoting segregation. Furthermore, the introduction of a tethered female into either swarm, resulted in no form recognition, and the female were inseminated equally by both M and S form males (Diabaté et al. 2009). In the very few cases where there are more than one form occupying the same swarm, there is little reported cross mating, although this could be down to touch or olfactory recognition at close proximity.

An alternative interpretation of mosquito swarm behaviour is provided in the form of frequency matching, an auditory-driven behaviour using tethered mosquitoes. Frequency matching sees opposite sex pairs of four genera match fundamental frequencies or harmonic components of their flight tones. *Toxorhynchites brevipalpis* are a non-swarming mosquito where males and females are of similar size and fly at overlapping WBFs. Upon acoustic stimulation, *T. brevipalpis* alter their WBF within 8 Hz (Gibson et al. 2006). Frequency matching was first demonstrated in swarming mosquitoes in *Aedes aegypti* (Cator et al. 2009), and shortly after in *Cx. quinquefasciatus* (Warren et al. 2009). With males and females of the respective species flying at different fundamental frequencies, the convergence of frequencies occur at the harmonic level. Despite this, the fundamental component of the female flight tone was established as most important as presenting sounds with the fundamental removed results in a significant decrease in phonotaxis to the sound source during swarming. In contrast, when presenting sine tones only, the change in behaviour was insignificant (Wishart et al. 1959). Frequency matching also provided the first evidence that females were able to respond to acoustic stimulation. The degree of successful matching is dependent on whether or not the female has already mated, with unmated females more than three times more likely to match compared to females that had been inseminated (Cator, Arthur et al. 2009). In *Anopheles gambiae* forms it was shown that frequency matching occurred more frequently in same form pairs (M+M or S+S [14 in 24]) than in mixed form pairs (M+S [2 in 24]) (Pennetier, Warren et al. 2010), which suggests that there is in swarm identification, which uses acoustics as a cue.

2.0 Materials and Methods

2.1 Mosquito care

Adult male and female *Cx. quinquefasciatus* mosquitoes were acquired from collaborators at Greenwich University, and the London School of Tropical Disease and Hygiene, originally obtained from Burkina Faso. The adult mosquitoes were kept in a 30cm^3 cage, enclosed in T1 sized Tubigauze (Nu-Care products Ltd), with a 4 mm stainless steel frame. The cages were kept in polythene bags to maintain humidity (70 – 75 % rH). Females were fed on defibrinated horse blood (TCS Biosciences, Butolph Claydon, Bucks, UK) delivered through a membrane feeder (Hemotek 5WI). Females then laid eggs rafts on an isotonic solution (0.1% aquarium salt – Aqualibrium™) in small tubs (30x15x20cm). The larvae which hatched from the eggs were fed on cat biscuits (Purina® GO-Cat® - with Tuna and Herring) for approximately 10 days, until pupae developed. Pupae were then removed from their large containers, and distributed randomly to smaller containers (150 ml capacity) and placed in cages until adults hatched. The random allocation of pupae limited inbreeding. For experiments that required virgin mosquitoes, pupae were separated into multiwell plates (Corning® Costar® TC 12x3.8 cm^3) which were covered with Parafilm®. When they emerged they were sexed, and separated into 'Virgin only' cages. The adult mosquitoes are fed a basic carbohydrate diet of 10% Sucrose solution soaked into cotton wool and kept in a 25^{o}C environment maintained by a convection heater on a thermostat in a 12:12 light/dark cycle to maintain circadian rhythm (Charlwood et al. 1979). All experiments were performed within one hour of the dark cycle to replicate dusk conditions.

2.2 Electrophysiological recordings

Mosquitoes were immobilised by cold narcosis (males were placed in a freezer at -17^{o}C for 45 seconds) and placed on a freezer block to maintain cold body temperature until the mosquito was either tethered for tethered flight recordings or attached to a small brass block (4x3x3mm) for electrophysiological recordings. To attach the brass block to the mosquito, a small amount of beeswax was added to one

side of the block, which was then heated with a soldering iron to melt it. The block was then fixed onto the dorsal thorax of the mosquito and the wax allowed to solidify, which secured the mosquito and its wings to the block. A small bead of superglue (Loctite®) on a stainless steel wire (40 SWG – Thackray, Leeds) was dabbed between the head and thorax and between the pedicels and the head. A bead of glue is also applied at the junctions of the legs to reduce tarsal movement. This reduced all movements of the mosquito which reduce noise for electrophysiological recordings. All electrophysiological recordings were conducted on a vibration isolation table (Newport corporation, Model: M-VW-3036-OPT-99-9-28-92). Mosquitoes attached to the brass block and were mounted and coupled on a ground electrode (EL212, WPI), with electrolyte gel (Sigma gel – Parker Laboratories INC) (figure 2.1).

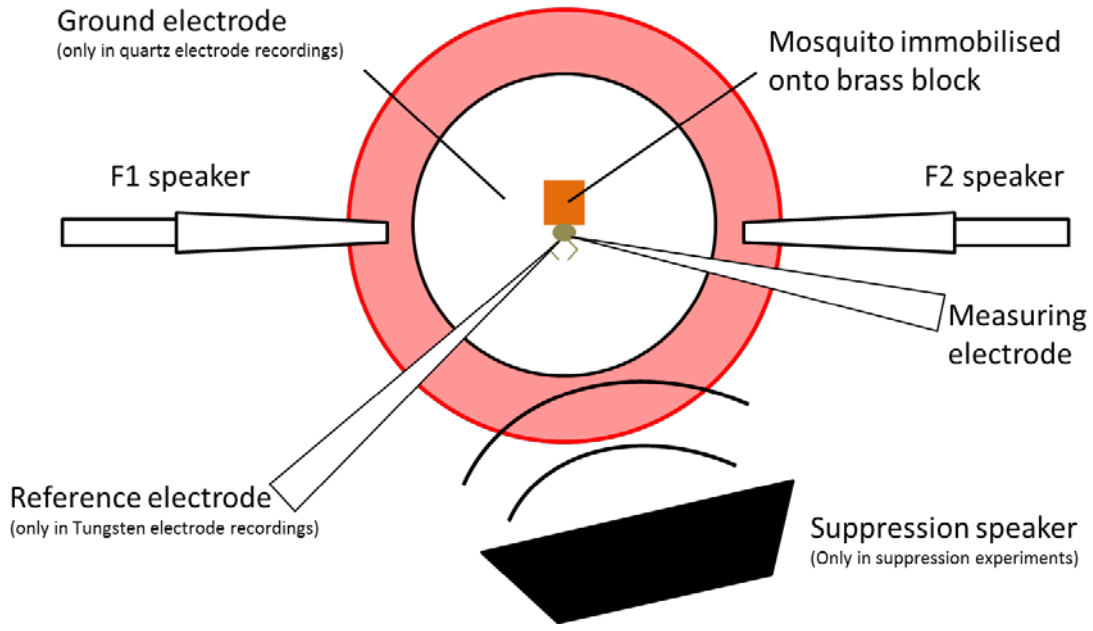

Figure 2.1. Setup for electrophysiological recordings, as viewed from above. The mosquito was fixed to a brass block, and electrically coupled to a ground electrode by electrolyte gel. The preparation was stimulated using two point source speakers. For tungsten electrode recordings, a primary measuring electrode was inserted into the JO, and a second reference electrode was inserted into the thorax of the mosquito.

Electrodes were inserted into the immobilised pedicels to obtain recordings of the compound JO potentials (Figure 2.1). Electrodes were constructed from either quartz glass or tungsten. For glass electrodes, quartz capillaries (Sutter instruments, 7.5 cm length, 1.0 mm inner-diameter, 0.7 mm outer-diameter, filamented) were pulled with a laser pipette puller (Sutter instruments Co. P-2000) to a resistance between 2-30 MΩ. Glass electrodes were filled with 2 M potassium chloride and mounted on a micromanipulator (Science products$_{GMbH}$). For fine control for electrode insertion, a piezo stepper (Science products$_{GMbH}$) was used. The voltage from the electrode was amplified 1000 times, with respect to the ground electrode. This signal was low pass filtered (custom made filter) at 5000 Hz and then through a DC restoration and finally fed into a data translation board (3010 data acquisition board, Data translation).

Tungsten electrodes were custom made (60 mm length, 250 µm shaft diameter, fine taper 10-15^{o}, epoxy insulated, 2-4 MΩ resistance – FHC, Bowdoin, ME USA 04287), and used in differential recordings. Differential recordings were made using a primary recording electrode and a secondary reference electrode to decrease electrical pickup. The reference electrode was positioned into the mosquito thorax, and a measuring electrode positioned in the JO using a piezoelectric stepper. All recordings were made under controlled conditions (temperature humidity and light), and within 30 minutes of preparation to ensure excellent physiological state and auditory sensitivity. The JO compound potential was measured in response to a 201 Hz pure tone before and after each experiment. If the amplitude of the JO compound potential had decreased by >5 dB, the data set would be discarded (2 in 20 discarded).

2.3 Acoustic stimulation & Calibration of electrophysiological recordings

Acoustic stimulation for electrophysiological recordings were made via a pair of modified DT48 headphone speakers, which were controlled from a custom programme (Matlab, *DPAdap.Yes*). The speakers were housed away from the preparation to reduce vibrations on the table and electrical pickup at the electrodes. Sound was propagated to the preparation via plastic tubing (7 mm inner diameter

and 1200 mm in length). All tones were calibrated using a white noise stimulus (Matlab, Calib2ch) against a known 94dB SPL 1 kHz sine tone (Brüel & Kjær 4230 sound level calibrator).

It is not possible to measure particle velocity directly via a microphone, so has to be calculated from sound pressure instead, using a pressure difference microphone, where voltage is proportional to particle velocity (Göpfert, Briegel et al. 1999). Bennet-Clark (1984) designed an unconventional particle velocity microphone, later improved by Professor Steven Errede from the University of Illinois (2013), which allows for a more accurate calculation of particle velocity. This is achieved by measuring the velocity difference of the membrane in the microphone head by integrating the energy from the stimulus into the circuit. This allows for an improved lower frequency range response. Sound pressure and particle velocity are non-linear in the near field (less than one wavelength), but are proportional in the far field (greater than one wavelength). All conversion calculations were therefore made in the far field. For full description of the calibration of the sound system, see **Appendix 1.0**.

Due to the linearity between voltage and particle velocity (Göpfert, Briegel et al. 1999), determining a co-efficient allows us to convert voltage from a microphone directly into particle velocity. In order to achieve this, first pressure was calculated with a 1 kHz 94 dB SPL tone (Brüel & Kjær 4230 sound level calibrator), and then converted into particle velocity by dividing by acoustical impedance, **z=p/u** (z = impedance, p = pressure, u = volume flow). Pressure can be calculated using equation **(e1.1)**, and rearranged to show pressure **(e1.2)** where $\mathbf{I^1}$ is a measured pressure, and $\mathbf{I^2}$ is a reference pressure (2×10^{-5} N/m^2), which equates to the human hearing threshold (Pickles 1988).

$$dB = 20\log_{10}(I^1/I^2) \qquad \text{(e1.1)}$$

$$\text{Pressure} = (I^2) \times (10^{(dB\ /\ 20)}) \qquad \text{(e1.2)}$$

Particle velocity is then determined by dividing SPL by acoustical impedance (413.5 Pa·s/m^3 at 20^{o}C). Measuring the same sounds through a microphone gives us the relative voltage, which allows us then to calculate a co-efficient. The co-efficient used in this thesis was 0.02616 (**Appendix 1.0**).

Pure tones were played to the preparation, which increased in intensity steps, described here as a level function, and were delivered as pure tones of 82 ms duration with 8 ms rise/fall time, to avoid broadband transients at the onset and offset of the stimulus. Acoustic stimulation was delivered via a 5 kHz low-pass filter and generated using a DT3010 board. To reduce acoustic distortion, stimulation levels were reduced to voltages below the operating limitations of the speakers. For DP suppression experiments (**Chapter five**) a constant suppression tone was delivered simultaneously with the male- and female-like tones (F1 – 700 Hz and F2 – 400 Hz) through a separate Beyerdynamics DT 770 speaker placed 7.5 cm from the preparation (Figure 2.1). Masking tones were produced using the sine wave function of a Philips PM5193 function generator and a step level voltage function.

2.4 Temperature control for electrophysiological recordings

A mosquito was fixed to a brass block and ground electrode (as described above) and then mounted on a ball of blue-tac and placed inside a custom-made stainless steel chamber and secured with a plastic screw. The chamber was attached to a Peltier element and heat sink. Temperature was controlled by a custom-made device with a negative feedback loop, which altered the current fed through the Peltier element in response to the temperature read by a thermal resistor (Figure 2.2). A ball of cotton wool was positioned at the back of the metal chamber, and soaked with water, to maintain humidity.

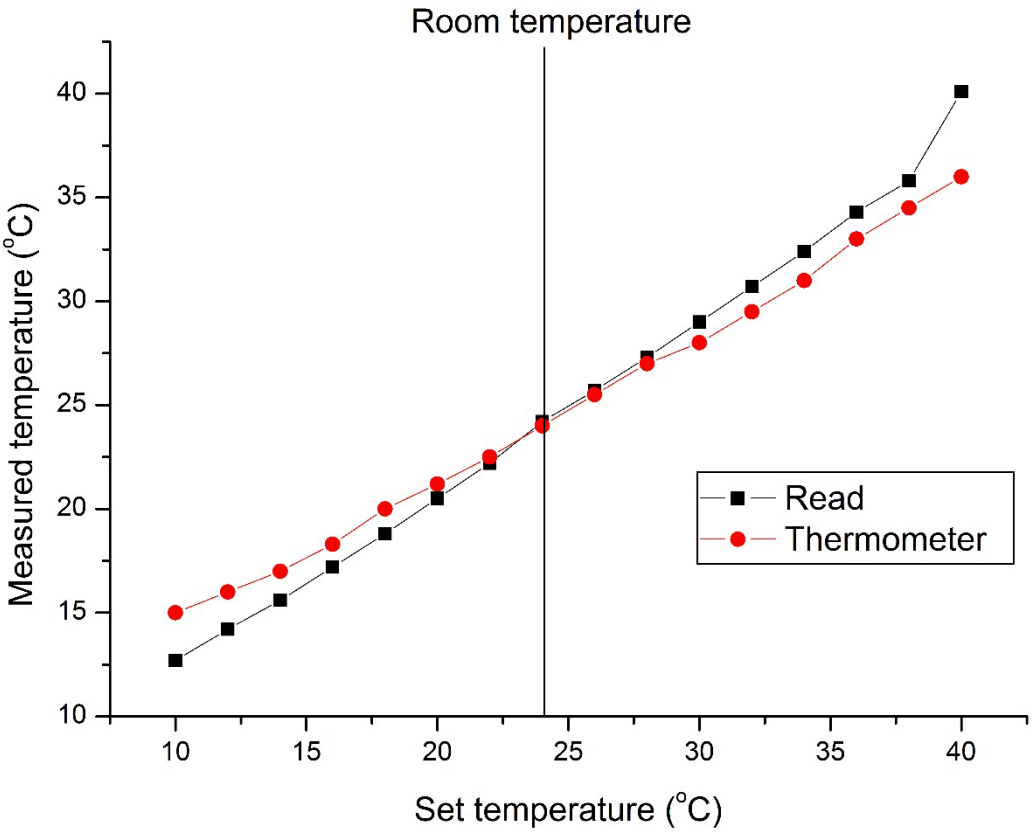

Figure 2.2 Peltier calibration. Relationship of temperature read on the power supply against temperature measured using a thermometer. During recordings, the set temperature on the power supply had to be offset to the actual temperature shown in this graph.

2.5 Data analysis

Threshold JO compound potential tuning curves were derived by determining the minimum PVL to establish a JO compound potential 5 dB above the average noise floor, at the frequency of the stimulation. The JO compound potential was measured at the frequency of acoustic stimulation. To measure the JO compound potential at specific frequencies the data was frequency transformed using a Fourier Transform. The noise floor was calculated as an average of four FFT points either side of the target frequency.

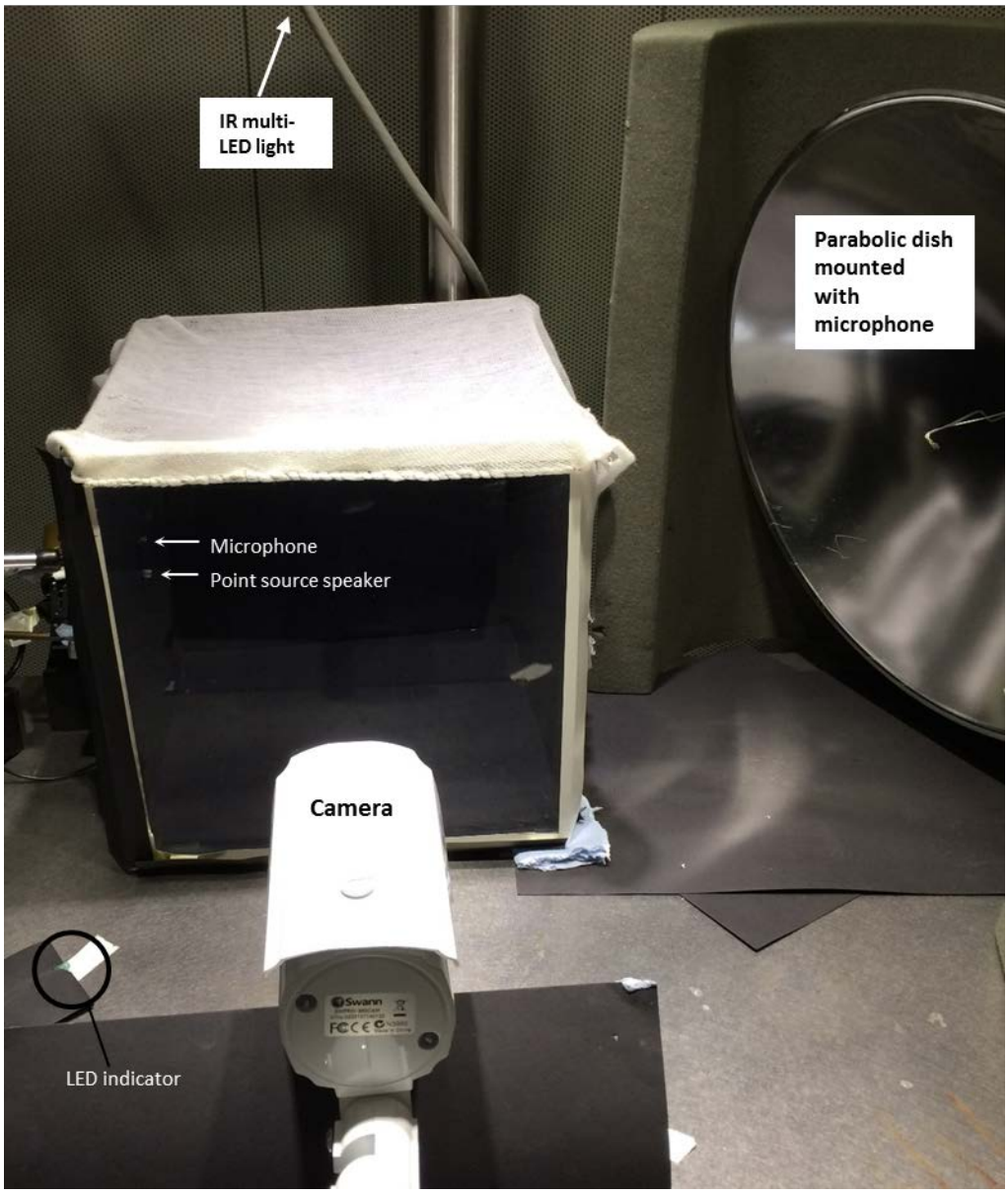

Figure 2.3. Behavioural flight arena. A 30 cm^3 4 mm stainless steel frame enclosed by medical tubigrip. Acoustic stimulation was delivered through a 7 mm plastic tube as a point source in the centre of the enclosure that was coupled via the tubing to a speaker located outside of the enclosure. A near field microphone was positioned within 20 mm of the point source to measure responses close to the tube opening, and a parabolic pressure microphone was used to measure flight tones throughout the cage. All recordings and stimulation were made using a laptop via a sound card and amplifier (see materials and methods section).

2.6 Behavioural experiments

All behavioural experiments were made in a 30 cm^3 stainless steel flight arena (Figure 2.3), positioned on a vibration isolation table (Newport corporation, Model: M-VW-3036-OPT-99-9-28-92), inside a sound attenuated booth (IAC Ltd, Winchester, UK).

The flight arena during recordings was kept at constant environmental conditions (temperature, humidity) and provided with dusk light levels typical during natural swarming behaviour. A swarming marker (black disc, 13 cm radius) was placed on the floor of the arena to stimulate flight behaviour typical of swarming. Swarming is defined as flying in controlled loops, to maintain 'station-keeping' with respect to the swarm marker (Gibson 1985). A Knowles 23132 pressure microphone was mounted at the focal point of a ~61 cm parabolic reflector (Edmunds), and placed just outside the arena to record overall WBF activity (Figure 2.3). There were two versions of the flight arena, one for acoustic only recordings (**Chapters four and five**), and one for audio and visual dual recordings (**Chapter two**). In acoustic only recordings the flight arena was enclosed by T1 sized Tubigauze (Nu-Care products Ltd). In audio and visual recordings, three sides of the metal frame was covered with matt-black cotton fabric which is non-reflective to infra-red (IR) light, while the front side was covered by a transparent acrylic screen enabling the camera to view the interior of the chamber. The ceiling was covered with white cotton gauze to allow the chamber to be illuminated by two IR multi-LED lights positioned 1 m above the cage. The flight arena was equipped with an IR video camera (Swann® Pro-880), positioned 30 cm in front of the clear screen. Digital video recordings at 30 frames s^{-1} of the flying mosquitoes were obtained using Debut Video Capture software v1.88 (NCH® software). The video-recorded flight paths were then digitized using Kinovea (v0.8.23) software. The synchronized video-spectrogram sequences in the supplementary movies were composed using Adobe® After Effects. Copula formation was verified via TrackIt 3D® (SciTrackS, GmbH) zoom tracking software that displayed an image of each mosquito in real time.

An adapted Audio Techniques ATH A700AX (5–35,000 Hz range with flat frequency response 100–25,000 Hz) speaker was housed away from the flight arena to reduce near-field vibrations. Sound was delivered as a focal sound source to the centre of

the cage through a plastic tube (7mm diameter and 1100mm in length) which was held in place using a magnetic clamp (Noga, CPC). A calibrated (Göpfert, Briegel et al. 1999) near-field microphone (Knowles NR-3158, Ithaca, NY, USA) was mounted and positioned ~4 cm from the speaker probe tip. Voltages from each microphones were amplified 100-fold with a purpose-built two-channel preamplifier and the output of each channel was digitized at 192 kHz using a Fireface® UC sound card. The digital outputs were then recorded using Spectrogram 16 (Visualization Software, LLC) at a sampling rate of 48 kHz and frequency resolution of 5.9 Hz. Spectrogram 16 was also used to analyse and extract data on the time, frequency and amplitude of all acoustic signals. Artificial sound stimuli were generated using the sine wave function of Test Tone Generator 4.4 (EsserAudio® 2011) software. With the exception of the behavioural audiograms, all tone bursts had a fixed duration (5 or 10 s, depending on the experiment), were cosine windowed at onset, and offset to avoid broad-band acoustic transients. Calibrated pure tones simulating the sound intensity of the fundamental component of the flight tones of tethered-flying female mosquitoes were based on measurements with the particle velocity microphone placed 2 cm in front of their heads. The mean (± standard error) particle velocity for this reference distance was $5.7\times10^{-5}\pm1.9\times10^{-6}$ m s^{-1} (N=23).

Individuals or groups of male mosquitoes were placed inside the flight arena at the time of maximum circadian activity, and free to establish swarming behaviour. After a ~10 min period of adaptation to conditions inside the arena, the mosquitoes started to fly spontaneously, whereupon sound recording and stimuli presentation were initiated. All behavioural experiments were conducted at 30±2 °C, which is within the range of temperatures of the natural habitat of the *Cx. quinquefasciatus* mosquitoes (Gokhale et al. 2013). To characterise temperature dependant processes, the temperature of the sound attenuated booth was altered by use of a convection heater (Micromark, MM30070N) that heated to a maximum of 34.9 ^{o}C, and cooled to a minimum of 21.1 ^{o}C by an air conditioning unit (Amcor SF12000E). Temperature inside the cage was monitored using a probe (DHGate) attached to a digital display outside the booth. Measurements of the temperature of tethered flying mosquitoes were taken using a FLIR® TG165 Thermal Imaging IR Thermometer (Figure 6.2).

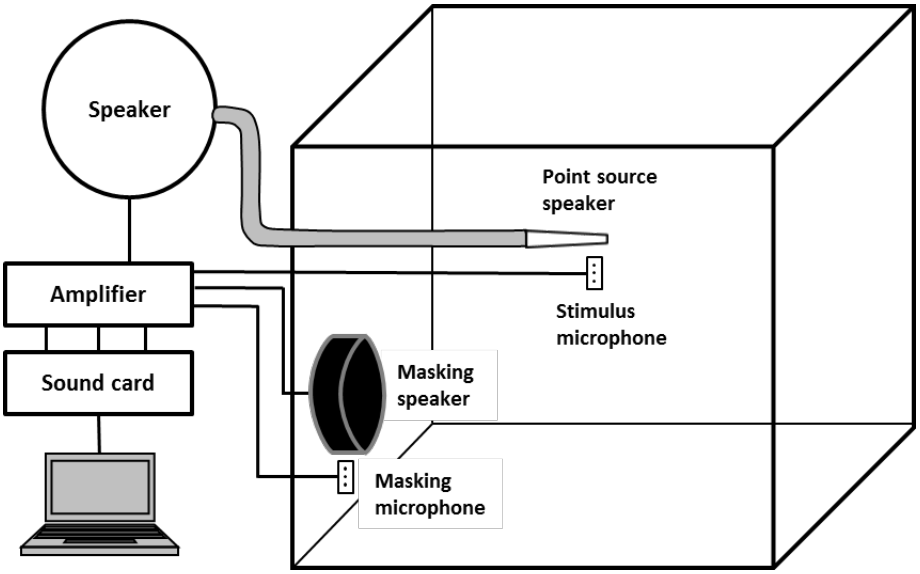

Figure 2.4. Behavioural flight arena for masking experiments. A 30 cm^3 4 mm stainless steel frame enclosed by medical tubigrip. Acoustic stimulation was delivered through a 7 mm plastic tube as a point source in the centre of the enclosure that was coupled via tubing to a speaker located outside of the enclosure. A near field microphone was positioned within 20 mm of the point source to measure responses close to the tube opening. A masking speaker and second near field microphone was positioned just outside the cage, and camouflaged by the cage outer material to remove any visual stimulation cues. All recordings and stimulation were made using a laptop via a sound card and amplifier.

For masking experiments, tones were played from a third speaker (Beyerdynamics DT 770), placed at one wall of the flight arena, thus distanced 15 cm from the centre and from the stimulus speaker (Figure 2.4). A second near-field microphone was placed ~2 cm from the masking speaker. Each microphone identified which of the sound sources the male mosquitoes produced RFM behaviour towards (Figure 2.5). Pure tones produced from the masking speaker were referred to as masking tones, and were enveloped with a cosine onset and offset, produced with Test Tone Generator 4.4 (EsserAudio®, 2011). Both the stimulus and masking tones were delivered simultaneously for 10 seconds. The inter-trial interval between presentations was ~5 seconds. Three acoustic frequencies were used as probe tones: 340 Hz, 400 Hz and 450 Hz. The particle velocity of the probe tones was $5x10^{-5}$ ms^{-1}

at a reference distance of 2 cm, which is a similar sound intensity produced by tethered-flying females at the same distance. The frequency of the masking tones varied throughout the experiments, ranging between 100-1000Hz and with a particle velocity of ~$8x10^{-5}$ ms^{-1} at a reference distance of 2 cm.

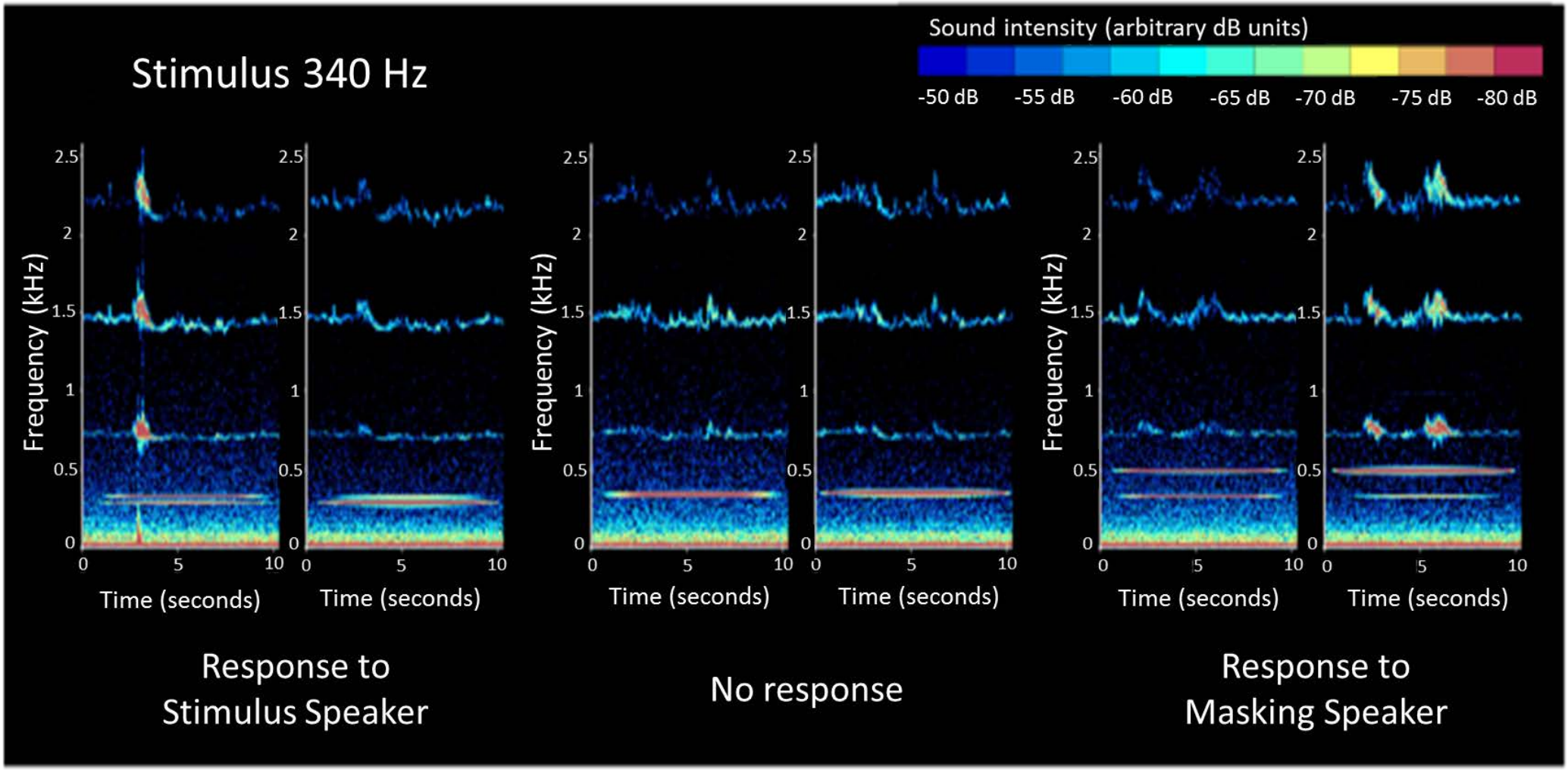
Stimulus 340 Hz
Sound intensity (arbitrary dB units)
-50 dB
-55 dB
-60 dB
-65 dB
-70 dB
-75 dB
-80 dB
Frequency (kHz)
Time (seconds)
Response to Stimulus Speaker
No response
Response to Masking Speaker

Figure 2.5: Example spectrogram of the WBFs of free-flying males when stimulated with a simultaneous stimulus/mask tones presentation. Stimulus tone 340 Hz. In response of tone presentation, male mosquitoes could either present a RFM response towards stimulus speaker, no conspicuous response, or present a RFM response towards the masking speaker. For each single interaction shown, the left spectrogram displays the wing beats recorded by the microphone near the stimulus speaker and the right spectrogram displays the activity recorded by the microphone near the masking speaker. The identification of the speaker to which the showed phonotaxis and RFM behaviour was determined by comparing the sound intensity of the WBF in the 2 sound channels: the sound intensity of RFMs near a microphone registered responses 20-30 dB higher than the furthest microphone. Occasionally (<5% of the records), a male displayed RFM to both speakers during a single 10 second stimulation; in this situation, we registered the response to the first speaker.

Appendix 1.0

Sound system calibration manual

Calibrating speakers

- Open Matlab
- Open *Existing GUI*
- Click *Calib2ch.fig*

Programme parameters: Sampling: 50 kHz, Ave: 10, F1: 1 kHz

Place the near-field microphone (Knowles NR-3158) in the position of the mosquito, facing the left speaker (with 3 small holes pointing out), switch on microphone.

Press "*channel 0*" on programme – This will produce a primary yellow curve (altering attenuation will reduce harmonic pickup).

Stimulate a *BK* pressure microphone using a known 94 dB 1 kHz tone (Brüel & Kjær 4230 sound level calibrator). Add the reading on the measuring amplifier to the 94 dB from the calibrator, which give a maximal level (=0).

Example: Reading off amp 4 dB + 94 dB = **98 dB** (maximal level)

Press "*channel SIN*" on programme – With the *BK* pressure microphone in the position of the mosquito.

- Speaker produces a sine tone at 1 kHz
- Read off level on measuring amp [here: 30 dB], and subtract that from the maximal level (e.g. **98** – 30 = **68 dB**)
- enter *68* dB calculated into pop up box

Now switch microphone round to face right speaker

Press "channel 1" – produces white noise, and secondary blue curve (altering attenuation will reduce harmonic pickup).

Press "*Save*" and "*Read*"

The calibration factor will now be displayed in the cal.cal file in the "*C:\Exdata*" (4th number in the data file).

Converting voltage output to pV

Place a *BK* pressure microphone on one corner of the table facing in, and place a large speaker at the other end (minimum of 1.5 wave lengths away), also facing in.

Replace the "*DT48left speaker middle*" with the output of the large speaker so now the stimulus tone plays through the large speaker.

Use the calibrator (Brüel & Kjær 4230 sound level calibrator) to stimulate the *BK* pressure microphone with a 94 dB 1 kHz tone, and calculate maximal level (see above).

Example: Reading off amp 8.5 dB + 94 dB = **102.5 dB**

Now play the sine tone through the large speaker (via the *calib2ch.fig* program), and take reading off amp (e.g. 37.5).

Example: 102.5 - 37.5 = **65 dB**

The equation to calculate pressure is:

$$\underline{\mathbf{dB = 20\log_{10}(I^1/I^2)}}$$

Where $\mathbf{I^1}$ represents a measured pressure, and $\mathbf{I^2}$ represents a reference pressure. The reference pressure, as is relative to the threshold of human hearing, is 2×10^{-5} Pa. Use this information to fill out parts of the equation.

$$65 \text{ dB} = \mathbf{20\log_{10}\ (I^1 / \underline{2 \times 10^{-5}})}$$

Rearrange the formula to read:

$$\text{Measured pressure } (\mathbf{I^1}) = \mathbf{(2 \times 10^{-5}) \times (10^{(65\ /\ 20)})}$$

Which for this case results in:

$$\mathbf{Pressure = \underline{0.03557\ (N/m^2)}}$$

To calculate particle velocity from here, divide pressure by acoustical impedance:

Example: pV = Pressure (Pa) / Acoustical impedance (z)

0.03557 / 413 = $\underline{8.632 \times 10^{-5}\ (ms^{-1})}$

Now place the Knowles microphone above the SPL microphone (ensuring that the Knowles is plugged into the oscilloscope) and play the same 1 kHz tone (from calibration program) and read the voltage on the oscilloscope.

Example: 3.3 mV (0.0033 V)

We now know that **8.632×10^{-5} ms^{-1}** generates **3.3 mV** from the far field, which allows us to calculate a co-efficient that will directly translate a particle velocity into voltage, and vice versa. This co-efficient will allow, when making figures, to calculate the known voltage measured by the microphone into particle velocity. This information can also be used to determine the correct level of constant tone for two tone experiments (See **Calibrating the constant tone**).

The co-efficient to calculate voltage into particle velocity can be derived by dividing particle velocity by voltage:

Example: $8.632 \times 10^{-5} / 0.0033$ **= 0.02616**

With this co-efficient, it is possible to calculate particle velocity or voltage by plugging in the co-efficient into these equations:

(8.632×10^{-5})/ co-efficient = voltage

0.0033 x co-efficient = particle velocity

Calibrating the constant tone in two-tone experiments

In order to calculate a constant tone for two-tone experiments (f2-f1, f1-SO, 2f1-f2), it's necessary to play a constant tone which is relative to the beating wing of a female mosquito (at the distance of wing to flagellum – approximately 2 mm).

This is measured in pV, and needs to be converted into dB.

The particle velocity of the wing beat of a mosquito at 2 mm is 1.2 x 10^{-3} (Female *Cx. quinquefasciatus*).

The particle velocity mentioned here is based on the direction of the sound source being propagated perpendicular (90^{o}) to the shaft of the flagellum. It is most likely that the sound propagates at a 45^{o} angle relative to the flagellum. This means that the energy from the particle displacement can be decomposed into two vectors; one perpendicular to the flagellum and the other parallel with the flagellum (Figure S1). In order to determine the correct stimulation levels, particle velocity needs to be modified.

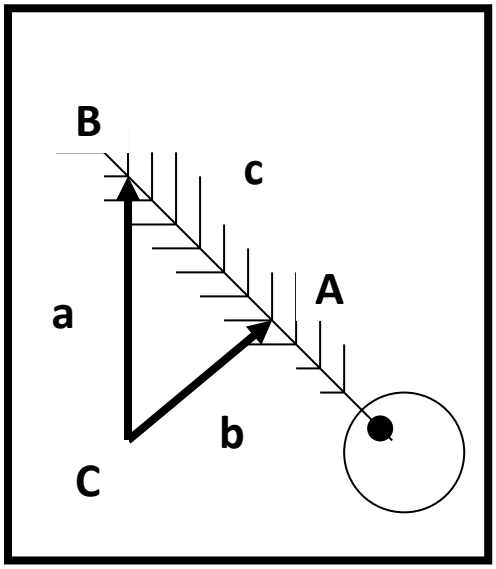

Figure S1: Recalculate particle velocity via basic trigonometry.

Here we wish to calculate the particle velocity of **a**, which is the effective movement. **b** is the reference particle velocity at 2 mm, which is 1.2 x 10^{-3} (see above).

Using trigonometry:

a / SIN(A) = b / SIN (B) = c / SIN (C)

So in this case we know that because **A** = 90 degrees → SIN (90) = 1

B = 45 degrees → SIN (45) = 0.707

Which re-arranges to be:

a / 1 = b / 0.707

a = b / 0.707

a = 1.2 x 10^{-3}, so to calculate the SIN45 of **b** we need to find **b.**

1.2 x 10^{-3} = b / 0.707

1.2 x 10^{-3} x 0.707 = b

b = <u>8.484 x 10^{-4}</u>

As calculated in the **"Converting voltage output to pV"** section, it is possible to use a co-efficient to convert particle velocity into voltage, which is generated in the far field.

8.484 x 10^{-4} / co-efficient

8.484 x 10^{-4} / 0.02616 = 32.4 mV

This voltage is now the voltage, which is require to achieve 1.2 x 10^{-3} pV through the speaker.

Keep playing the frequency of the female WBF through the *DPAdapYES.fig* programme in Matlab, and systematically increase the intensity, until the desired voltage is achieved (in this case 32.4mV). This dB level will now be the constant tone for f2.

3.1 Chapter One: The Johnston's Organ of male *Culex quinquefasciatus* is mis-tuned to the wing beat frequency of female conspecifics

3.1.1 Introduction

The Johnston's Organ (JO) was speculated, as early as 1855, to be a dedicated acoustic receiver to localise female mosquitoes (Johnston 1855). When the male mosquito is presented with sounds close in frequency to the female wing beat frequency (WBF), it results in the rotation of the hypopygium and antennae towards the direction of the sound (Kahn et al. 1949, Gibson 1985). The frequency tuning of the JO and the flagellum have been characterised using electrical recordings of the JO compound potential, and mechanical recordings of the flagella displacement using contactless lasers. The most sensitive frequencies of the JO, as determined through measurements of the JO compound potentials, are between 250 and 300 Hz across several haemophilic mosquito genera (Tischner 1955, Keppler 1958, Belton 1974, Cator, Arthur et al. 2009, Warren et al. 2009, Arthur et al. 2010, Pennetier, Warren et al. 2010, Lapshin 2012). The most sensitive frequencies of the flagellum, determined through its displacement, range between 370 and 500 Hz (Tischner 1955, Göpfert, Briegel et al. 1999, Gibson and Russell 2006, Warren, Gibson et al. 2009, Pennetier, Warren et al. 2010). In *Cx. quinquefasciatus,* the most sensitive frequency responses of the JO and flagellum are 300 Hz and 380 Hz (Warren, Gibson et al. 2009). The difference in tuning derived from mechanical displacements of the flagellum and the JO compound potential can be attributed to the low-pass filtering properties, as the signal is passed through neural tissue within the JO (Arthur, Wyttenbach et al. 2010).

How does the frequency tuning of the JO compare with the WBF of free-flying mosquitoes? So far, any comparison between JO tuning and the WBF has been done using tethered mosquitoes (Cator, Arthur et al. 2009, Warren, Gibson et al. 2009, Pennetier, Warren et al. 2010). The WBF of tethered male and female *Cx. quinquefasciatus* is approximately 542 Hz and 428 Hz (Warren, Gibson et al. 2009); the male JO, however, is most sensitively tuned to ~300 Hz (Warren, Gibson et al.

2009). Similarly, the WBF for male and female *Aedes aegypti*, is approximately 600 Hz and 400 Hz with the male JO most sensitively tuned to ~250 Hz (Cator, Arthur et al. 2009). In both cases, the tuning of the JO is mismatched below the female WBF by ~128 and ~150 Hz respectively. The WBF of *Drosophila melanogaster* is lower when tethered compared to free flight (Fry et al. 2005), thus, the mismatched tuning of the JO has been postulated to be due to unrealistic WBF's of tethered mosquitoes. In this chapter, I will measure the WBFs of free-flying (non-tethered) male and female mosquitoes and determine the frequency tuning of the male JO through measurements of the JO compound potential.

3.1.2 Results

Free-flight wing beat frequency of female and male *Culex quinquefasciatus*

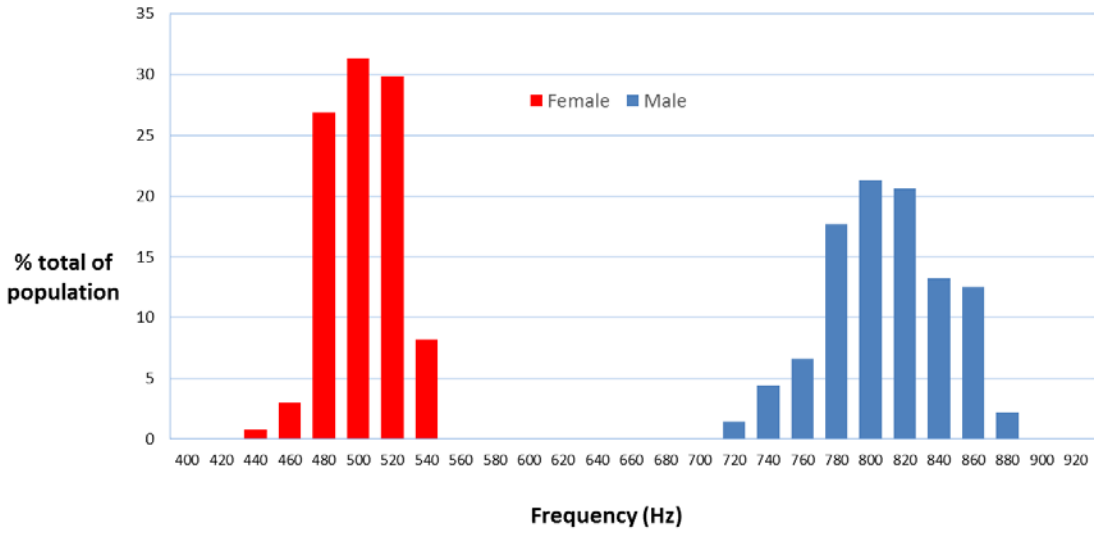

Figure 3.1: Frequency distribution of free-flying female (red) and male (blue) WBFs during swarming in a 30 cm^3 flight arena at 30°C, N=21 each. WBFs were recorded using a pressure difference microphone housed in a parabolic dish.

Female and male mosquitoes swarmed in a flight arena, during artificial dusk (one hour into their 12-hour dark cycle), when *Cx. quinquefasciatus* swarm. The flight arena was maintained at 30 °C to match the temperature of their natural habitat in Tanzania (Gokhale, Paingankar et al. 2013). The mean WBF of free-flying females is

493.3 Hz (range 430-527 Hz) and 798.0 Hz for males (range 713-874 Hz). The WBF of males and females are significantly different with no overlap of their ranges (Figure 3.1).

Frequency tuning of the JO

Compound JO potentials were recorded with electrolytically sharpened tungsten electrodes inserted ~5 µm into the JO through the pedicel wall. The temperature was maintained at 30 °C to match that at which the WBF was measured. Mosquito wing beats generate a fundamental tone and higher order harmonics (Kahn et al. 1945, Wishart and Riordan 1959, Bennet-Clark 1971, Gibson and Russell 2006, Warren, Gibson et al. 2009), but here immobilised mosquitoes were presented with

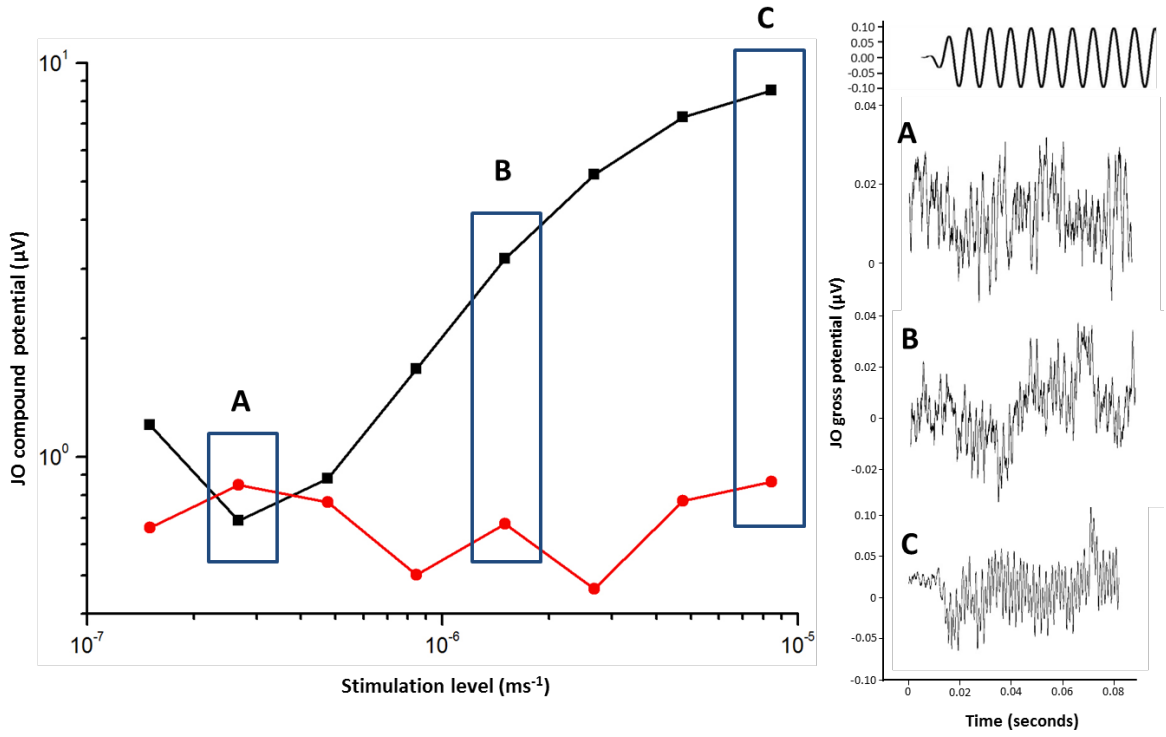

Figure 3.2: Example threshold data. Immobilised mosquitoes were presented with pure tones, which increased in intensity in 5 dB steps, until a JO compound potential (black) occurred 5 dB above the noise floor (red). Left; graphic of JO compound potentials that increase in amplitude with an increase in stimulation intensity. Right; JO compound potentials as a function of time, at different stimulation intensities (depicted by the blue boxes). Top right, time trace of acoustic stimulation [402.8 Hz].

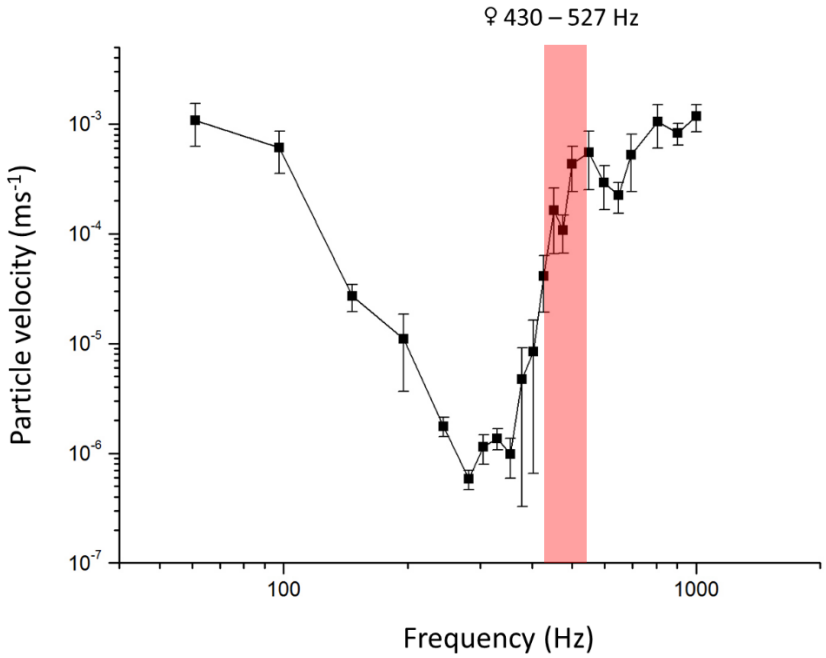

Figure 3.3. Threshold tuning curves of the male JO at 30°C. Thresholds were derived from the minimum particle velocity level necessary to elicit a JO compound potential 5 dB above the noise floor (see Figure 3.2). The WBF range of flying females is donated by the pink box. N=10.

pure tones. The flagellum was stimulated with a point source speaker perpendicular to the axis of the flagellum, and tones increased in intensity until a response 5 dB above the noise floor was established (Figure 3.2). Based on this threshold criteria, threshold tuning curves of the JO were derived, which indicated the most sensitive responses occurred at 333.1 ± 80.0 Hz at a particle velocity of 6.08 x 10^{-7} ms^{-1} with an absolute sensitivity comparable to previous studies (Warren, Gibson et al. 2009). Tuning bandwidth of the male JO is determined by calculating the width of the tuning curve measured 10 dB above the threshold, termed Q_{10dB} bandwidth. The Q_{10dB} bandwidth of the JO was 97.6 Hz (Figure 3.3).

3.1.3 Discussion

The frequency tuning of the JO has previously been compared to the WBF of tethered flying mosquitoes (Gibson and Russell 2006, Cator, Arthur et al. 2009, Warren, Gibson et al. 2009). The WBF of free swarming male and female *Cx. quinquefasciatus* here was 798 and 493 Hz, compared to 542 and 428 Hz from their tethered counterparts (Warren, Gibson et al. 2009). The frequency of the wing beats is determined by the upward and downward motion of the mosquito wings; with the dorsal longitudinal muscles depressing the wings by arching the mosonotum, and the dorsoventral muscles lift the wings by drawing the scutum downwards. Attaching a tether to the scutum will change its mass and/or stiffness and therefore change the mechanical resonance of the flight system. This is evidenced by tethered *Drosophila*, which generate a pattern of wing motion that is clearly different to that of free flight (Fry, Sayaman et al. 2005). In tethered *Drosophila*, the total stroke amplitude and WBF is reduced and the time course of stroke deviation is distorted (Fry, Sayaman et al. 2005). *Drosophila* regulate their flight speed by their flight angle, thus leaning forward to increase speed, much like a helicopter (David 1982). A tether that does not maintain this flight angle and provides no acceleration (because they are fixed) alters the feedback for the flies' velocity control system, which may result in attempts of *Drosophila* to accelerate continuously. In addition, tethering of mosquitoes, in particular, produces erratic flight patterns (Gibson and Russell 2006, Cator, Arthur et al. 2009, Warren, Gibson et al. 2009, Pennetier, Warren et al. 2010).

The frequency tuning of the male flagellum and JO has been shown to match the female WBF in tethered *Cx. quinquefasciatus, Anopheles gambiae* and *Aedes aegypti* (Cator, Arthur et al. 2009, Warren, Gibson et al. 2009, Pennetier, Warren et al. 2010). It is clear however, that the male's JO is tuned to frequencies lower than the WBF of free flying females (Figure 3.2). The most sensitive frequency of the male JO is 280 Hz compared to 382 Hz reported by Warren et al (2009). The sharpness of tuning, measured here as Q_{10dB}, is 2.87, sharper than the previously reported 1.11 (Warren, Gibson et al. 2009). These differences may be due to different temperatures used, that have shown to effect JO tuning, as well as WBF (Tamarina et al. (1979), Chapter 4). The temperature used here matched that during the swarming period of *Cx.*

quinquefasciatus in Tanzinia, where they were sourced. All other measurements of the WBF were at typical lab temperatures of 19-22^{o}C (Warren, Gibson et al. 2009). The most sensitive responses of the JO were to 280 Hz, whereas the lowest recorded WBF of free flying females was 430 Hz. This mismatch, of 150 Hz, between the most sensitive response of the JO and the lowest WBF of the free flying female, suggests that the male JO is mistuned to the females fundamental WBF.

Göpfert, Briegel et al. (1999) first measured a mechanical mismatch of 80 Hz between the best frequency of the male flagellum and the WBF of a tethered female *Aedes aegypti*. The mismatch was believed to be due to the tether, and they claimed that the lower WBF of free-flying mosquitoes would be a closer match to the JO tuning. The free flight WBF measured here, was higher than in tethered mosquitoes, which fails to account for the mismatch to tuning in tethered mosquitoes. In order for male mosquitoes to detect the female WBF, she would have to fly at frequencies outside the range measured here. There are reports of female WBF as low as 200 Hz during early eclosion (Tischner et al. 1955), but males of all mosquito species require at least several hours to a full day until they reach sexual maturation (Beach 1980). The mismatch between male JO tuning and the female WBF has led others to conclude that the biological function of the JO is lacking which is surprising for the most sensitive arthropod detector known (Göpfert, Briegel et al. 1999, Göpfert et al. 2001).

3.2 Chapter two: Free-flight mating behaviour and phonotactic tuning of male mosquitoes

3.2.1 Introduction

It has long been established that male mosquitoes are attracted to sound, and show positive phonotaxis towards the WBF of a female, irrespective of its source (Mayer 1874, Child 1894, Howard 1901, Maxim 1901, Roth 1948, Wishart and Riordan 1959, Downes 1969, Belton 1994). Examples include male mosquitoes showing positive phonotaxis to vibrating tuning forks (Landois 1874) and the humming of an electric generator (Maxim 1901). In the absence of acoustic stimulation, swarming males ignore a non-flying female mosquito (Lutz 1924). The WBF of the female is therefore necessary and sufficient for males to demonstrate phonotaxis toward female mosquitoes, without the need for visual or olfactory cues (Downes 1969, Boo 1980). In the last 10 years, auditory-driven behaviour of mosquito flight was studied using tethered mosquitoes and it was found that opposite sex pairs, of four genera, attempt to match fundamental frequencies or harmonic components of their flight tones (*Toxorhynchites* [(Gibson and Russell 2006)] *Culex* [(Warren, Gibson et al. 2009)], *Anopheles* [(Pennetier, Warren et al. 2010)], and *Aedes* [(Cator, Arthur et al. 2009)]). This auditory behaviour was thought to precede the grasping and copulation of opposite sex pairs of mosquitoes in swarms (Roth 1948). Frequency convergence of the higher harmonics of the flight tones of both sexes has been reported in tethered *Cx. quinquefasciatus*, potentially as a mechanism for recognition of conspecific sexual partners (Warren, Gibson et al. 2009, Pennetier, Warren et al. 2010). The wing beat frequencies (WBF) of males fluctuate during their approach to female flight tones, but these changes have not been quantitatively analysed (Kahn, Celestin et al. 1945, Roth 1948, Wishart and Riordan 1959, Belton 1994).

The particle displacement component of wing beats (so called near-field sound) vibrates the flagellum, which connects to the ~7,000 mechanosensitive scolopidia, of the nanometre-sensitive Johnston's Organ (JO) (Belton 1974, Boo et al. 1975, Clements 1999, Göpfert, Briegel et al. 1999, Göpfert et al. 2000). The frequency

tuning of the flagellum and the JO of male *Cx. quinquefasciatus* has been characterised (Warren, Gibson et al. 2009), and it is implicitly assumed to match their frequency-specific phonotactic behaviour (Wishart and Riordan 1959). There is no quantitative analysis of positive phototaxis in male *Cx. quinquefasciatus*, so here free-flight phonotactic behaviour of males to pure tones is characterised by measuring their 2D flight tracks and WBF. This auditory-driven behaviour is then compared to the frequency tuning of the JO and range of the WBF of conspecific females (**Chapter one**).

3.2.2 Results

Phonotactic and auditory-motor behaviour of male mosquitoes to a tethered female mosquito

The flight paths and WBFs of individual swarming male mosquitoes were recorded in the presence of a tethered flying female in a flight arena (Figure 4.1, Figure 4.2). Male *Cx. quinquefasciatus* mosquitoes were released into a flight arena (Figure 4.1) under ambient lighting at 30^{o}C (the temperature in Tanzania during dusk, where they were obtained), with a tethered flying female placed on one wall (Figure 4.1). Male mosquitoes form swarms at dusk, so experiments were also timed to take place within one hour into their 12-hour dark cycle. The duration of the recorded sequences, when both sexes were flying simultaneously, ranged between ~1.5 minutes and ~11 minutes. The mean WBF of the free-flying males and tethered females were 739±5.0 Hz and 411±4.8 Hz (N=9).

The male displayed continuous looping flight (white trace Figure 4.1) until he repeatedly approached the tethered female, in a darting action. The male mosquito displayed a stereotypical modulation of his WBF when flying within 4 cm or touching the female. This behaviour was characterised by a rapid increase in the male's WBF followed by rapid WBF oscillations before a gradual decrease in his WBF as he departed from the female. Each male displayed this behaviour on average 6.2±1.0 times per minute, while flying continuously. In contrast, when the tethered female was prevented from flying by using the tarsal reflex (by positioning a small piece of

paper under her legs), males (N=3) did not display any conspicuous changes in WBF or attempt to approach the female during three recordings lasting on average 14 min. The tethered female occasionally increased and modulated her mean WBF, similar to the male onset and rapid frequency modulation (RFM) behaviour; however, this occurred only as a direct consequence of physical contact by the male.

The initiation of RFM is a male-specific response, which was confirmed by releasing a virgin free-flying female in the presence of a tethered flying male. In all of the recorded sequences (N=3), females displayed continuous looping flight for several minutes without ever being attracted to the tethered male or exhibiting any conspicuous changes in acoustic or flight behaviour in response to the male. Tethered males did not display RFM behaviour in response to free-flying females, as shown in free flight.

Phonotactic and auditory-motor behaviour of male mosquitoes to pure tones

Male *Cx. quinquefasciatus* mosquitoes were released into a slightly modified flight arena (Figure 4.2), containing a point source speaker instead of the tethered female. During swarming, the WBF was continuously recorded using a pressure-difference microphone (Knowles 23132), housed in a parabolic dish (Figure 4.2). As a measure of the mosquitoes' phonotactic responses, a second microphone (Knowles 23132) was positioned within 3 cm of a point-source loud speaker, which played pure tones. The RFM behaviour illustrated in Figure 4.3 indicated phonotaxis to the point source speaker, which was confirmed by digital video recordings. Here, RFM behaviour was an acoustic indicator of phonotaxis, and occurred solely in response to acoustic stimulation from the sound source.

During swarming, five-second tones were played by the point-source speaker, which elicited phonotactic behaviour coincident with stereotypical changes in WBF (Figure 4.3). Male mosquitoes made swift darting movements towards the speaker when within 4 cm, which coincided with changes in WBF (Figure 4.1). The

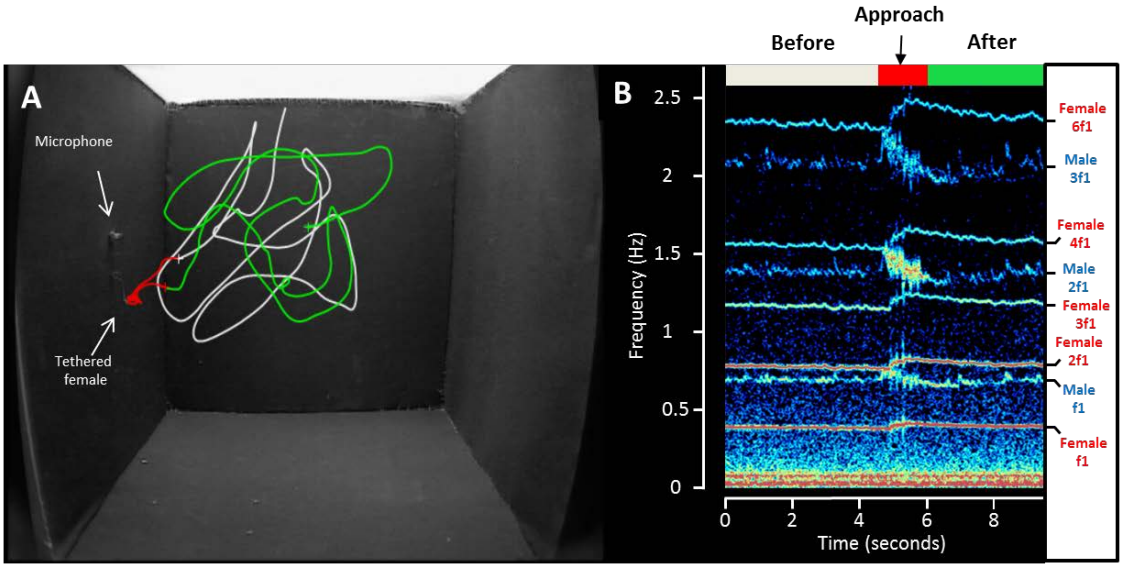

Figure 4.1: Phonotactic behaviour of male *Cx. quinquefasciatus* and the WBF of the male and a tethered flying female. A. Flight path of the male mosquito before (white) during (red) and after (green) interaction. B. Spectrogram of the WBFs of male (blue) and female (red) recorded in A. The flight path in A. is correlated with the white, red and green bar at the top. Data collected by Patrico Simões.

stereotypical acoustic response is comprised of four phases; (1) latency, (2) onset, (3) rapid frequency modulation (RFM) and (4) offset (Figure 4.3). Pure tones were played from the speaker to determine the frequency range to which male mosquitoes displayed RFM responses. The stimulus level was set to that measured 2 cm from the front of the head of a tethered flying female mosquito (see Materials and Methods).

In total, 69 individual RFM events were recorded acoustically and visually from one swarm of 12 males (note: using this method, it is not possible to discriminate between individual mosquitoes). The WBF measured immediately before tone stimulation was 742±9 Hz (mean ± SE) and during the latency period (time from start of tone to a significant increase in the WBF indicating the start of the response), the male's WBF remained essentially unchanged (ΔWBF=2±1 Hz; Figure 4.4). The latency period, from the start of the acoustic stimulation until a steep increase in WBF, had a large range

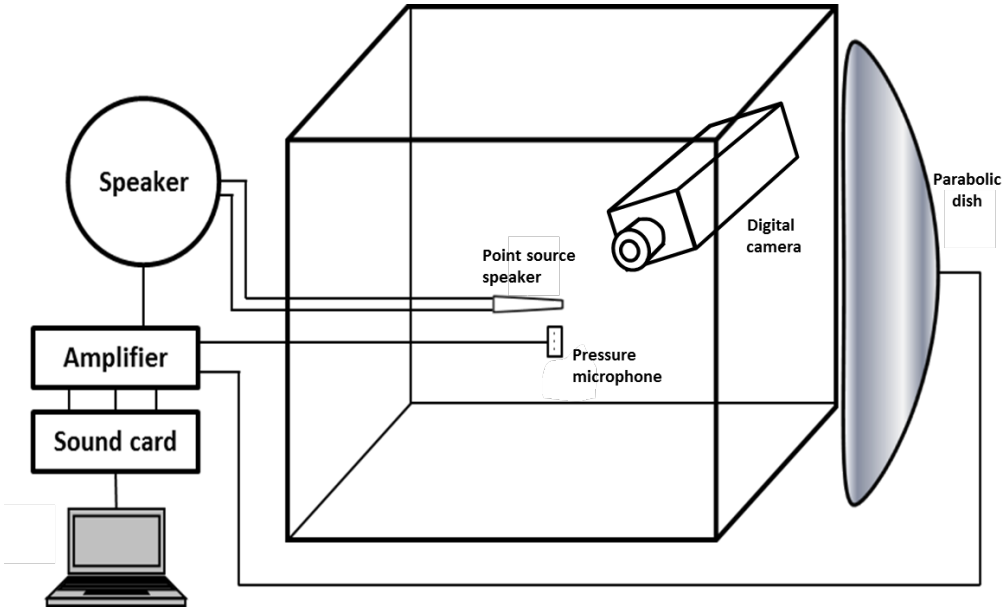

Figure 4.2. Behavioural flight arena. For simultaneous video/ audio recordings, the metal frame (4 mm stainless steel cubed frame [30 cm^3]) was covered with matt-black cotton fabric which is non-reflective to infrared (IR) light, while the front side was covered by transparent acrylic enabling the camera to view the interior of the chamber. The ceiling was covered with white cotton gauze to allow the chamber to be illuminated by two IR multi-LED lights positioned 1 m above the cage. Acoustic stimulation was delivered through a 7 mm plastic tube as a point source, coupled via the tubing to a speaker located outside of the arena. A pressure-difference microphone was positioned within 30 mm of the point source to measure responses close to the stimulating speaker. An additional pressure-difference microphone was housed in a parabolic reflector to measure WBFs away from the point source speaker. All recordings and acoustic stimulation were made using a laptop via a sound card and amplifier (sampling rate of 48 kHz).

between 161 and 3510 ms (mean: 1479±94 ms). A likely cause of the variable latency period is that the mosquito was too far from the speaker to detect the sound, and only begins a response when in hearing range of the speaker (Figure 4.1). The onset (2) of the acoustic response marked the beginning of phonotaxis to the sound source, as confirmed by video recordings. Coincident with phonotactic responses recorded with

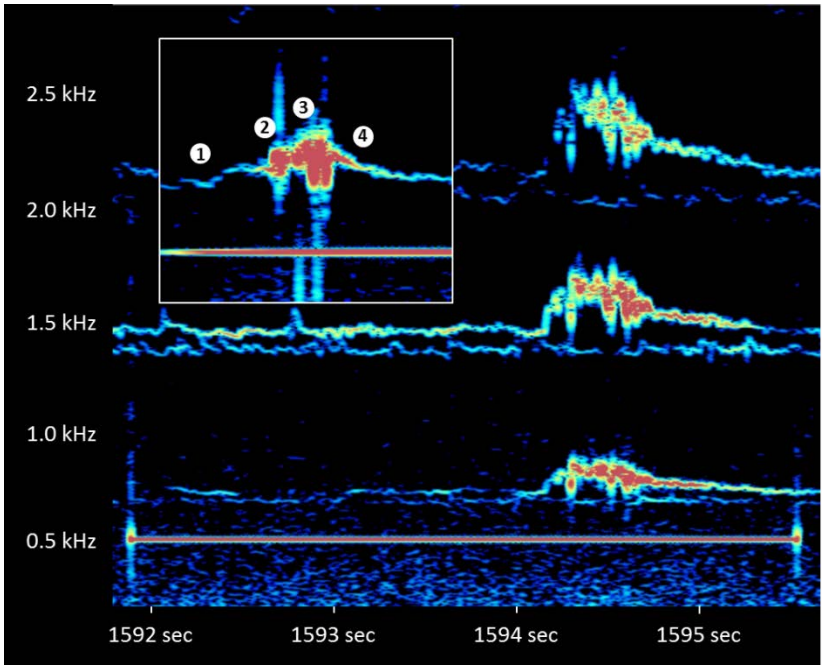

Figure 4.3. Typical acoustic response of a male mosquito to a pure tone from a point source speaker. Spectrogram of the fundamental WBF of a male mosquito and a constant sine wave stimulus at 520 Hz with a cosine onset and offset (bottom trace). The typical acoustic response is enlarged in the inset, which is separated into four acoustically distinct components. (1) Latency, (2) Onset, (3) Rapid frequency modulation (RFM), and (4) Offset. Data collected by Patrico Simões.

the camera, the response was characterised acoustically by a swift increase in WBF of 85 ± 3 Hz in 327 ± 37 ms, equivalent to a rate of change of ~260 Hz·s^{-1}. The onset phase was followed by the RFM phase, which lasted 1148 ± 79 ms, and occurred when the mosquito was within ~4 cm of the sound source.

During the RFM phase it was observed, when flying in close proximity (~4 cm or less) to the sound source, male mosquitoes would display a series of short, tight loops around the point source, even attempting to grasp the plastic tubing protruding out from the side of the cage. During the RFM phase, the frequency bandwidth of the WBFs increased to 87 ± 6 Hz compared with a bandwidth of 25 ± 1 Hz measured during the latency phase (Unpaired Student's *T-test*, t=12.31, N=30, P<0.001). Based on video recordings, the offset phase coincided with male flight away from the speaker (Figure 4.1), which lasted 1246 ± 63 ms.

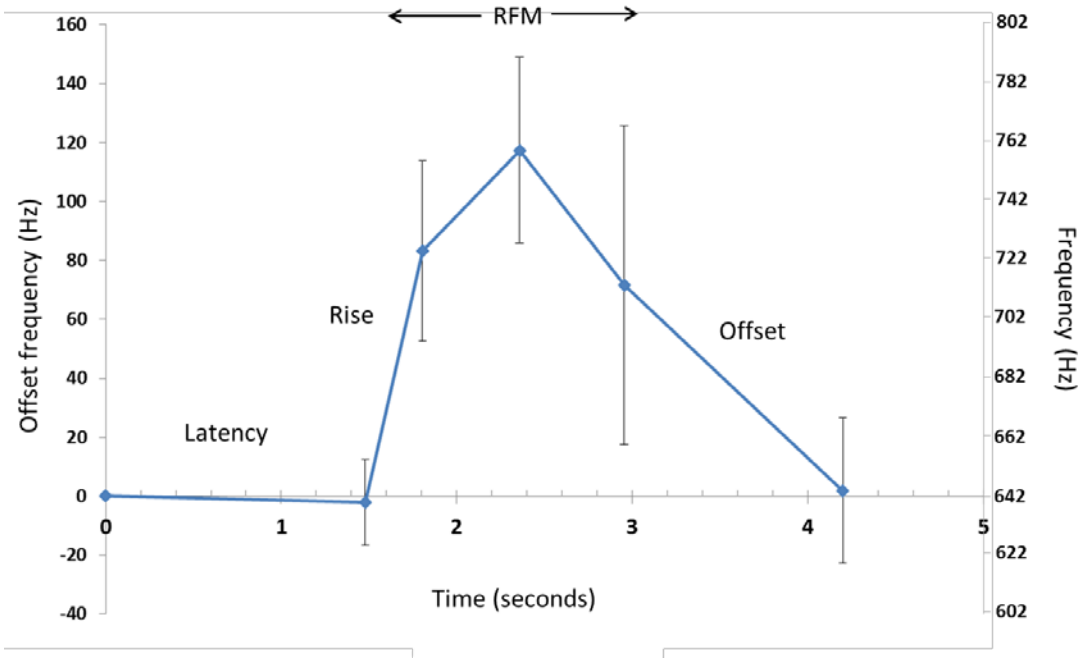

Figure 4.4. Quantitative analysis of the characteristic acoustic response (n=68). Time 0 indicates the start of the stimulus tone. Frequency at time 0 shows mean WBF during latency (offset = 0). The left scale (offset frequency) is the WBF difference in relation to the frequency at time 0. Data collected by Patrico Simões.

In contrast, no conspicuous phonotactic or RFM behaviour was observed in virgin free-flying females (N=7), stimulated with 5-second pure tones with frequencies ranging from 200-2000Hz at the same particle velocity level as males.

Frequency tuning of RFM behaviour of males

Free-flying males were stimulated with pure tones to determine the range of frequencies to which males exhibited RFM (mean PVL $5.7x10^{-5} \pm 1.94x10^{-6}$ ms^{-1}, n=23). Free-flying male mosquitoes exhibited the RFM behaviour only to tones between 280-640 Hz. Within this range, more than 75% of the tested males exhibited a response to tones between 340-540 Hz (Figure 4.5, n=13). The frequency range over which males display RFM behaviour encompasses the WBF ranges of conspecific free-flying female mosquitoes (430-527 Hz, n=30). To test the repeatability of the RFM behaviour within individuals, each free-flying male (n=7) was presented with

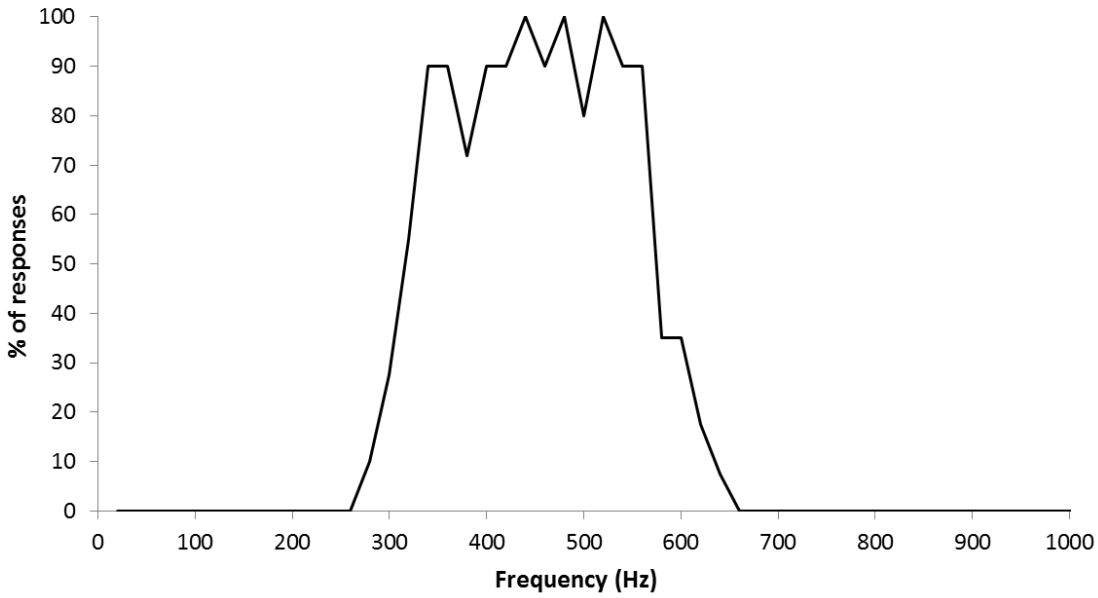

Figure 4.5: Percentage of free-flying male mosquitoes (n=13) displaying RFM as a function of the stimulus frequency (10-second pure tones at a PVL of $5.7 \times 10^{-5} \pm 1.94 \times 10^{-6}$ ms^{-1}; n=23). Frequencies up to 2500 Hz were tested, but no responses were detected below 250 Hz, or above 650 Hz. Each of the 48 tones were presented randomly and only once to each male mosquito. Data collected by Patrico Simões.

seven consecutive 460 Hz pure tone stimuli (10 s duration, inter-trial interval of 5 s). Males responded with RFM to 95.9 ± 2.63 % of the seven consecutive 460 Hz pure tones (5 out of 7 mosquitoes responded to all presentations) with no responses to 860 Hz tones.

Particle Velocity Level threshold to elicit RFM behaviour

The behavioural threshold is the minimum particle velocity level to elicit RFM in swarming males. The frequency specificity of RFM behaviour was determined by playing pure tones across a range of frequencies to six swarms of 7-10 males (Figure 4.6). The PVL of the speaker was increased at a rate of 0.4 dB s^{-1} from $\sim 1 \times 10^{-8}$ ms^{-1} until an RFM response was detected from at least one male or until the PVL reached

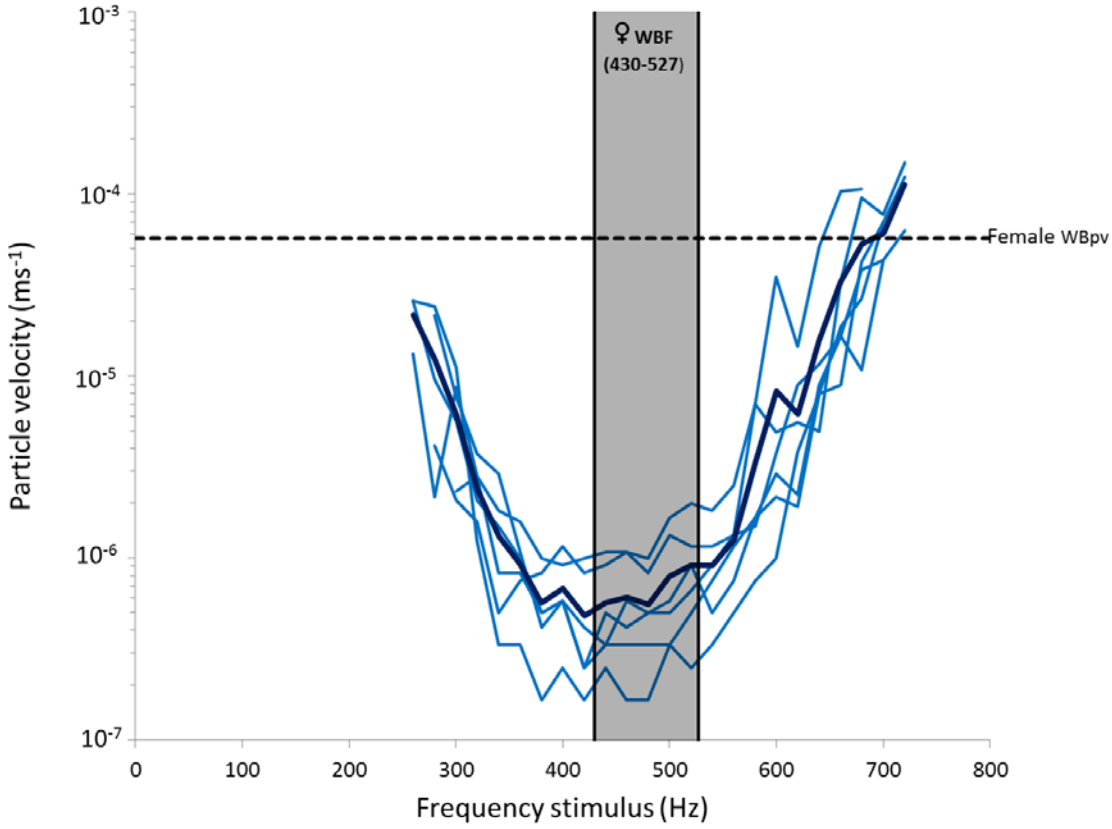

Figure 4.6: Behavioural threshold frequency tuning curve at 30 °C. The PVL at which male mosquitoes displayed RFM to pure tones, which increased in amplitude at 0.4 dB·s^{-1} (Individual responses, thin light blue and mean response, thick dark blue. The range of the female WBF depicted by the grey box. N=6. This procedure was repeated across a range of frequencies with a 5-10 s gap between pure tone presentations. All PVL values were calculated relative to a reference distance of 2 cm in front of the sound source. Data collected by Patrico Simões.

4x10^{-4} ms^{-1}. The particle velocity level that elicited the RFM and the WBF of the male at response onset were both recorded.

The most sensitive responses were elicited at frequencies between 340-560 Hz (ANOVA $F_{1,23}=14.64$, $P<0.001$), thus encompassing the range of WBFs for conspecific free-flying female mosquitoes (grey shaded area, Figure 4.6). Lower and upper frequency responses were recorded as far as 260 Hz and 720 Hz. Tone frequencies between 340 and 560 Hz elicited responses at the lowest thresholds

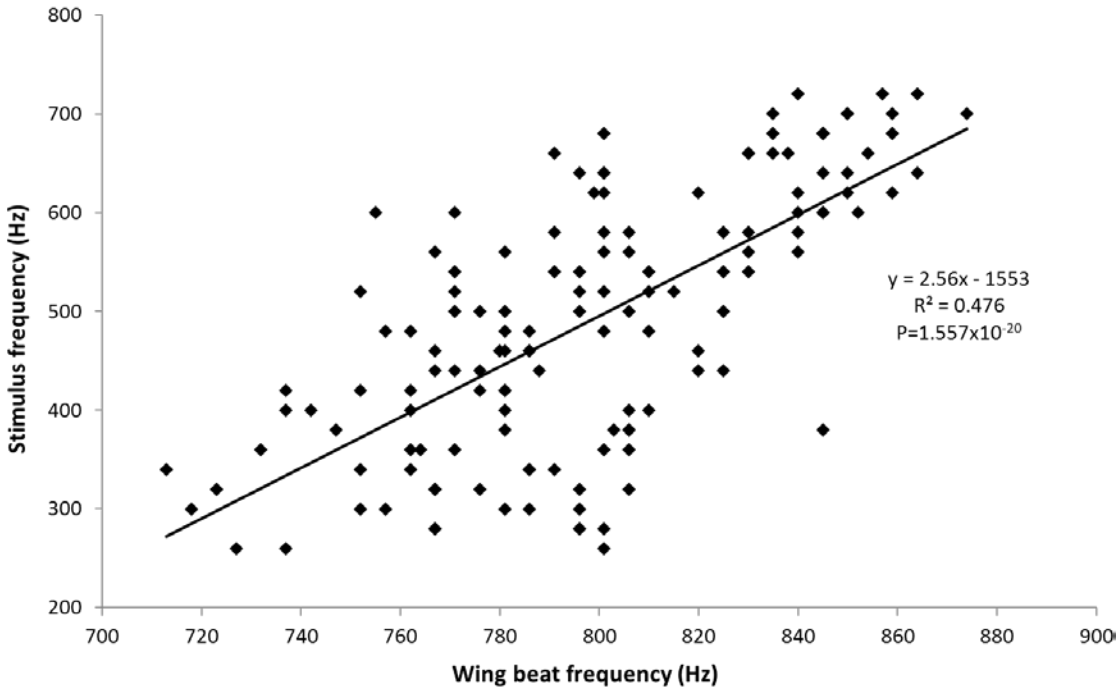

Figure 4.7: The relationship between the WBF of males and the sound source stimulus frequency (R^2=0.476, Stimulus=2.56x ♂WBF-1553; Pearson's r=0.69, F= 8.1 x $10^{-20,}$ p=1.557x10^{-20}). Data collected by Patrico Simões.

(ANOVA F1,23=14.64, P<0.001), and encompass the range of WBFs for conspecific free flying female mosquitoes (430–527 Hz, 492±4 Hz, N=30; Figure 4.6 grey shaded area). The positive correlation between the WBF (as measured at the onset of the RFM behaviour of the responding males) and the frequency of the stimulus tone shows that lower frequencies of stimulation are most likely to elicit responses from males with a lower WBF, and higher frequencies elicit responses from males with a higher WBF (Figure 4.7).

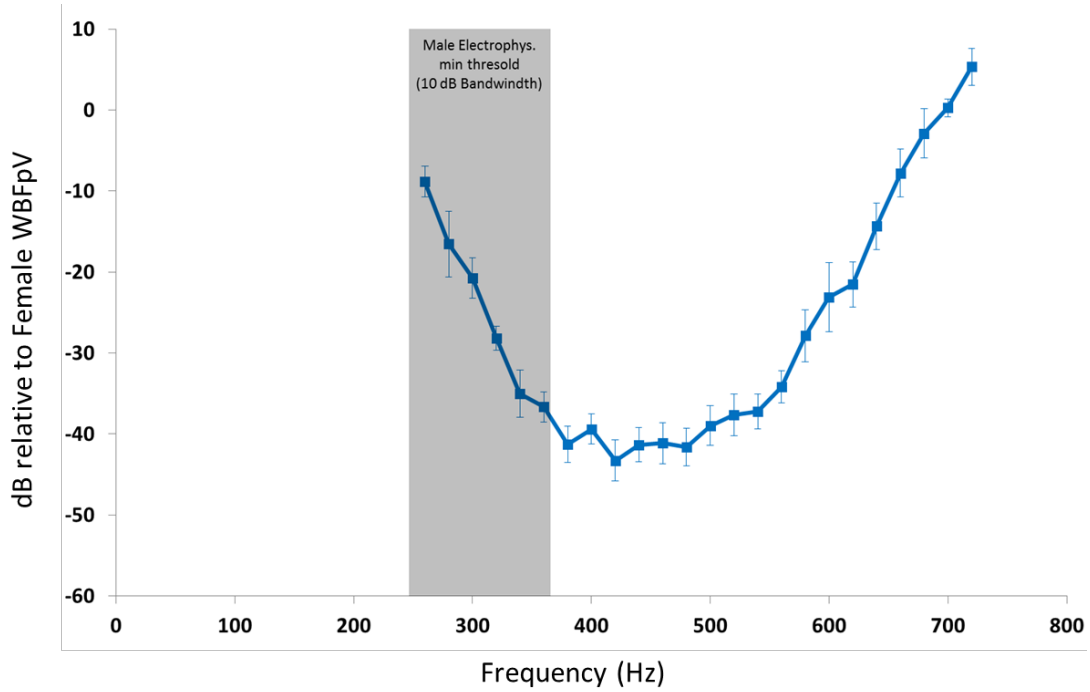

Figure 4.8: Behavioural threshold (expressed in dB PVL relative to the particle velocity of the female WBF (♀WBpV) from Figure 4.6) of the RFM response as a function of stimulus tone frequency. Grey bar: 10 dB bandwidth of JO compound potential tuning curve (Figure 3.1). Behavioural data collected by Patrico Simões.

3.2.3 Discussion

This chapter reveals a unique and repeatable phonotactic behaviour of free-flying male mosquitoes characterised by stereotypical changes in his WBF when stimulated with sounds that mimic the female WBF. This characteristic auditory-driven motor response was then used to derive a behavioural tuning curve, which was compared to tuning of the JO. Previous insight to mosquito auditory-driven behaviour has so far been derived from free-flight phonotactic recordings (Wishart and Riordan 1959) and tethered recordings of harmonic convergence in three haemophilic mosquitoes (Cator, Arthur et al. 2009, Warren, Gibson et al. 2009, Pennetier, Warren et al. 2010).

Wishart and Riordan (1959) measured the response rates of free-flying *Ae.aegypti* male mosquitoes when stimulated with artificial pure tones, and reported maximum responses of 56% at 550 Hz. These response rates are considerably lower than the

response rates reported here. Wishart and Riordan (1959) stimulated 5 second pure tones through a 4.8 cm aperture, attached to a vacuum, which would collect the attracted mosquitoes. The experimental conditions used by Wishart are likely to have resulted in a lower behavioural response, with half the duration of acoustic stimulation, in comparison to stimulation used in this chapter, and the complicated behavioural arena, with free flying mosquitoes only able to detect the stimulation when in line with the speaker and the aperture. The experimental paradigm in this chapter allowed the mosquitoes to detect the stimulation as long as they were within hearing range of the sound, and from all angles. *Ae.aegypti* female mosquitos' swarm at 426 Hz but Wishart's experiments show that male mosquitoes are most attracted to tones 124 Hz higher, whereas the mosquitoes here responded more sensitively to frequencies inside the female swarming WBF (Figure 3.1). The repeatability of RFM behaviour was high at 460 Hz, which represents a typical female WBF (Figure 4.5) however, when the duration of the stimulation was reduced to 1 second, the proportion of males responses was still 45±7.26 %, comparable to Wishart's (1959) rate of responses to 5 second tones. Although significantly lower than the proportion of response to 10 second stimulation, 1 second stimulation reinforces the robustness and speed of this pre-mating behaviour.

Male mosquitoes performed phonotaxis and changed their WBF to both tethered flying female and pure tones from a loud speaker with no noticeable difference. Analysis of the mosquitoes known phonotactic responses combined with analysis of their acoustic responses, shown to be important in sexual behaviour and/or mate selection, help us understand mosquito mating behaviour (Kahn, Celestin et al. 1945, Roth 1948, Cator, Arthur et al. 2009, Warren, Gibson et al. 2009, Pennetier, Warren et al. 2010). In the last decade, auditory-driven behaviour of mosquito flight was studied using tethered mosquitoes (Gibson and Russell 2006, Cator, Arthur et al. 2009, Warren, Gibson et al. 2009, Pennetier, Warren et al. 2010). Tethered flight has been known to distort insect WBF, as described in **Chapter one** (Fry, Sayaman et al. 2005), and prevented the mosquito's ability to move freely in a 3D environment, and free-flight studies have been limited in their interpretation of mosquito behaviour, largely due to the lack of video recordings and/or audiograms. The analysis presented

here shows that male mosquitoes, during phonotactic behaviour, display a very distinct and repeatable auditory response. This behaviour is likely to have some sexual context despite not being directly related with the formation of a copula.

Male *Cx. quinquasciatus*, which fly at low frequencies, tend to respond to low frequency stimulation, while mosquitoes that fly at high frequencies, respond preferentially to higher frequencies (Figure 4.7). This strong correlation suggests that the detection of female-like tones (and consequently the expression of RFM) by male mosquitoes is dependent on their own WBFs, as shown to be the case for harmonic convergence in three mosquito genera (Cator, Arthur et al. 2009, Warren, Gibson et al. 2009, Pennetier, Warren et al. 2010). WBF is correlated with body size, which can be influenced by food treatment during the larval phase, with an increased body size resulting in lower WBF (Belton 1986, Ogawa et al. 1986, Reiskind et al. 2012, Cator et al. 2016). Mating success is increased for pairs of the same size, thought to be driven by interactions between large female and males (Cator and Zanti 2016), although it is believed that male size is an important determinant of fitness (Benjamin et al. 1994) and larger males generally achieve an increased rate of reproductive success (Roff 1977, Yuval et al. 1993).

The purpose or function of the male's acoustic behaviour, and the RFM flight in particular, could represent i) a consequence of specific movements of the front and middle legs while first stretching forward and then grasping the sound source (Roth 1948, Charlwood and Jones 1979); ii) a controlled flight behaviour which maintains males in flight while attempting to seize and engage terminalia with the female (Charlwood and Jones 1979); or iii) a sexual signal to the nearby female. Equally, it is also possible to rule out some roles of RFM behaviour. Free-flying female mosquitoes do not engage in any sexual behaviour when presented with a tethered male, and the tethered males do not engage in RFM behaviour when the female flies within 4 cm.

The JO of male mosquitoes is tuned to frequencies around 280 Hz, and thus to frequencies ~150 Hz below the flight tones of free-flying female mosquitoes (**Chapter one**). The behavioural audiogram here (Figure 4.6) is matched with the female WBF. When comparing the behaviour threshold data from Figure 4.6 and the

10 dB bandwidth of the JO from **Chapter One**, there is a clear mismatch (Figure 4.8). It therefore remains puzzling why the frequency tuning of the JO is mismatched to the female WBF. The 10 dB JO bandwidth (245 – 360 Hz) and most sensitive behavioural responses (340 – 560 Hz) do overlap, but only at the extremes.

3.3 Chapter three: The JO of male mosquitoes is tuned to an acoustic distortion product

3.3.1 Introduction

Male mosquitoes, including *Aedes aegypti, Anopheles gambiae* and *Culex quinquefasciatus,* aggregate in swarms and detect and locate the wing beats of approaching females (Roth 1948, Gibson 1985, Belton 1994, Clements 1999). The female's wing beats are detected by the males Johnston's organ, which provides spatial information to the male (Clements 1999). The male locates and gives chase to the female until he grasps her mid-flight; if successful, a mating copula is formed (Roth 1948). The sound-capturing flagellum pivots about its base at the same frequency of a pure tone acoustic stimulus (Göpfert, Briegel et al. 1999). These flagellar vibrations are transmitted to the JO at the frequency of the female WBF, however the JO compound potentials occur at a frequency component at twice that of the stimulus, so-called frequency doubling. Frequency doubling is thought to reflect the activation of opposite groups of sensory neurons at opposing sides of the JO stretched once every period (Belton 1974, Clements 1999, Göpfert, Briegel et al. 1999, Göpfert and Robert 2000, Jackson et al. 2009).

In response to pairs of tones, mimicking the male's own flight tones and those of a nearby female, the flagellum vibrates not only at the two tone frequencies but also at distortion products (Göpfert and Robert 2000, Göpfert and Robert 2001, Warren, Gibson et al. 2009, Pennetier, Warren et al. 2010, Mhatre et al. 2013). Distortion products are produced by a nonlinear system through the mixing of two input signals and are found in every acoustic receiver so far tested (reviewed in Whitehead et al. (1996)). The largest distortion product in tympanal ears are 2f1-f2 (where f1 and f2 represent two stimulus frequencies where f1<f2) (Kemp 1979, Rosowski et al. 1984, Coro et al. 1998, Kössl et al. 1998, Van Dijk et al. 2006, Möckel et al. 2007). In the mosquito flagellum, the largest distortion product is f2-f1 (Warren, Gibson et al. 2009). Acoustic distortion products measured mechanically at the flagellum are also transduced into compound neural potentials by the JO (Cator, Arthur et al. 2009, Jackson, Windmill et al. 2009, Warren, Gibson et al. 2009, Pennetier, Warren et al. 2010). Thus, mosquitoes detect distortion products, which is thought to aid harmonic

convergence (Cator, Arthur et al. 2009, Warren, Gibson et al. 2009, Pennetier, Warren et al. 2010). This is evidenced by measurements of low frequency (<30 Hz) f2-f1 distortion products between the higher order harmonics to which the mosquitoes matched. Although these low-frequency distortion products were transduced, unlike the high frequency tones that produced them, they lie in an insensitive low frequency region of the JO's frequency response (Warren, Gibson et al. 2009).

In this chapter, I test the hypothesis that the male JO is tuned, not to female WBF itself, but instead to the frequency difference between the fundamental WBF of male and female. This may explain the mismatch in tuning of the male JO to the female free-flight WBF (**Chapter one**). The f2-f1 distortion product was calculated based on measurements of the free-flight WBF of male and females mosquitoes. In addition to plotting the measured f2-f1 distortion product, I measured its level and frequency dependence.

3.3.2 Results

The JO of male mosquitoes is tuned to difference tones generated through interaction between male's and female's WBF

Compound JO potentials were recorded in response to pairs of pure tones. The first tone, f1, mimicked the flight-tone of a nearly female and varied in frequency and level. The second tone, f2, mimicked the frequency and sound level of the male's own WBF and was therefore fixed in frequency and level (795.8 Hz, 4.3×10^{-3} ms^{-1}). An example of the distortion product (f2 – f1) in the JO compound potential is shown in Figure 5.1. Note: during no stimulation and stimulation, spontaneous oscillations (SOs) are present in all healthy mosquitoes (Warren et al. 2010). The nature and function of SOs are still unknown.

The behavioural audiogram from Figure 4.8 (**Chapter two**) was re-plotted as a function of the frequency difference between the WBFs of male mosquitoes just prior to the onset of their RFM behaviour and the tone stimulus (Figure 5.2). Based

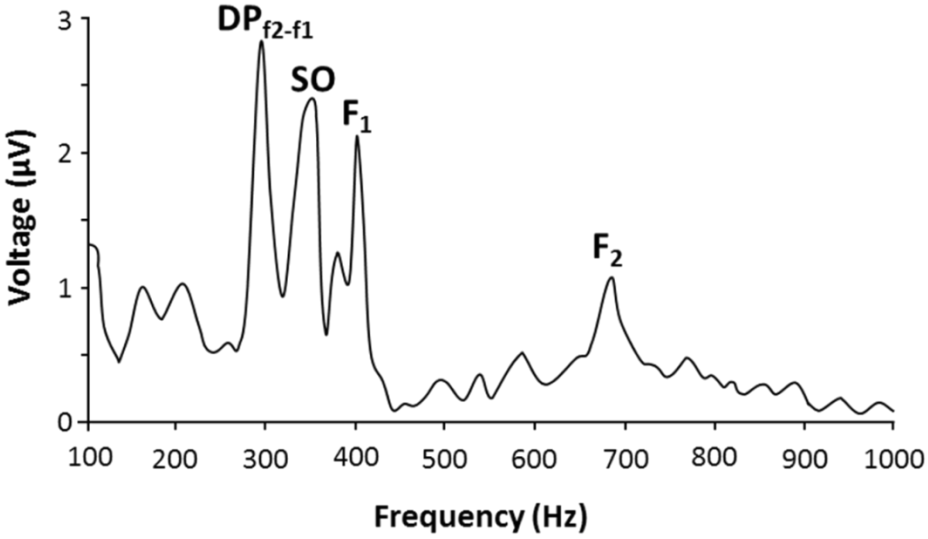

Figure 5.1: Frequency spectrum of the JO compound potential when stimulated by two tones (f1=400 Hz and f2=696 Hz) delivered through separate speakers. The JO compound potential has peaks in its frequency spectra at f1, f2 and at the f1-f2 distortion product (696 – 400 = 296 Hz). Spontaneous oscillation are indicated by SO.

on the quadratic curve, fitted to the behavioural audiogram (dB=0.001f^2–0.689f +77.81; R^2=0.761, F_2=211.9, P<0.001; dB, threshold relative to ♀WBpv; f, frequency), the 10 dB bandwidth extended between 244 and 444 Hz (Figure 5.2). This behavioural sensitive range is in close relation to the 10 dB bandwidth of the JO (Figure 5.2, grey bar), with the most sensitive point of the quadratic curve being inside the JO sensitive range, whereas the behavioural responses as a function of the stimulus frequency are grossly mismatched (**Chapter two**).

The amplitude of the f2-f1 distortion product of the JO compound potential depends on both the frequency and level of the female flight tone (f1) (Figure 5.3). An increase in the particle velocity level of f1 leads to an increase in the JO compound potential. The DP frequencies that would be produced within the range of free-flight WBFs (measured in **Chapter one**) of male and females are between 430 and 527 Hz. Within this range of distortion products (DPs; 319.7 [turquoise] and 368.6 [green]) responses are >100 times more sensitive and tend to saturate at high stimulus levels (Figure 5.3). DPs that would be produced with free-flight WBF which are uncharacteristically

low (<250 Hz, DP; 551.7 [orange] and 698.1 [red]), slopes have a weak dependence on the PVL. DPs that would be produced with free-flight WBF which are uncharacteristically high (>550 Hz, DP; 246.7 [blue] and 148.8 [black]) produced slopes with a logarithmic dependence on PVL.

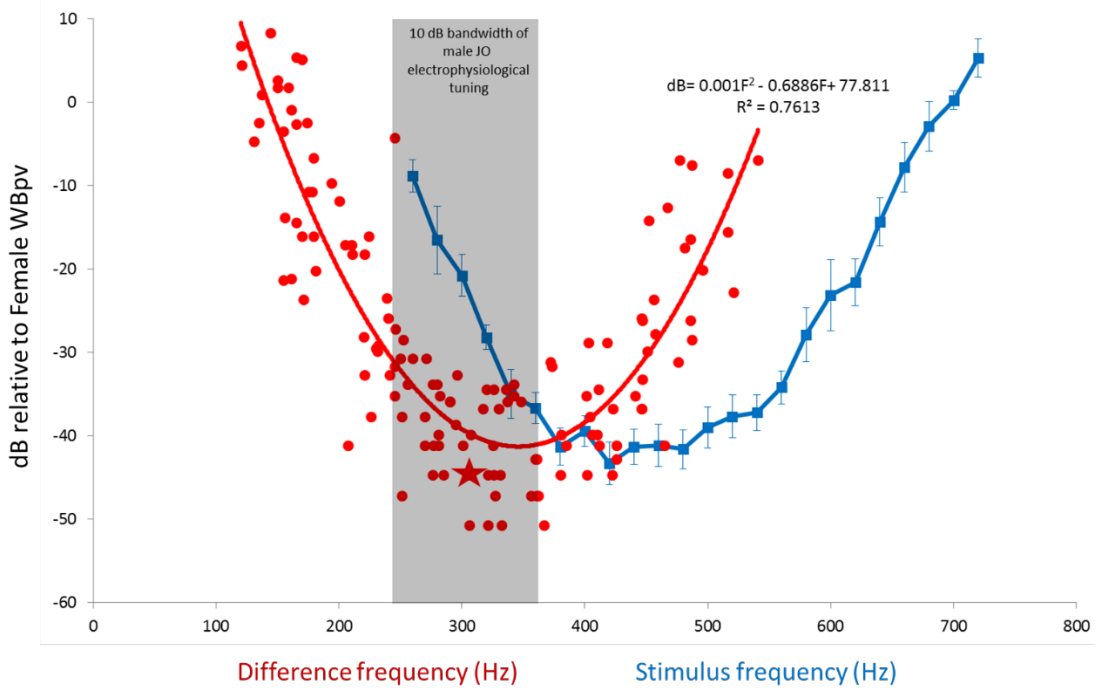

Figure 5.2: Threshold frequency tuning of the RFM response as a function of the f2-f1 distortion product. The distortion product (red) was calculated by taking the difference between the stimulus tone frequency (blue) and the males' WBF (measured before the onset of the acoustic behaviour). Threshold is expressed in dB relative to the ♀WBpV from Figure 4.3. Example of difference frequency response (red star); 786 Hz [WBF] – 480 Hz [stimulus tone frequency] = 306 Hz [distortion product]. Grey bar: 10 dB bandwidth of JO compound potential tuning curve, as a function of stimulus frequency. Behavioural data collected by Patrico Simões.

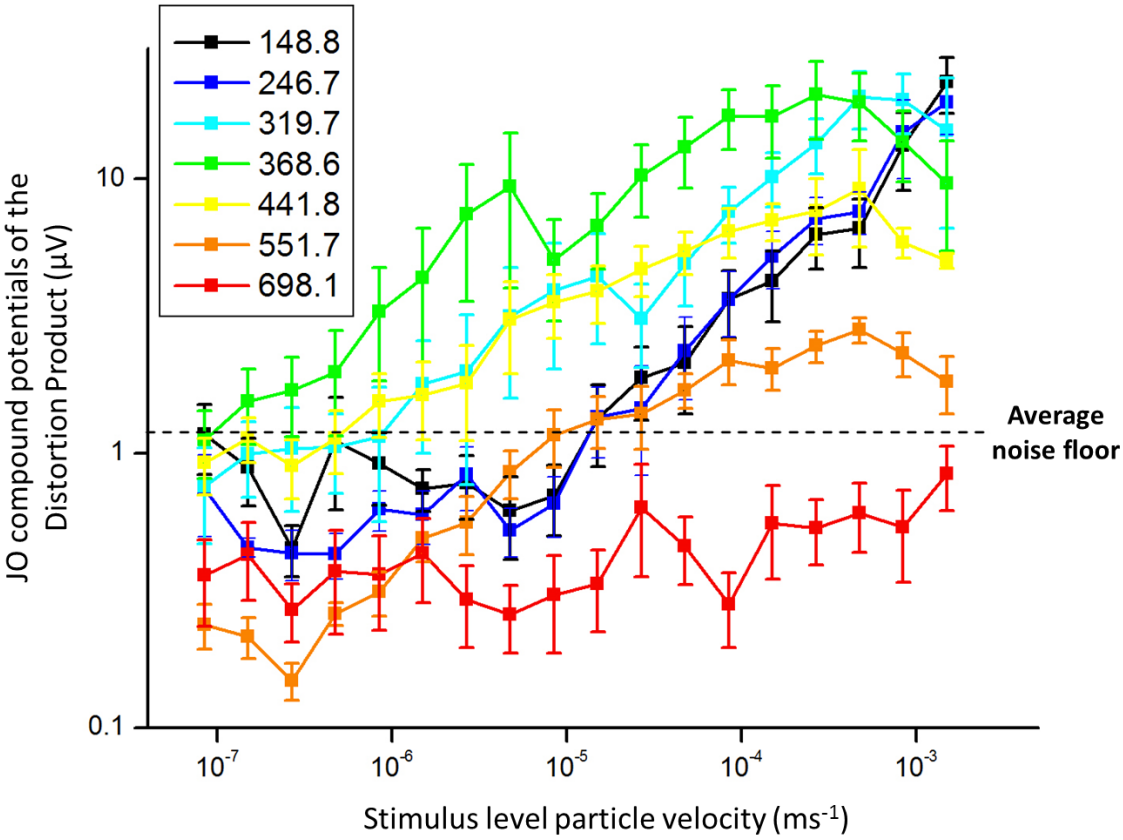

Figure 5.3 Magnitude of the f2-f1 distortion product JO compound potential as a function of stimulus level of f1. Different frequencies [f1] are shown in the key (in Hz) and a second tone [f2] was of constant frequency, 795.8 Hz and particle velocity level, 4.3x10-3 ms^{-1}. N=9, mean ± SE.

The quadratic curve from Figure 5.2 represents the predicted DPs from the free-flight WBF of male and females. This was superimposed on the iso-level plots of the magnitude of the distortion product JO compound potential as function of the f2-f1 DP (Fig 5.4). The lowest point of the quadratic curve represents the most sensitive behavioural RFM responses (~340 Hz). The predicted behavioural best frequency and the maximal JO compound potentials (368 Hz) are similar in frequency (Figure 5.4).

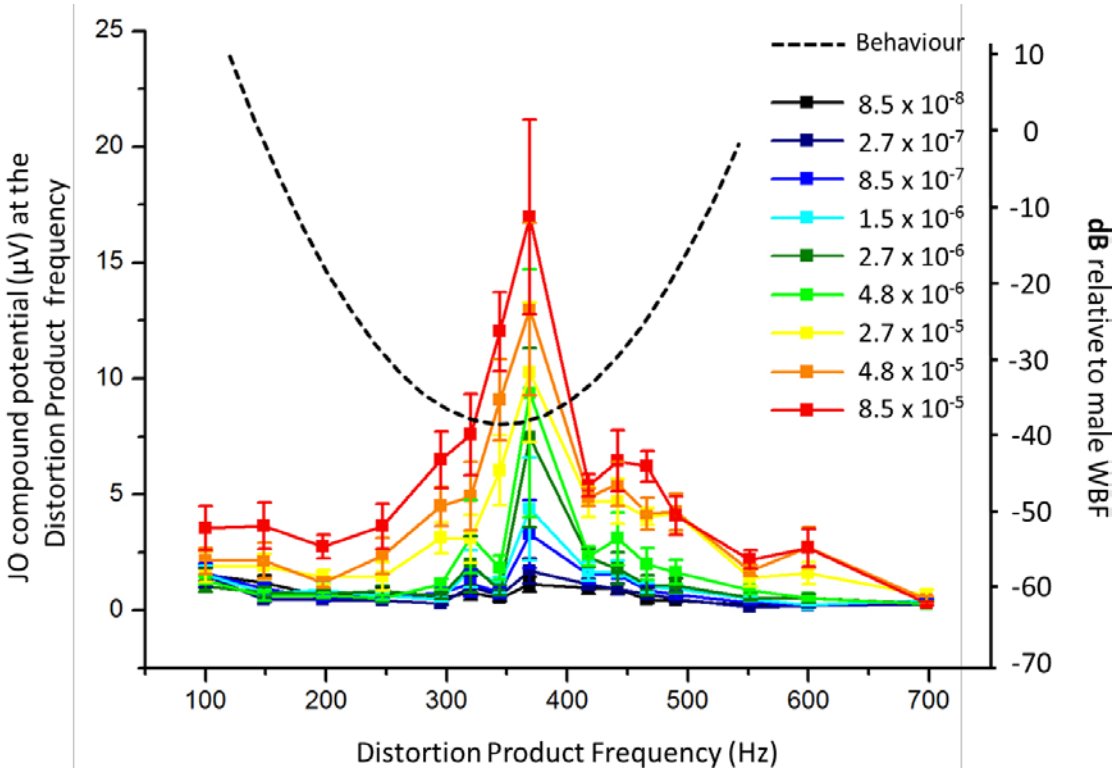

Figure 5.4: Magnitude of the f2-f1 distortion product JO compound potential as a function of the frequency of the distortion product. The frequency of f1 was fixed at 795.8 Hz and its particle velocity level (in ms^{-1}) is indicated in the key. The frequency of f2 was varied and had a constant particle velocity level of $4.3x10^{-3}$ ms^{-1}. Upon the presentation of both tones, the mechanics of the flagellum generate a unique sound, called a distortion product (see Figure 5.1). The dashed line represents the quadratic fit to the calculated f2-f1 distortion product calculated from the behavioural tuning curve in Figure 4.6 (N=9). Behavioural data collected by Patrico Simões.

3.3.3 Discussion

In this chapter, I test the hypothesis that free-flying male mosquitoes are able to detect distortion products more sensitively than the two primary tones. The two primary frequencies, f1 and f2, represent the fundamental WBF of the female and male mosquito and the f2-f1 distortion product is produced through nonlinear mixing of f1 and f2. To test this hypothesis I compared the frequency-specific behaviour

(**Chapter two**) of free-flying male *Culex quinquefasciatus*, with frequency tuning of the JO. The JO responds most sensitively to frequencies in between 250 and 350 Hz and free-flying males respond most sensitively to frequencies between 330 and 570 Hz, which highlights a clear mismatch between these two measures of auditory sensitivity.

The frequency tuning of the JO matches the frequency tuning of the predicted f2-f1 distortion product (figure 5.2). This intermodulation DP is generated in the nonlinear mechanics of the flagellar vibrations (Göpfert, Briegel et al. 1999). The electrophysiological responses recorded from the JO here are more narrowly tuned than the non-linear antennal mechanical responses that provide a source for the DPs (Warren, Gibson et al. 2009). A comparison of the responses generated in the JO of single tones outside the JO 10 dB bandwidth (female WBF – 493 Hz) compared to the difference tone between the male and female WBF (f1 – 493 Hz, f2 – 798 Hz) reveals that the difference tone is much more sensitive. Stimulating the JO with a single tone of 493 Hz requires a stimulation of 4.4×10^{-4} ms^{-1} to establish a threshold response, which is two orders of magnitude higher than the particle velocity required of the f2 frequency, in two tone stimulation (5.4×10^{-6} ms^{-1}). This provides strong evidence that male mosquitoes utilise DPs to more sensitively detect females than detecting the flight flight-tone itself.

Distortion product JO compound potentials generated by the male–female flight-tone frequency difference become compressive with increasing stimulus level. They are >100-fold more sensitive than those generated more than half an octave lower in frequency, which increase linearly with level. The appearance of compression in the DP level functions that increases with frequency and level from frequencies just below the resonant frequency, is reminiscent of non-linear compression in the active mechanics of the mammalian cochlea (Robles et al. 2001) and the bullfrog sacculus (Martin et al. 2001). This indicates possible shared principles of operation in structures that share function but differ profoundly in structure and underlying mechanisms. If male mosquitoes are utilising DPs as a means to detect female mosquitoes, they are unique in exploiting their own flight tone to more sensitively detect an approaching female than detecting the female flight-tone itself. The

predicted and calculated DPs, based on the males WBF at the onset of RFM behaviour and the stimulation tone, overlay the JO tuning which incidentally supports the hypothesis that males are using the DP to orientate and fly towards females.

The exact function of the male's RFM flight remains uncertain, but it is clearly a significant component of mosquito mating behaviour. It is likely to represent a pre-copulatory controlled flight to maintain a close-range position while attempting to seize and engage terminalia with the female (Roth 1948, Wishart and Riordan 1959, Charlwood et al. 1979) and/or a specific and open-loop sexual signal to the nearby female. Nonetheless, this highly robust and stereotypical behaviour has enabled us to further understand the sensory mechanisms by which males detect the presence of females and could provide an unusual opportunity to further investigate how mosquitoes integrate the demands of flight and orientation with those for communication and hearing during flight. The most common strategy employed to combat target mosquito species is Integrated Vector Management (IVM), which uses a two-step release model. The two-step release model implements a suppression on the mosquito population (using genetically sterile males), followed by a genetic introduction of a second line of mosquitoes which encode products that inhibit parasite development without having major fitness effects on the mosquito host. The risk of reducing the mosquito population [during suppression], is it either invites another species to replace the existing suppressed species, and continue the transmission of disease, or competition from the initial vector population, which remains. Albeit at a lower population density initially, displacement with a new vector species that remains competent is less likely than with a strategy of population suppression alone. Due to the repeatability of RFM behaviour, there is an important behavioural assessment assay for the mating fitness of laboratory bred male mosquitoes, especially in the context of quality control in programmes based on male release methods (Phuc et al. 2007, Carvalho, Costa-da-Silva et al. 2014, Lees et al. 2014, Benelli 2015, Diabate et al. 2015).

3.4 Chapter four: Temperature affects wing beat frequency and frequency tuning and spontaneous oscillation frequency of the JO of *Culex quinquefasciatus*.

3.4.1 Introduction

Ambient temperature and humidity affects the wing beat frequency (WBF) and flight performance of mosquitoes, which includes distance flown, flight duration, and flight speed (Rowley et al. 1968), for instance the WBF of *Aedes agyppti* increases 9.4 $Hz \cdot {}^{o}C^{-1}$ (Tamarina, Zhantiev et al. 1979). It is logical that temperature affects the mechanical properties of insect cuticle and the biomechanical elements, which help determine the WBF of flying insects (Machin et al. 1962, Pringle 1967). Tuning of the JO is also temperature dependent with shifts of the best frequency of 16.9 $Hz \cdot {}^{o}C^{-1}$ (Tamarina, Zhantiev et al. 1979). The physiological basis of these changes in the antennal sound-receivers of mosquitoes remains unknown; however, the temperature dependence of auditory tuning in the tympanal hearing organs of *Cicada* were due to changes in the electrophysiological properties of the auditory neurons, not mechanical responses of the tympanum. Another temperature dependent process of the mosquito JO, are spontaneous oscillations, which are thought to represent tuning properties of the JO; this provides further indirect evidence of temperature dependant tuning of the JO (Warren et al. 2010). Some Sphinx moths have the capability to stabilise their thoracic temperature within 2-3 ^{o}C whilst in free-flight, independent of the air temperature, whilst smaller moths with much larger wings can raise their body temperature up to 46 ^{o}C (Heinrich 1974). Although some large insects are able to increase their core temperature during flight, smaller insects such as *Drosophila*, have neither the flight metabolism nor evaporation can alter the body temperature sufficiently, as the body is cooled quickly by convection (Church 1959).

Although the mean temperature, in which many of the vector mosquitoes swarm in the wild, is 30 ^{o}C (Gokhale, Paingankar et al. 2013), the majority of measurements of WBF and frequency tuning of the JO were obtained at lab temperatures, between 19 and 23 ^{o}C (Göpfert, Briegel et al. 1999, Warren, Gibson et al. 2009, Arthur, Wyttenbach et al. 2010, Pennetier, Warren et al. 2010). Temperature is positively

correlated with WBF in *Aedes aegypti* and could affect JO tuning (Tamarina, Zhantiev et al. 1979). Thus, a change in temperature will influence the generation of distortion products (DPs), which could be used by males to detect female mosquitoes (**Chapter three).** Here I investigate the temperature dependence on free-flying WBF of male mosquitoes and the frequency tuning of the JO. Finally, I will characterise the temperature dependence of the phonotacitc behaviour, which represents a behavioural output of an interaction of the temperature dependence of the WBF and JO tuning.

3.4.2 Results

Temperature dependence of wing-beat frequency measured during free-flight and body temperature during flight.

To measure the WBF of swarming male mosquitoes across a range of temperatures, the flight arena (30 cm^3) was cooled to a minimum of 21.1 ^oC, and heated to a maximum of 34.9 ^oC (see materials and methods). Once cooled or heated the temperature was allowed to return to room temperature, where recordings would take place. During heating and cooling, the WBF was measured every 0.1 ^oC change in temperature (Figure 6.1). The WBF of free-flying male *Culex quinquefasciatus* increased with temperature with a strong positive correlation (Figure 6.1) [$y = 11.818x + 424.47$, $R^2 = 0.5741$, $p<2.04 \times 10^{-13}$]. WBF increased at 11.7 $Hz \cdot {}^oC^{-1}$ with a mean shift in WBF of 163 Hz over a temperature range of 13.8 ^oC (21.1 – 34.9 ^oC).

The core temperature of flying tethered mosquitoes is not influenced by prolonged tethered flight across a range of ambient temperatures between 26.7 and 32.2 ^oC (Figure 6.2). The core temperature of the mosquitoes remained at 24 – 26 ^oC throughout 10 mins of tethered flight (N=14).

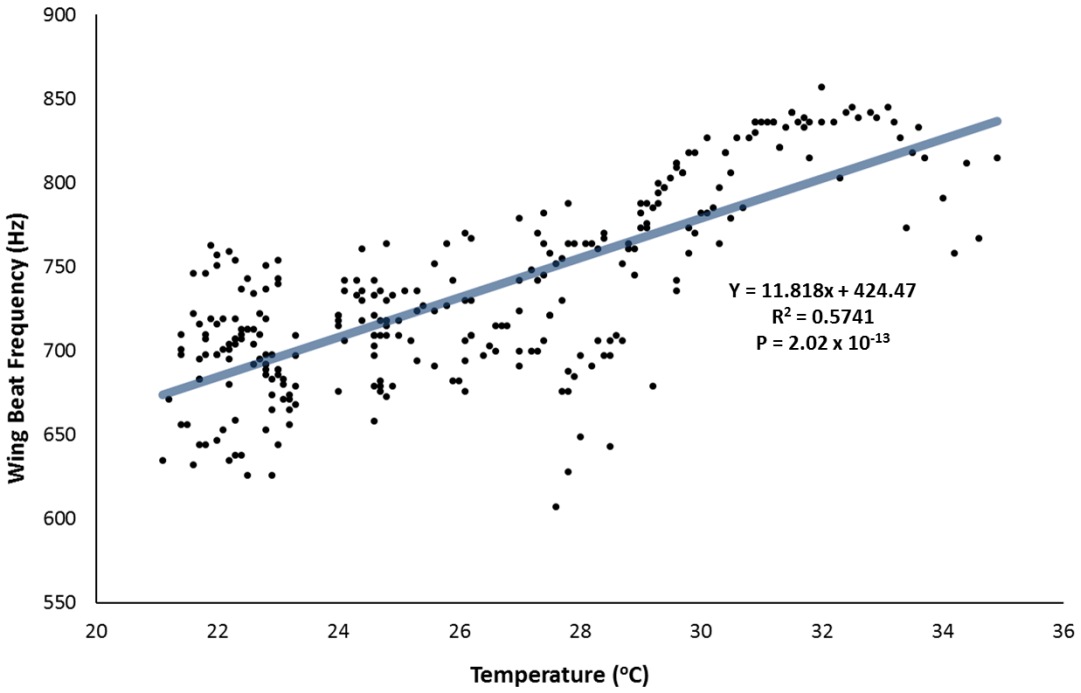

Figure 6.1: Temperature dependence of wing beat frequency during free-flight. Five sets of six mosquitoes swarmed at artificial dusk in a flight arena (30 cm^3). The flight arena was cooled to a minimum of 21.1 °C using an air conditioning unit, and heated to a maximum of 34.9 °C using a convection heater.

The frequency tuning, upper frequency range and spontaneous oscillations of the JO compound potential are positively correlated with temperature

Immobilised mosquitoes were presented with pure tones from a point source speaker at a constant particle velocity (1 x 10^{-5} ms^{-1}) at either 21 °C (Figure 6.3) or at 30 °C (Figure 6.4). A pure tone generates a compound JO potential at the fundamental frequency (f1 – Figures 6.3 and 6.4) and at multiple harmonic levels (2f1, 3f1, 4f1 etc). Compound JO potentials in response to the fundamental frequency of the pure tones at 21 °C were detected over a frequency range of 120 Hz to 400 Hz. When measured at 30 °C, the upper frequency range of responses to the fundamental of the stimulus tone extended to 580 Hz without any notable change in responses to lower frequency stimulation (Figure 6.4). Spontaneous oscillations (SOs) are present before and after acoustic stimulation but are suppressed during acoustic

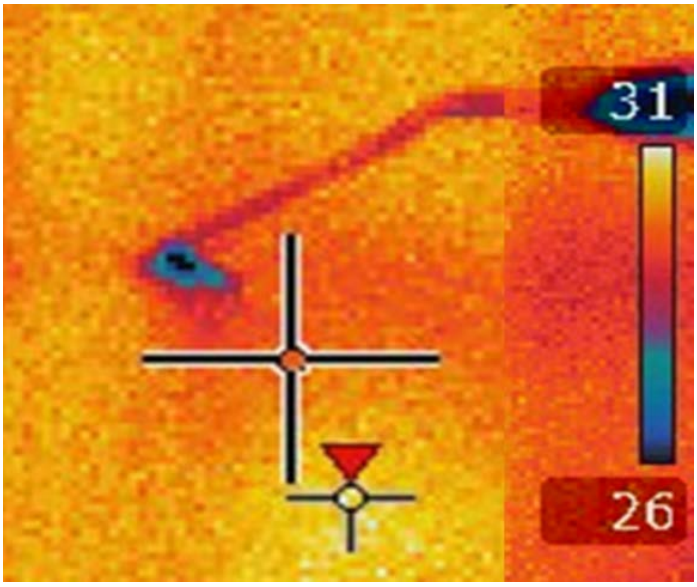

Figure 6.2: Temperature measurement of a tethered flying male *Culex quinquefasciatus* using a thermal imaging camera. The mosquito does not generate detectable heat during flight, and maintains a cooler core temperature than surrounding conditions. Temperature at crosshairs = 29.7 ^{o}C, maximum temperature = 30.6 ^{o}C, mosquito core temperature 25.3 ^{o}C.

stimulation at frequencies close in frequency to the SOs (Figure 6.3 and 6.4). When the ambient temperature is 21 °C, the SO frequency is centred on 360 Hz with strong second and third harmonics (Figure 6.3 – upper trace). The frequency of the SOs is increased to 480 Hz at 30 °C.

Threshold tuning curves of the male JO compound potential from an individual mosquito were derived at five different temperatures, which ranged from 20 – 36 ^{o}C (mean interval temperature of 4 ^{o}C ± 1.08 ^{o}C) (Figure 6.5). The best frequency of each tuning curve increased with temperature. Absolute sensitivity is defined here as the lowest stimulus level to elicit a compound potential at least 5 dB above the noise floor. At the lowest temperature (20 ^{o}C), the threshold responses were most sensitive to relatively low frequencies (135 – 140 Hz), and were relatively insensitive ($5x10^{-5}$ ms^{-1}) (Figure 6.5). When the temperature was increased, the sensitivity of the compound potentials and the frequency of the best frequency also increased. At the highest temperature (36 ^{o}C), the compound JO potentials were most sensitive and

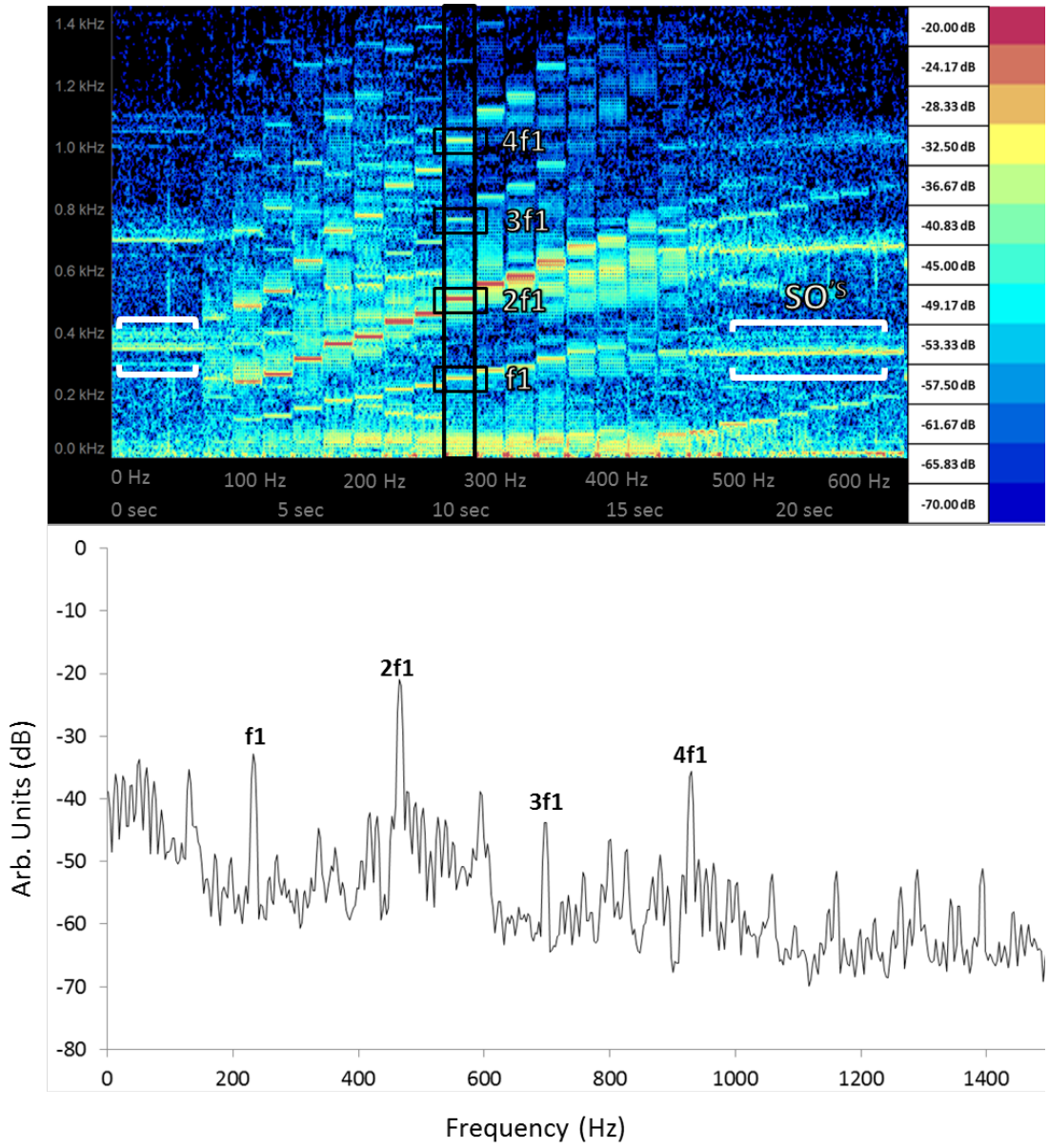

Figure 6.3: Spectrogram and frequency spectrum of the JO compound potential at 21°C. Preparation stimulated with a pure tone frequency sweep (51 – 1001 Hz in 25 Hz steps stimulating at 1 x 10^{-5} ms^{-1}). Top: Spectrograms provide a visual representation of the frequency (Y-axis) and level of the response (colour coded, Z-axis) as a function of time (X-axis). Bottom: Frequency spectrum of the period denoted by the black rectangle in the spectrogram.

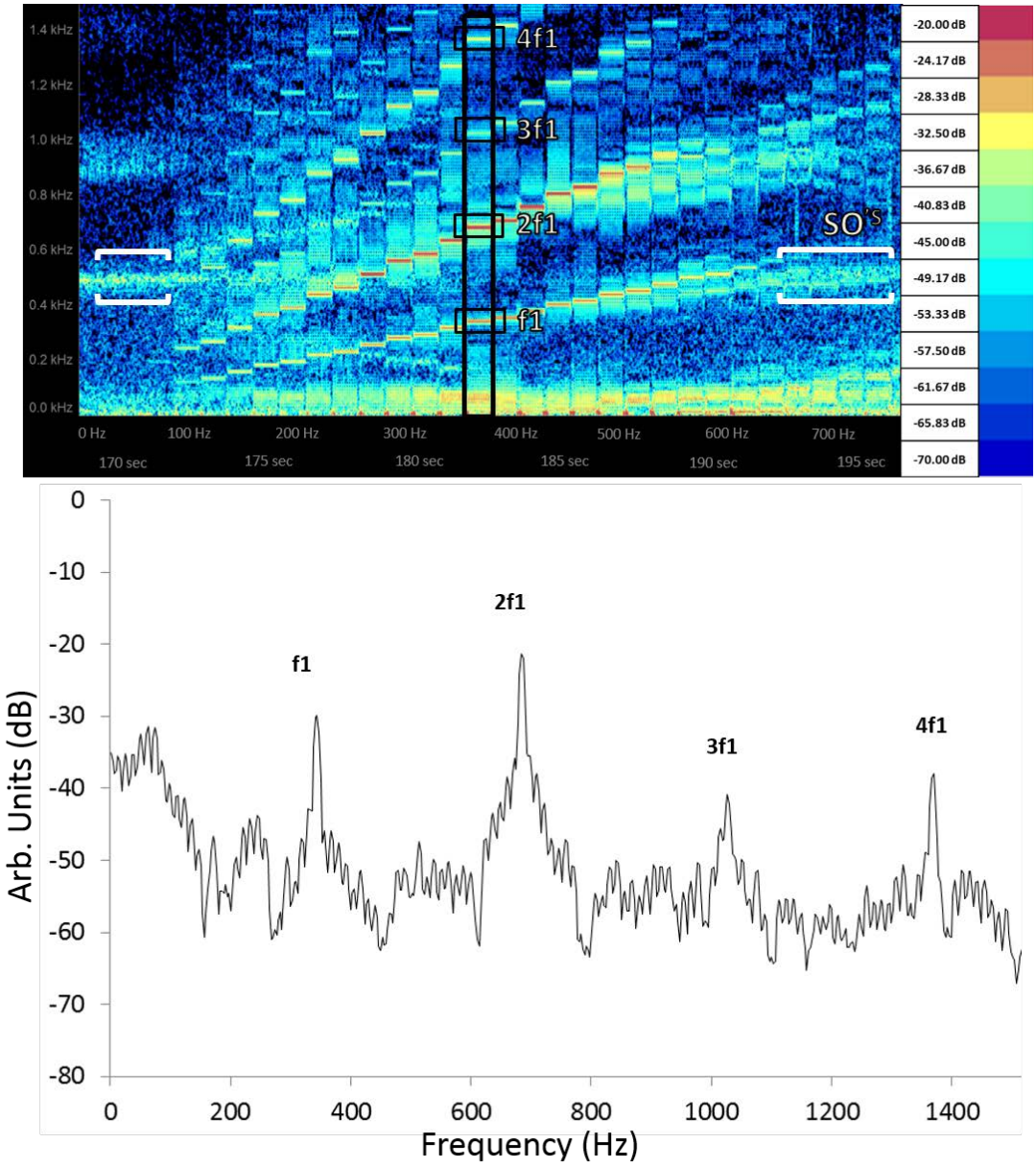

Figure 6.4: Spectrogram and frequency spectrum of the JO compound potential at 30°C. Preparation stimulated with a pure tone frequency sweep (51 – 1001 Hz in 25 Hz steps stimulating at 1 x 10^{-5} ms^{-1}). Top: Spectrograms provide a visual representation of the frequency (Y-axis) and level of the response (colour coded, Z-axis) as a function of time (X-axis). Bottom: Frequency spectrum of the period denoted by the black rectangle in the spectrogram.

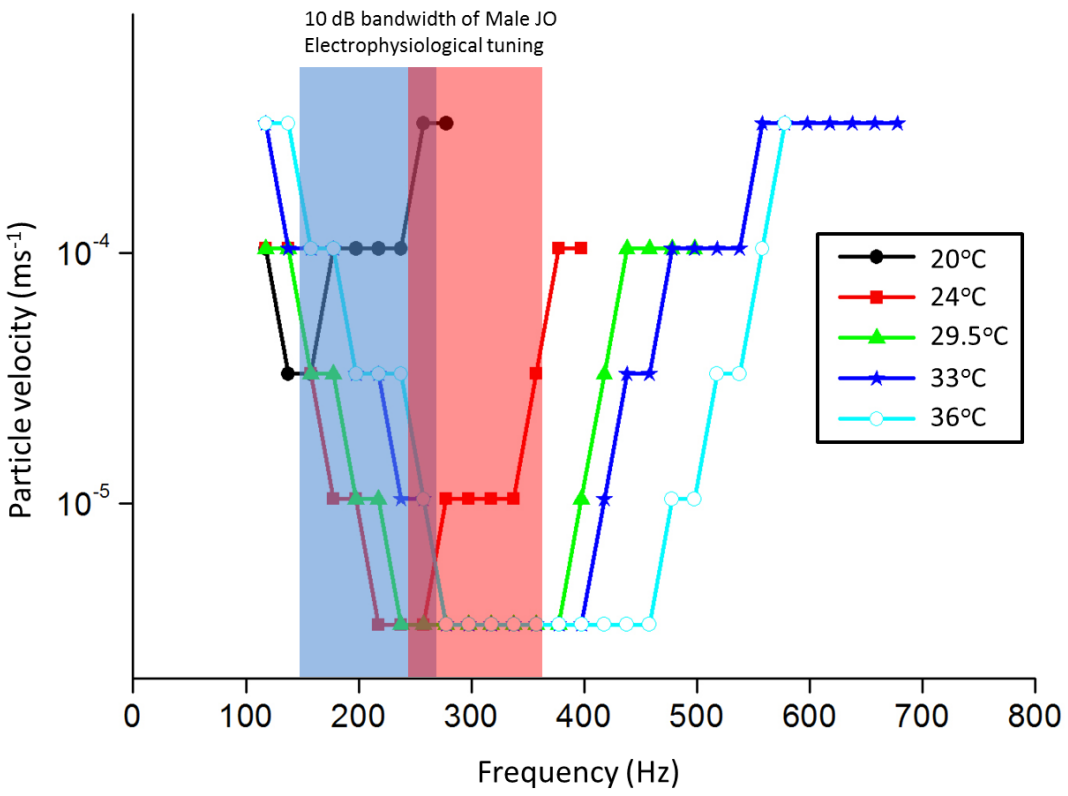

Figure 6.5: Compound JO potential threshold tuning curves of a male JO at different temperatures. Threshold responses were classified when JO compound potentials were 5 dB above the noise floor. Recordings performed at various temperatures (see key-inset [20 – 36 °C]) in an individual male mosquito. Bars indicate 10 dB bandwidth of JO tuning at 21 °C (blue [N=10]) and 30 °C (red [N=10]) under the same stimulation conditions.

the threshold frequency tuning curves were most broadly tuned; sensitive to frequencies between 280 – 460 Hz at 3.3 x 10^{-6} ms^{-1} (Figure 6.5).

For comparison, the Q_{10dB} bandwidth was derived from two quantitative JO tuning curves at 21 °C and 30 °C for 10 mosquitoes each, and plotted on Figure 6.5 (illustrated by the blue and red bars respectively). Frequency tuning of the quantitative JO tuning curve at 21 °C, responses were most sensitive to frequencies of 201 Hz with a Q_{10dB} frequency bandwidth of 125 Hz. The black line of the individual mosquito (20 °C) falls within the quantitative bandwidth (blue bar). At 30 °C the compound JO potentials derived from quantitative JO tuning are most sensitive to

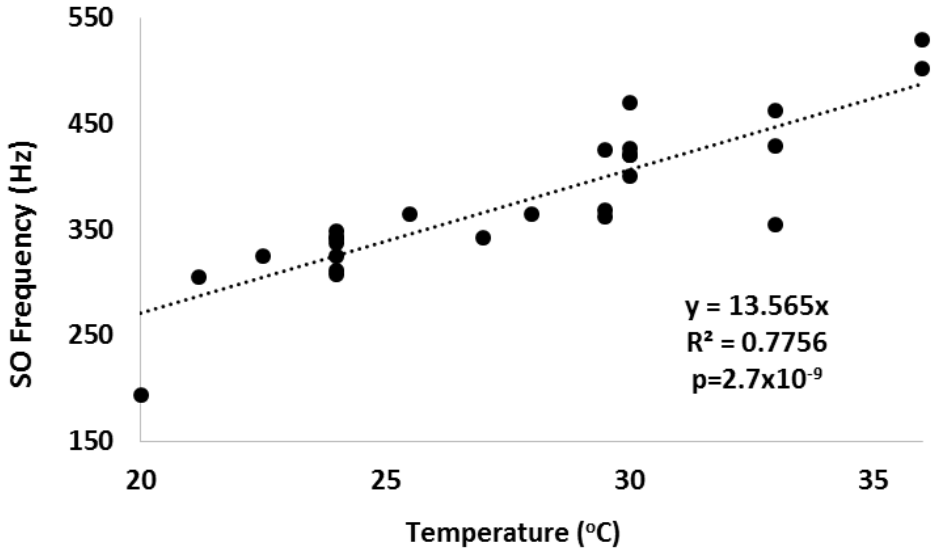

Figure 6.6: Temperature dependence of spontaneous oscillation frequency (SOs) in the absence of acoustic stimulation. SOs recorded in the JO compound potentials using sharpened tungsten electrodes. N=26.

tones with frequencies of 280 Hz and have a similar Q_{10dB} frequency bandwidth of 120 Hz. The tuning of the individual animal at 29.5 °C falls into that quantitative bandwidth (red bar). Compared to recordings at 21 °C, responses at the higher temperature (30 °C) revealed an upwards shift of the best frequency of ~80 Hz, demonstrating a shift of 13.1 Hz·°C^{-1}, which was consistent with the shift in the best frequency in the individual animal. SOs also increased in frequency at 14 Hz·°C^{-1} (Figure 6.6).

The influence of temperature on the acoustic behaviour of free flying male *Culex quinquefasciatus* mosquitoes

Six swarms of 7-10 males were released in a behavioural arena (Figure 4.2, same protocol as **Chapter two).** Pure tone were played from a loud speaker and the PVL increased at a rate of 0.4 dB s^{-1} from ~1x10^{-8} ms^{-1} until an RFM response was detected from at least one male or until the PVL reached 4x10^{-4} ms^{-1}. The mosquitoes here swarmed in the flight arena under twilight conditions under two different

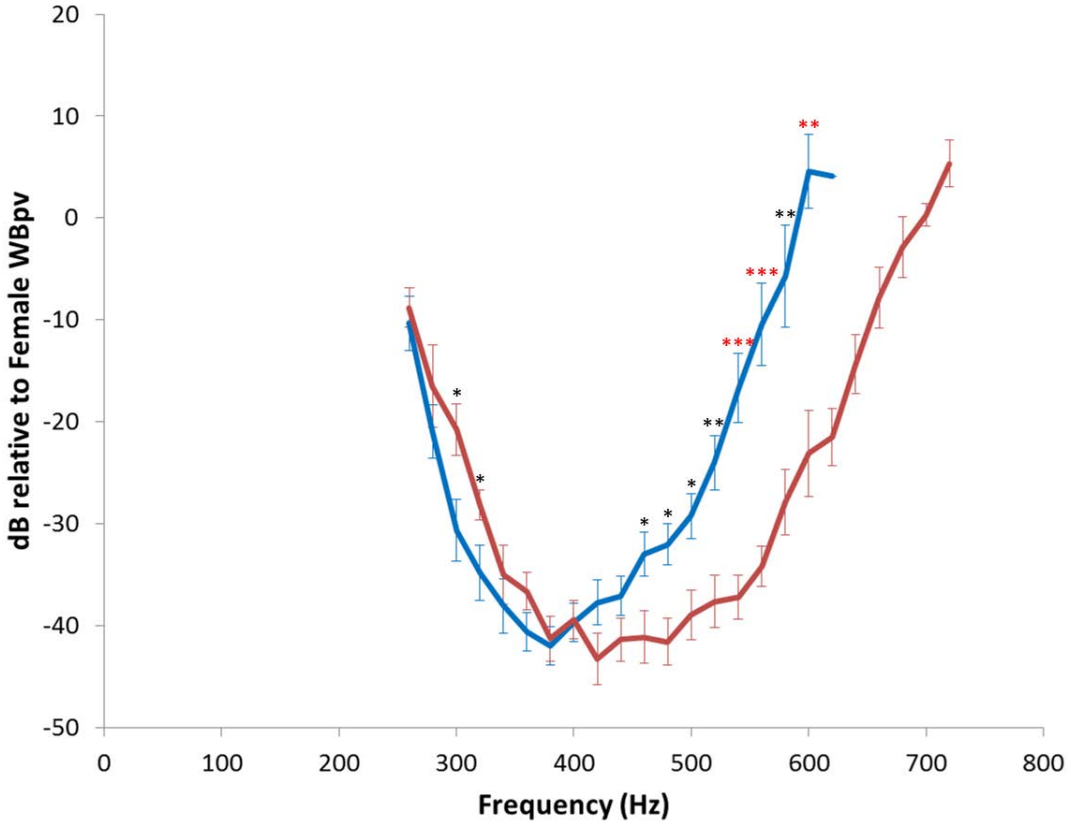

Figure 6.7: Behavioural threshold frequency tuning curve measured at 21 °C (blue, N=5) and 30°C (red, N=6). The PVL at which male mosquitoes displayed RFM to pure tones. The pure tone was increased in amplitude at 0.4 $dB \cdot s^{-1}$ from ~$1x10^{-8}$ to $4x10^{-4}$ ms^{-1}. This procedure was repeated across a range of frequencies with a 5-10 s gap between pure tone presentations. All PVL values were calculated relative to a reference PVL of a tethered mosquito from 2 cm. Each point represents the mean of all data points +/- standard error from all mosquitoes. Single asterisks: $p<0.05$, double asterisks $p<0.01$, triple asterisks $p<0.001$ (two-tailed T test). Red asterisks show significance after applying Bonferroni's Holm correction method. Data collected by Patrico Simões.

temperatures, which represent lab and field temperatures (21 °C and 30 °C respectively). Male mosquitoes demonstrated the same RFM response as seen in Figure 4.2 (**Chapter two**). At 21 °C, mosquitoes produced RFM responses most sensitively when stimulated with tones of 380 Hz (Figure 6.7 - blue) and responded

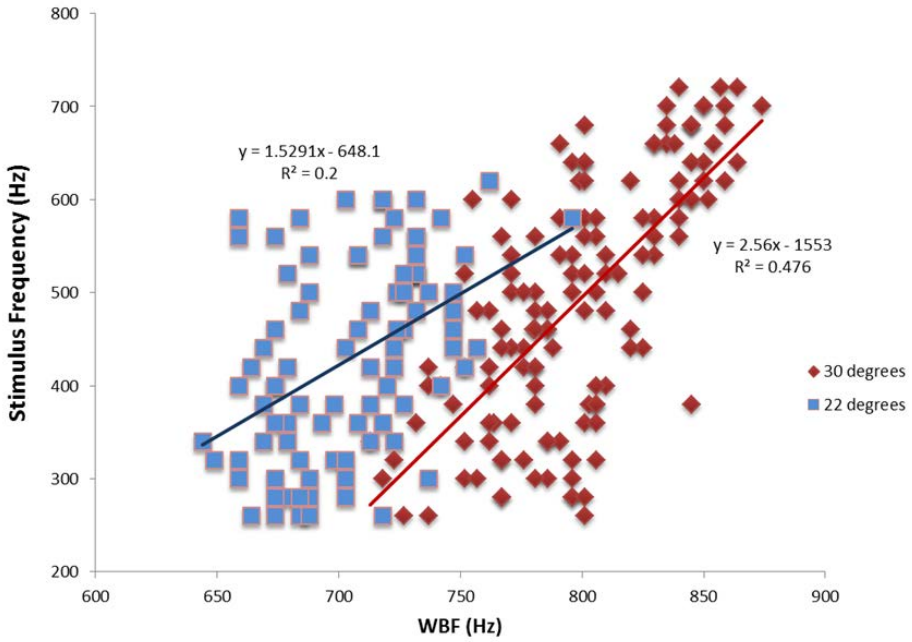

Figure 6.8: Correlation of the WBF of a male and the frequency, which the male displays, phonotaxis. Blue 21°C (stimulus=1.53x ♂WBF-648; Pearson's r=0.45), Red 30°C (stimulus=2.56x ♂WBF-1553; Pearson's r=0.69, ANCOVA $P=2.36x10^{-10}$). Data collected by Patrico Simões.

up to a maximum frequency of 620 Hz. At 30 °C, male mosquitoes produced RFM responses most sensitively when stimulated to 425 Hz tones (Figure 6.7 - red) and RFM could be elicited up to a maximum 720 Hz. At frequencies above 400 Hz, there was a significant increase in sensitivity between the two temperature conditions. For example, at 600 Hz, responses were 27 dB more sensitive at 30 °C in comparison to 21 °C (Figure 6.1). Frequencies above 440 Hz require significantly higher particle velocity levels to elicit a compound JO potential at 21 °C in comparison to 30°C. The 45 Hz shift in tuning is equivalent to a change of 5 Hz·°C^{-1}.

Behavioural tuning

The positive correlation between the WBF, as measured at the onset of the RFM behaviour of responding males, and the frequency of the stimulus to which they

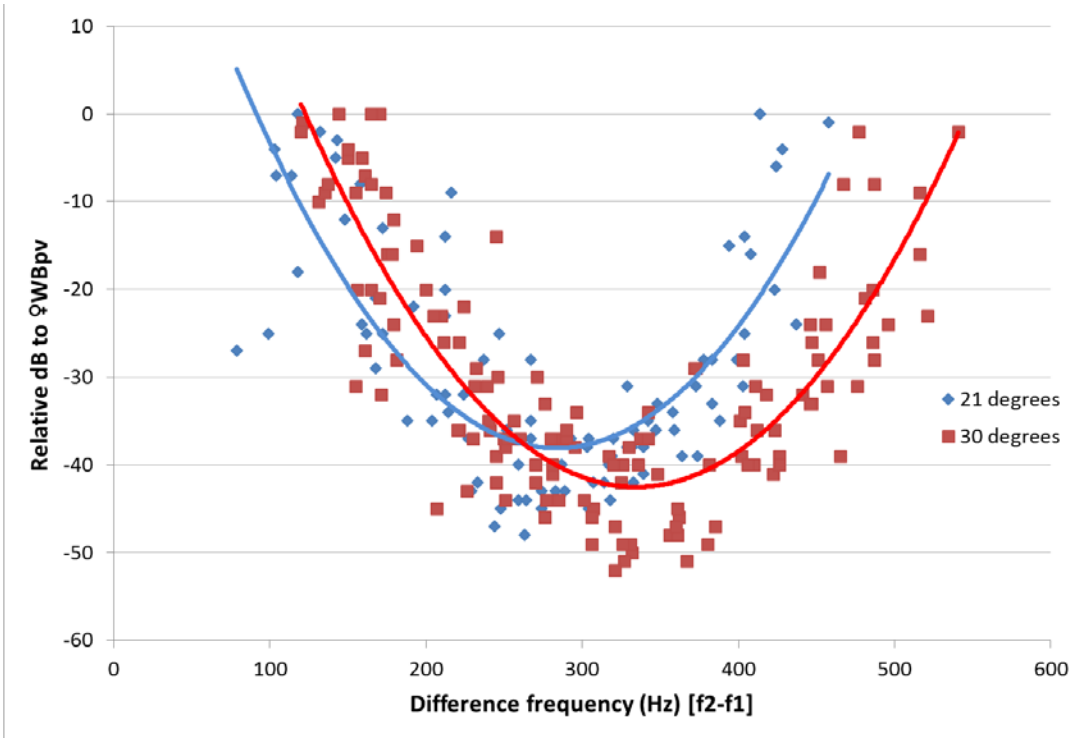

Figure 6.9 Hz: Behavioural tuning as function of difference frequency. The pre-mating behaviour as a function of the difference between the males' WBF measured before the onset of the acoustic behaviour and stimulus tone frequency (scatter plot fitted with quadratic curve). Behavioural responses measured in two temperature conditions; 21 °C (blue) and 30 °C (red).

respond is shown in Figure 6.8. At 21 °C, the correlation between WBF and temperature is weak ($R^2 = 0.2$) with a shallow slope (blue in Figure 6.8). WBF in cooler conditions were much lower at 796 Hz and the stimulus frequency to which they showed phonotaxis was lower at 620 Hz. At 30 °C, the mean and the highest WBF. There was a moderate positive correlation ($R^2 = 0.476$). WBF's were measured as high as 874 Hz and responses were recorded as high as 720 Hz. The behavioural tuning of each mosquito was re-plotted as a function of the difference tone (f2-f1), where f1 is the frequency of the stimulus tone and f2 is the frequency of its WBF immediately prior to performing an RFM response to the stimulus tone (As described in Chapter Three (Figure 5.2)). The scatter plot was fitted with a quadratic curve (Figure 6.9). At 21 °C the quadrative line of best fit indicates that the most sensitive DP responses occurred at 280 Hz, while most sensitive DP responses occurred at 330 Hz at 30 °C

(as seen in Figure 5.2). The frequency difference between the two temperatures of the lowest point of the quadratic curve is ~50 Hz, although sensitivity is not greatly affected with a difference of 4 dB (Figure 6.9).

3.4.3 Discussion

In this chapter, I characterised the temperature dependence of WBF, frequency tuning of the JO and phonotactic behaviour. There is a positive correlation of WBF and frequency tuning of the JO with temperature. This results with changes in the phonotactic behaviour, which relies on both WBF and the detection of the WBF by the JO.

A positive correlation between temperature and mosquito WBF and JO tuning was first reported by Tamarina et al. (1979) and spontaneous oscillations of the JO, which are thought to represent tuning of the JO, also temperature dependant (Warren et al. 2010). The JO tuning shift of 13.1 $Hz \cdot {}^{o}C^{-1}$ correlates well with Tamarina, Zhantiev et al. (1979), which reported similar rates in *Aedes aegypti* (16.9 $Hz \cdot {}^{o}C^{-1}$). The JO responses recorded here occurred at a range of 120 – 720 Hz at 30 ^{o}C (Figure 6.4), as opposed to between 100-400 Hz at 21 ^{o}C. Phonotactic behaviour is similarly affect by temperature as at 30 ^{o}C responses are recorded to frequencies between 250 and 720 Hz, however at the lower temperature, responses are decreased in range from 250 to 620 Hz. WBF was similarly influenced by temperature changes as rate change of 11.7 $Hz \cdot {}^{o}C^{-1}$, again comparable with literature (9.4 $Hz \cdot {}^{o}C^{-1}$, Tamarina, Zhantiev et al. (1979)).

The core temperature of large insects has been shown to rise during flight (Church 1960), however the core temperature of flying tethered mosquitoes, measured here, remained unchanged, irrespective of the ambient temperature. The rate of heat loss is greater in smaller insects such as mosquitoes and *Drosophila,* and in hot ambient conditions (e.g. 40 ^{o}C), small flying insects only heat up at a rate of 0.1 $cal/cm^2/min$ (REF). Mosquitoes can however increase rate of temperature in strong, direct sunlight, but because mosquitoes create swarms and mating copula during dusk (Church 1960), this is unlikely to happen.

In Chapter Three, it is hypothesised that male mosquitoes use distortion products to detect females. The distortion product postulated to be used by male *Culex quinquefasciatus* (f2-f1) is generated at the difference between the males own WBF (f2) and the WBF of a female (f1). Both WBF and JO tuning are influenced by temperature with dependencies of 11.7 $Hz \cdot {}^{o}C^{-1}$, and 13.1 $Hz \cdot {}^{o}C^{-1}$ respectively. The different temperature dependencies between WBF and JO tuning result in an shift of behavioural tuning of 50 Hz over 9 ^{o}C (5.5 $Hz \cdot {}^{o}C^{-1}$) (Figure 6.9). The temperature dependent changes in male JO tuning allow a coupling of sender (WBF) and receiver (JO tuning) – known as temperature coupling hypothesis (Ritchie et al. 2001). This enables males to detect females over a range of temperatures.

Temperature affects tuning in range of auditory receptors such as, the *Cicada* tympanal organ (Fonseca et al. 2007), Leopard frog saccular hair cells (Smotherman et al. 1999) and the chick cochlea (Fuchs et al. 1990). An increased temperature leads to an upward shift in the best frequency of the auditory receptors and an increase in absolute sensitivity but no change in the sharpness of tuning. These finding correlate well with properties measured from the male JO, where there is an increase in absolute sensitivity of 23.6 dB when temperatures are increased from 21^{o}C to 30^{o}C and an upward shift in JO tuning by ~80 Hz. Although the shift of 80 Hz is much smaller than a shift of 5 kHz in cicada, it represents a similar shift in relation to the overall hearing range. In addition, the tuning sharpness remained similar in both animals irrespective of the temperature.

The world has been undergoing climate change for the last 200-300 years with average temperatures reaching new highs (Houghton 1996). The coupling of the temperature dependence of the male JO tuning with the female's WBF predicts that sexual behaviour of mosquitoes is unlikely to be negatively affected.

3.5 Chapter five: Acoustic masking of auditory behaviour reveals male mosquitoes listen for frequency differences and not for female flight tones.

3.5.1 Introduction

Acoustic communication is used by a wide range of animal species to emit and receive acoustic signals conveying information about potential mates or rivals (Bradbury et al. 2011). However, the acoustic landscape of these species often contains a number of unknown sound sources, which can impair the ability of receivers to detect and classify the acoustic signals. The origin of this noise is variable, but it is most notably due either to same-species, different-species or anthropogenic acoustic activity (Brumm et al. 2005, Wiley 2006, Schmidt et al. 2015). Acoustic masking of a signal by background noise, in turn, shaped evolutionary adaptations in both the senders and receivers to cope with noise. For senders, these adaptations are generally adjustments to the signal properties, such as loudness, duration, timing or frequency, whereas for the receivers the adaptations can involve the reception and neural processing of sound by the peripheral or central nervous systems (Brumm and Slabbekoorn 2005, Römer 2013, Schmidt and Balakrishnan 2015). The underlying behavioural and physiological mechanisms causing acoustic masking in animals, and particularly in insects with tympanal hearing organs, have been studied intensively mainly through experimental stimulation of the receivers with two simultaneous tones (Boyan 1981, Bailey et al. 1986, Nolen et al. 1986, Farris et al. 2002, Kostarakos et al. 2015).

Male mosquitoes form swarms over visual markers where they fly in a looping pattern, often in large numbers (Knab 1906, McIver 1980, Gibson 1985). When a female approaches the swarm, the males detect the female flight-tones and a mating chase ensues (Roth 1948, Wishart and Riordan 1959, Charlwood and Jones 1979, Gibson 1985, Belton 1994, Clements 1999). Free-flying males exhibit a stereotypical modulation of their WBF coincident with phonotactic behaviour to the fundamental frequency of female flight-tones mimicked by a pure tone from a speaker (**Chapter two**). This robust and repeatable modulation of the WBF is termed Rapid Frequency

Modulation (RFM) and provides a high throughput approach to understand the effect of acoustic masking to auditory-led behaviour.

Mosquitoes detect the near-field component of sound (air particle velocity) through sinusoidal displacement of their flagellum to the sound source (Göpfert and Robert 2001). Thus, local short-distance noise sources have the potential to interfere with male mosquito acoustic behaviour. Antennal vibrations in mosquitoes are detected by and transduced into electrical signals by several thousand sensory scolopidia, which compose the auditory Johnston's organ (JO) housed in the pedicel at the base of each of the flagellum (Boo 1980). It is hypothesised that the JO is tuned to detect the difference in frequency between the male's own wing beat frequency (WBF) and that of the female (**Chapter three**). Specifically, the JO detects the intermodulation distortion products (DPs) generated in the mechanical vibrations of the antenna due to nonlinear interaction between the male and female flight-tones (Göpfert, Briegel et al. 1999). This means that male mosquitoes must fly in order to detect and locate the flight-tones emitted by females.

Here I report the acoustic masking of the RFM behaviour in free-flying male mosquitoes and compare to the suppression of distortion product JO compound potentials. The paradigm used here is similar to those that have been employed for behavioural and physiological masking in insects (Boyan 1981, Bailey and Morris 1986, Nolen and Hoy 1986, Farris and Hoy 2002, Kostarakos and Römer 2015). Similar paradigms have been used in humans and other mammals (Sellick et al. 1979, Cheatham et al. 1982, Robles and Ruggero 2001, Lee et al. 2009, Versteegh et al. 2013). This is the first study describing the role of masking in the acoustic behaviour of mosquitoes, and indeed, in insects with antennal hearing. Furthermore, if there is a strong correlation between the suppression of RFM behaviour and the suppression of distortion product compound JO potentials, it serves to strengthen the distortion product hypothesis outlined in chapters two and three.

3.5.2 Results

Male mosquito RFM can be disrupted through acoustic masking

Pure stimulus tones delivered from a loud speaker were used to elicit robust RFM of swarming male mosquitoes (32 swarms, three mosquitoes per swarm). The particle velocity of the stimulus tones was $5x10^{-5}$ ms^{-1} at a reference distance of 2 cm, similar sound intensity produced by tethered-flying females at the same distance. The frequency of the masking tones varied throughout the experiments, ranged between 200-600 Hz and with a particle velocity of ~$8x10^{-5}$ ms^{-1} at a reference distance of 2 cm in front of the mosquito. Frequencies outside of 300 – 550 Hz did not produce significant suppression of RFM behaviour (G-test goodness-of-fit: stimulus: 340 Hz, $G \geq 5.16$, $p \leq 0.023$; stimulus: 400 Hz, $G \geq 3.87$, $p \leq 0.049$; stimulus: 450Hz, $G \geq 4.60$, $p \leq 0.032$). The likelihood of eliciting RFM was similar and not significantly different (G-test of independence: $G=0.596$; d.f.=2; $P=0.742$) for stimulus frequencies of 340 Hz, 400 Hz and 450 Hz (81%, 85% and 89%, respectively). A second tone was played from a second loud speaker (masking speaker) simultaneously with the stimulus tone to disrupt RFM phonotactic behaviour. Two sound pressure microphones were placed within 2 cm to both the masking speaker and the stimulus speaker. Each microphone identified which of the sound sources male mosquitoes directed their RFM responses towards (Figure 2.4 and Figure 7.1). The effect of masking frequency on the probability of RFM response is shown in Figure 7.2. Stimulus tone-only presentations elicited a high percentage of RFM responses towards the stimulus speaker (Figure 7.2 A-C [black horizontal line]; stimulus 340 Hz: 75%; 400 Hz: 81%; 450 Hz: 84%). There was a significant suppression of the RFM response towards the stimulus speaker when compared to stimulus-only presentations (Figure 7.2 A-C, blue areas; stimulus 340 Hz: masking frequencies= [300-500 Hz], $G \geq 5.31$, $p \leq 0.021$; stimulus 400 Hz: masking frequencies= [320-550 Hz], $G \geq 4.37$, $p \leq 0.037$; stimulus 450 Hz: masking frequencies= [250-500 Hz], $G \geq 9.01$, $p \leq 0.003$).

In addition to RFM responses towards the stimulus speaker, male mosquitoes can instead direct their response towards the masking speaker or display no response at

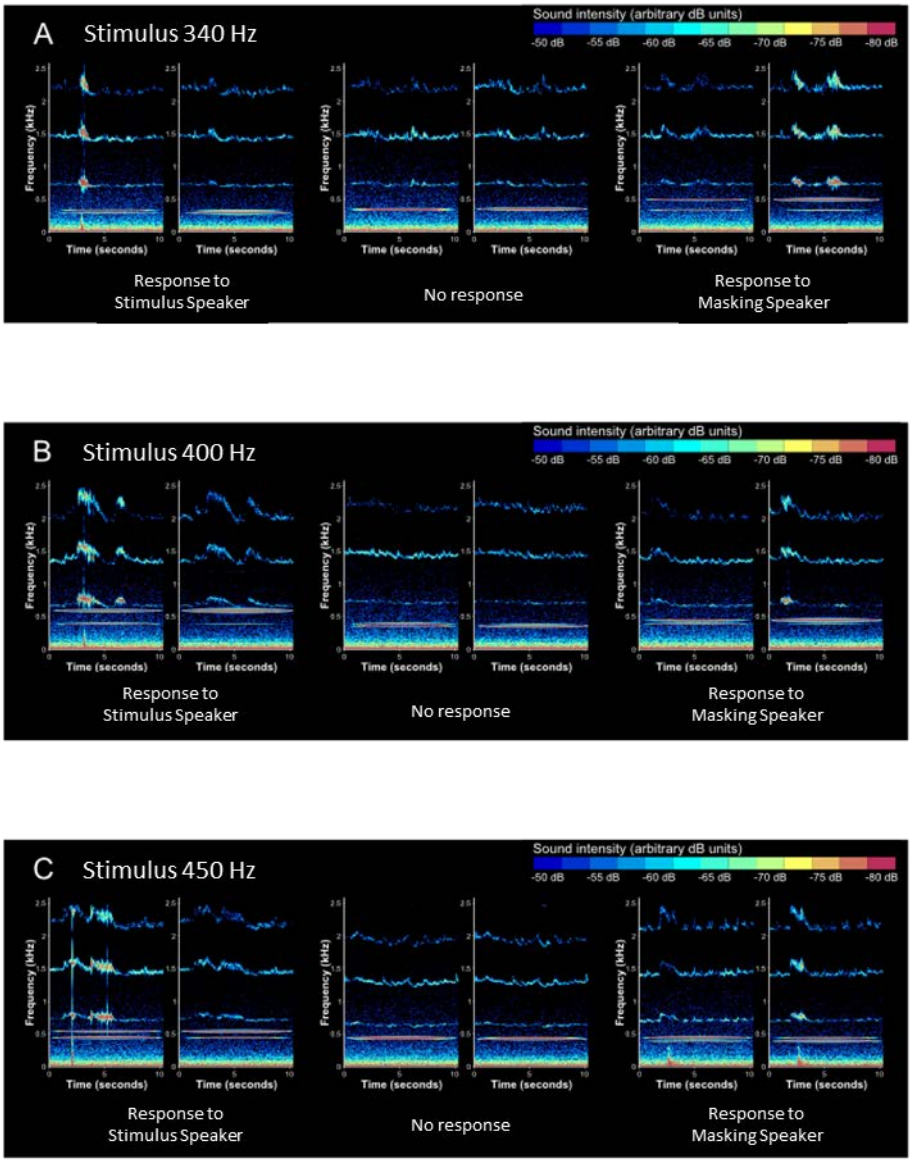

Figure 7.1: Spectrograms of the WBFs of free-flying males when stimulated with a simultaneous stimulus/mask tones presentation. A) Stimulus tone 340 Hz. B) Stimulus tone 400 Hz. C) Stimulus tone 450 Hz. In response of tone presentation, male mosquitoes could either present a RFM response towards stimulus speaker, no conspicuous response, or present a RFM response towards the masking speaker. For each single interaction shown, the left spectrogram displays the activity recorded by the microphone near the stimulus speaker and the right spectrogram displays the activity recorded by the microphone near the masking speaker. The identification of the speaker the male displayed his behaviour was obtained by comparing the sound intensity of the WBF in the 2 sound channels: the sound intensity of RFMs near a

microphone registered responses 20-30 dB higher than the furthest microphone. Occasionally (<5% of the records), a male displayed RFM to both speakers during a single 10 second stimulation; in this situation, we registered the response to the first speaker. Data collected by Patrico Simões.

all, continuing station keeping flight with no frequency modulation (Figure 7.2). Suppression of the RFM response towards the stimulus speaker appears to be dominated by attraction to the tones emitted by the masking speaker. I have termed this competition. RFM towards the masking speaker occurred significantly more often than towards the stimulus speaker for masking frequencies ~420±50 Hz (Figure 7.3 a-c, red areas; stimulus 340 Hz: masking frequencies= [360-450 Hz], G≥4.98, p≤0.026; stimulus 400 Hz: masking frequencies= [390-470 Hz], G≥18.22, p≤0.001; stimulus 450 Hz: masking frequencies= [400-470 Hz], G≥5.15, p≤0.023). However, the competition effect, i.e. the attractiveness of the masking frequency relative to the stimulus frequency, does not account for all the observed behavioural masking as masking frequencies also caused a significant suppression of RFM response to either speaker. The interference effect of the masking tone on the overall RFM response was observed for all stimulus frequencies, although more pronounced at 340 Hz (Fig. 2a-c, grey areas; stimulus 340 Hz: masking frequencies= [320-400 Hz], G≥11.53, p≤0.001; stimulus 400 Hz: masking frequencies= [320-470 Hz], G≥6.14, p≤0.013; stimulus 450 Hz: masking frequencies= [280-470 Hz], G≥4.85, p≤0028). The maximum interference effect (Figure 7.2 A) occurred when the male mosquitoes displayed RFM response to neither speaker (probability of 0.13 [lowest point of the black dotted curve]). When males did not display RFM during the stimulus/masking presentations, it was observed that their WBFs dropped ~10-15 Hz during stimulation and then gradually returned to their original WBF (Figure 7.2).

Acoustic masking relative to JO tuning

Masking of phonotactic RFM behaviour is maximal for frequencies ~80 Hz above the best tuning frequency range of the JO as quantified in chapter three (Figure 7.3 A). A

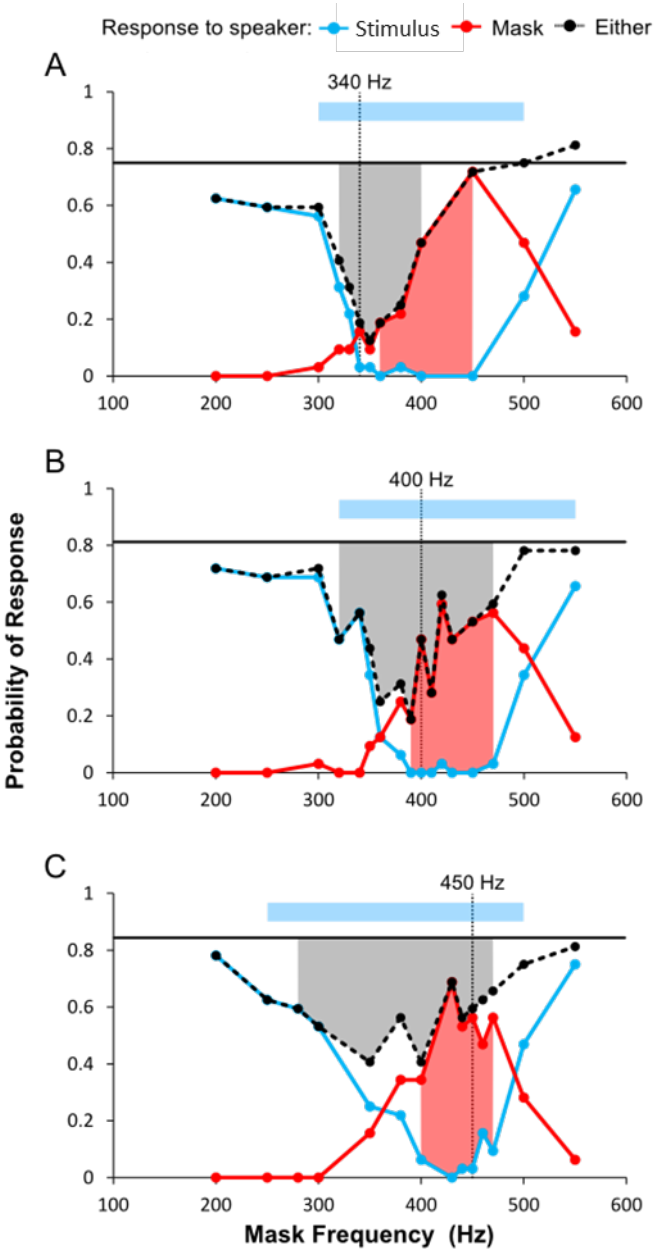

Figure 7.2: Acoustic masking of RFM behaviour is a consequence of both interference and competition by the masking tones. A) Stimulus tone 340 Hz. B) Stimulus tone 400 Hz. C) Stimulus tone 450 Hz. The probability of RFM response towards the stimulus speaker (blue line), masking speaker (red line) and to either speaker (dashed black line) are plotted as functions of the masking frequency (n =32 for each stimulus/masking pair). Particle velocity of the stimulus tones was $5x10^{-5}$ ms^{-1} at a reference distance of 2 cm. Horizontal black lines represent the probability of the RFM response to stimulus tone only. Blue range: masking frequencies causing significant

acoustic masking towards the stimulus sound source. Red range: masking frequencies causing competition, i.e., a significantly higher probability of RFM towards the masking sound source than to the stimulus sound source. Grey range: masking frequencies cause interference, i.e., a significantly lower probability of RFM response to either sound source relatively to the stimulus-only presentations. Data collected by Patrico Simões.

hypothesis for this mismatch is that male mosquitoes do not detect these tones *per se*, but rather f2-f1 DPs generated between the stimulus tones and the mosquito's own WBF. This was tested by a comparison of the tuning of the JO against the f2-f1 DP, calculated through the difference of the WBF of the responding males (measured just prior to the onset of RFM) and the masking tone frequency (Figure 7.3 B).

Regardless of the stimulus tone frequency, maximum behavioural masking (i.e. suppression of the RFM response to the stimulus speaker) was centred on the frequency difference (WBF-masking tone=300 Hz) and extended symmetrically either side by ~100 Hz (Figure 7.3 B). The frequency range of this suppression correlates with the optimal frequency tuning of the JO (Figure 7.3 B). In addition, the frequency of maximum tone competition (i.e. attraction towards the masking speaker) appears to be dependent on the stimulus-tone frequency, being close to 250 Hz for 340 and 400 Hz stimulus, and 300 Hz for 450 Hz stimulus tone (Figure 7.3 B). This relationship suggests that acoustic masking is caused by the influence of masking tones on the formation or detection of intermodulation distortion products (DPs) on the male's antenna or JO.

Acoustic masking of difference tone distortion products recorded in the compound JO potentials is centred on the most sensitive frequency

Male mosquitoes were immobilised and stimulated with pairs of pure tones which had particle velocity levels and frequencies mimicking the male's own fundamental WBF (F1) and a female's fundamental WBF (F2) (F1: 700 Hz, $4x10^{-4}$ ms^{-1}; F2: 400 Hz,

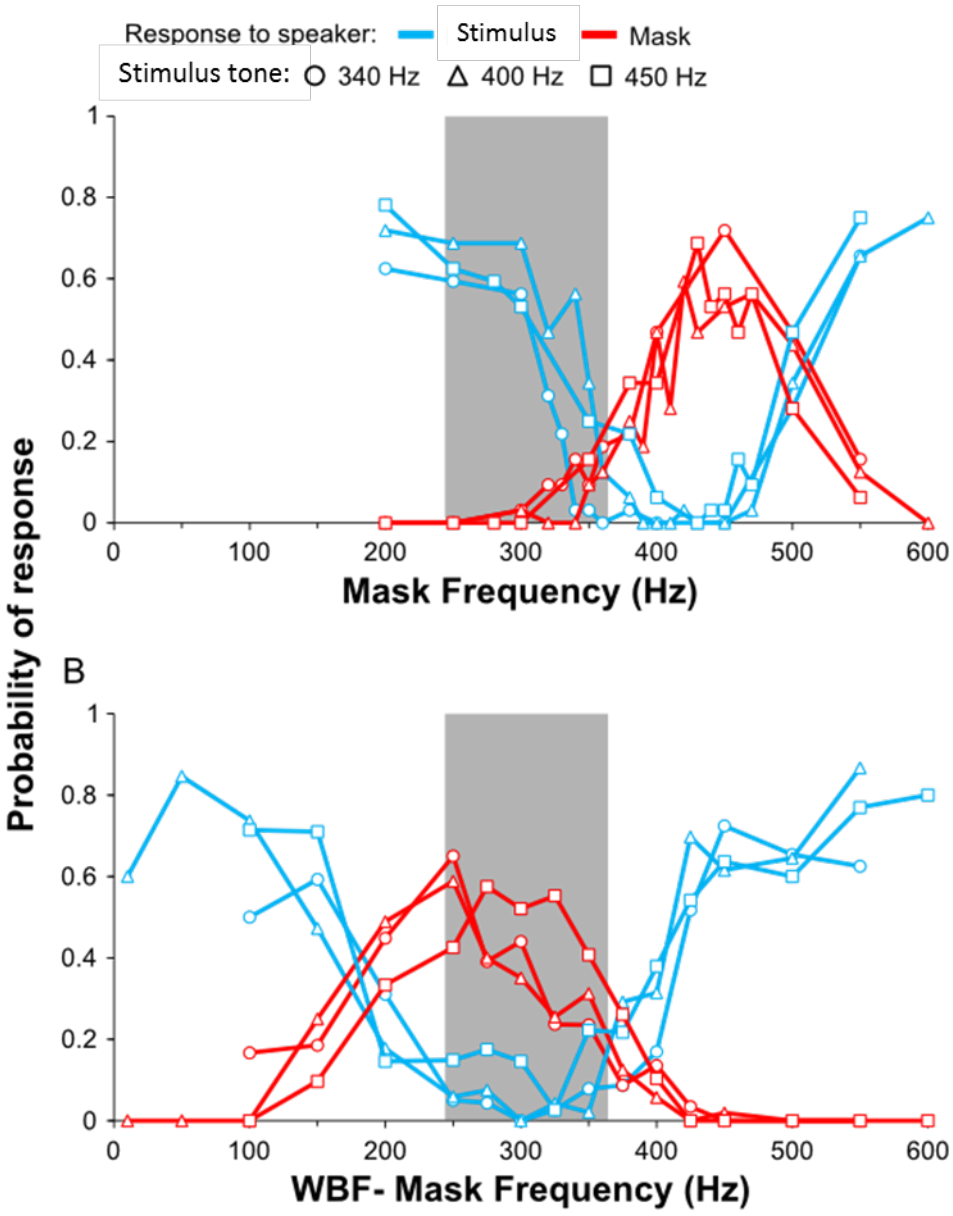

Figure 7.3. Acoustic masking of RFM response correlates with JO tuning when the probability of the response is replotted as function of frequency difference between the male's WBF and Mask frequency. A) Probability of RFM response to stimulus and masking speaker as a function of the masking tone frequency (as in Figure 7.2). A) Probability of RFM response calculated as a function of the frequency difference between the WBF of the male just prior the RFM response and the masking frequency. The grey rectangle represents the 10dB bandwidth tuning of the male's JO (Chapter one). Data collected by Patrico Simões.

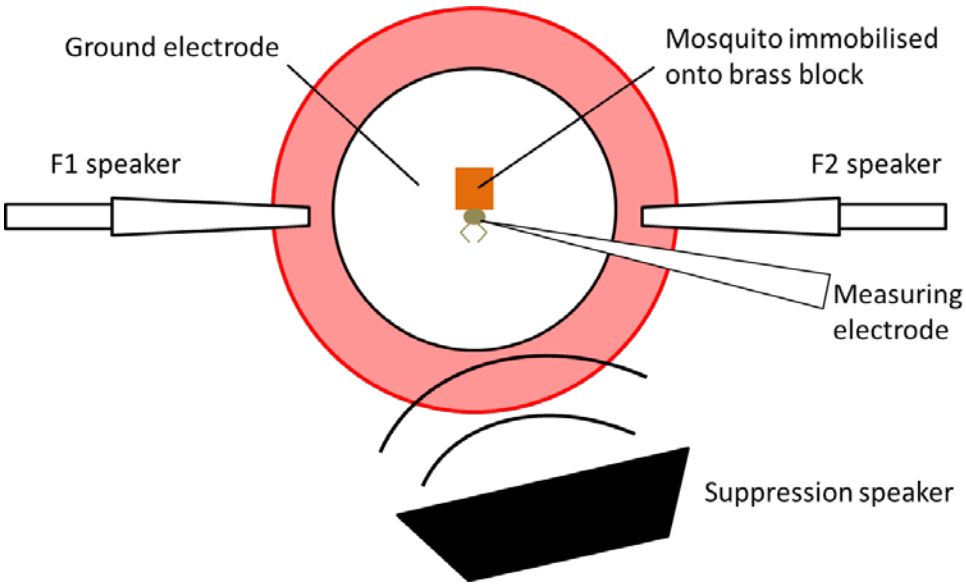

Figure 7.4. Physiological set up. Schematic of arrangement for delivering two tones (F1: 700 Hz, $4x10^{-4}$ ms^{-1}; F2: 400 Hz, $1x10^{-5}$ ms^{-1}) and masking tone to the antennae and recording electrical responses with sharp borosilicate electrodes from the JO.

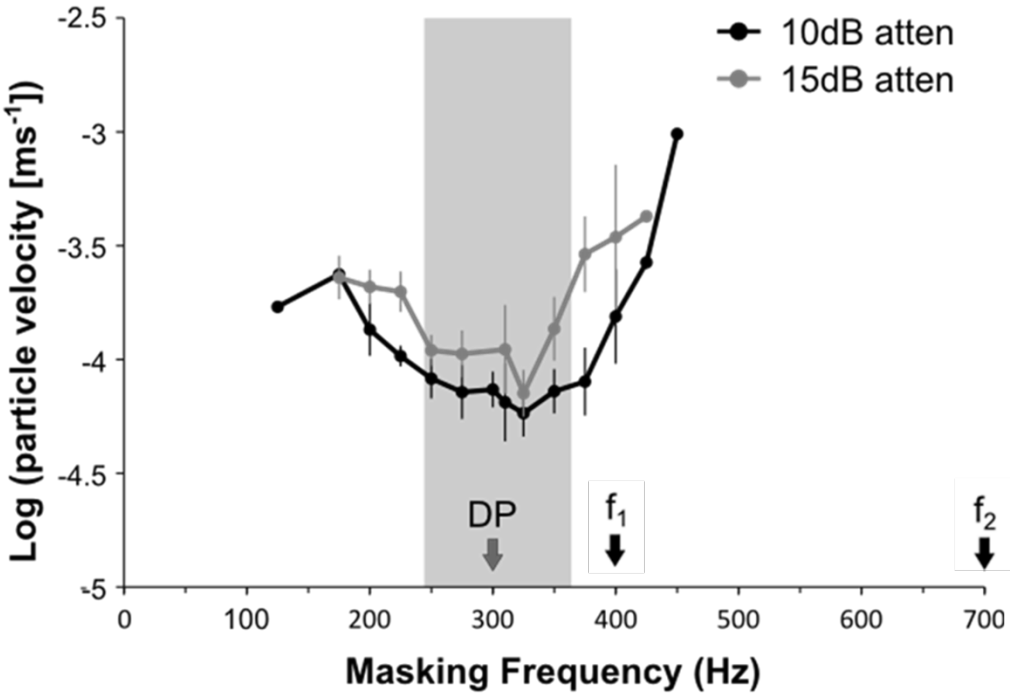

Figure 7.5. Distortion product JO compound potential suppression tuning curve. Difference tones (DP=300 Hz) were generated by the simultaneous presentation of two tones (f1=400 Hz; particle velocity = 4 x $10^{-4}ms^{-1}$ and f2=700Hz; particle velocity =

1 x $10^{-5}ms^{-1}$) simulating male and female flight tones, respectively. Curves represent the masking sound levels required to suppress the magnitude of the DP (F2-F1) response by 10 dB and 15 dB. The grey shaded region corresponds to the 10 dB bandwidth of the JO frequency threshold tuning curve (Chapter one).

$1x10^{-5}$ ms^{-1}) (Figure 7.4). The frequencies were transduced by the JO into compound JO potentials, and recorded through the insertion of a sharp tungsten electrode into the pedicel. In response to two-tone stimulation, the JO compound potential had frequency components at the F1 and F2 stimulus frequencies. In addition, the JO transduced the F2-F1 DP. To interfere with the generation of the F2-F1 DP a third pure tone was emitted from a third speaker (Figure 7.4).

The level of suppression by the third tone depends on its frequency and particle velocity level. The particle velocity level of the third tone was increased until the DP compound JO potential decreased in magnitude by 10 and 15 dB. The dependence of the DP JO compound potential of the frequency and particle velocity level of the third tone is plotted in Figure 7.5 (mean ±standard error, N=4).

The particle velocity level of the suppression tone required suppress the amplitude of the distortion product JO compound potential is shown in Figure 7.4. Analysis of variance revealed a significant effect of frequency of the suppressing tone on the 10dB and 15dB attenuation of the electric DPs' magnitude (10 dB: F=7.34, d.f=13, $p<0.001$; 15 dB; F=2.77, d.f.=10, p=0.031). Suppression is achieved most sensitively to 325 Hz, which is 45 Hz away from the JO best frequency, which is outside of the female WBF (Figure 7.5). These results support the hypothesis that acoustic masking is caused by the suppression of the DPs.

Discussion

Here I report the acoustic masking of the RFM behavioural response of free-flying male mosquitoes and suppression of the JO compound potential at the distortion product of two tones. These results indicate that the pre-mating behaviour of male mosquitoes, a function mediated by sound (Roth 1948, Wishart and Riordan 1959, Charlwood and Jones 1979, Belton 1994, Gibson and Russell 2006, Cator, Arthur et al. 2009, Warren, Gibson et al. 2009, Pennetier, Warren et al. 2010), can be impaired by acoustic masking. Acoustic masking is centred on a frequency range that not only encompasses the fundamental frequency of the flight-tones of free flying females (430-527 Hz), but it is also similar to the most sensitive frequencies of male behavioural audiograms (340-560 Hz) (**Chapter two**). Masking frequencies above 600 Hz did not suppress RFM behaviour, indicating that male flight-tones (713-874 Hz), and by extension, other males flying within a swarm, do not impair RFM behaviour.

Acoustic masking is mediated by two non-mutually exclusive processes; either by competing and being more attractive than the female-like stimulus tone or by interfering with the males' ability to detect or locate the stimulus tone. Acoustic masking is caused through suppression of DPs generated in the non-linear vibration of the antennae (Warren, Gibson et al. 2009, Pennetier, Warren et al. 2010). This is supported by comparisons between the re-plotted behavioural masking data as a function of the frequency difference between the stimulus tone and the male's own flight tone (Figure 7.3), the electrophysiological DP masking audiograms (Figure 7.5), and the frequency tuning of the male JO (**Chapter three**). These results provide further support for the hypothesis that male mosquitoes do not detect female flight tones *per se* but rather the difference in the fundamental frequencies of their own flight tones and those of a nearby female. It also supports the view that harmonic convergence (Cator, Arthur et al. 2009, Warren, Gibson et al. 2009, Pennetier, Warren et al. 2010, Aldersley et al. 2016) is perhaps an epiphenomenon that arises as a natural consequence of male and female mosquitoes attempting to hear the difference in frequency between their flight-tones (**Chapter three**).

Does acoustic masking bare any significance to mosquito swarming and the RFM component of male mating behaviour? Mosquito hearing relies on the detection by

the antenna of the particle velocity, and thus near-field, component of sound (Bennet-Clark 1998, Göpfert and Robert 2001). Consequently, any tone that might act as a potential acoustic masker should be within the close proximity (a few centimetres) of the male mosquito or much louder than could be produced by a flying mosquito. In natural conditions, male mosquitoes form relatively dense swarms while waiting for sexually receptive females (Gibson 1985, Clements 1999). Given that masking tones above 600 Hz do not suppress RFM behaviour, male-male acoustic interactions within the swarm should not impair the ability of an individual male mosquito to detect and locate potential mates. This is because the JO is tuned to frequencies well below those of the flight-tones of males (**Chapter three**). Furthermore, difference tones, due to nonlinear interaction in the antennal vibrations between a male's own flight-tones and those of another male, would be in the order of tens of Hz and thus in a very insensitive region of the electrical responses of the JO (Warren, Gibson et al. 2009, Lapshin 2012). Therefore, from a male mosquito's perspective, swarms are not a noisy environment for listening out for passing females.

Acoustic masking of the RFM behaviour is most effective for masking frequencies similar to those of the female flight-tones. In natural conditions that would occur only if a male within a swarm was to detect simultaneously the flight-tones of two nearby females. This situation, however, would occur only with unrealistically high densities of females nearby or within the swarm. Wishart and Riordan 1959 studied the attractiveness of *Aedes aegypti* males to various sounds and found the most attractive frequencies were centred on the female fundamental frequency and ranged optimally between 400-600 Hz, consistent with the findings of *Culex quinquefasciatus* (**Chapter two**). Crucially, this work showed that when two or more pure tones, which are attractive alone, are not attractive when present together. In some frequency combinations, this resulted in a > 95% reduction in the number of male mosquitoes trapped by their sound-lured vacuum trap (Wishart and Riordan 1959). The cause for that decrease was not determined, but it appears that, as presented here, acoustic masking and competition could be the underlying process.

According to the acoustic adaptation hypothesis (Morton 1975), acoustic signals evolved to be optimised to the habitats in which the species occurs, thus minimising the effects of attenuation and signal distortion. The high sensitivity of male mosquitoes to near-field sound, in particular to the WBF of female flight tones, appears to have a cost, which is a high susceptibility to acoustic masking when two tones of similar female-like frequencies are presented simultaneously. However, the probability that a male within the swarm encounters simultaneous and prolonged acoustic signalling from two females, would appear to be very rare indeed.

Interference and competition mediate acoustic masking of the male RFM response. On one hand, overall suppression of the response, i.e. interference, is to some degree expected. In other nonlinear systems, such as the electrical responses of hair cells in the mammalian cochlea, the stimulus and masking tones can suppress themselves mutually (Sellick and Russell 1979). As in the results presented here for the mosquito antenna, in the cochlea system, mutual suppression is greatest when masking and stimulus tones both fall within the local bandwidth of the receptor (Sellick and Russell 1979). On the other hand, the attraction of male mosquitoes to the masking sound source, i.e. competition, is likely to be related to the free-flight paradigm; stimulus and masking sound sources are spatially separated, so if both tone frequencies are attractive males can go to whichever tone appears loudest. Evidently, the perceived sound level will be dependent on the spatial location of the mosquito relative to the sound sources when stimulation occurs. It is also possible that a similar mechanism to the one found in the *Ormia ochracea* flies is present; in which the localization of conflicting sources are solved by a precedent effect, wherein the detection of small time differences (~10 ms) in sound reception are used to determine location of the first source detected (Lee, Elias et al. 2009).

4.0 General discussion

4.1 Male mosquitoes use distortion products to detect female mosquitoes

Male mosquitoes demonstrate positive phonotaxis and produce sensitive JO compound potentials, to tones, which are close in frequency to the female wing beat frequency (WBF). It was speculated since the early 19th Century that the male mosquito JO detects the fundamental WBF of a nearby female (Johnston 1855), of which males would pursuit and mate. In this thesis, the tuning of the male JO of *Culex quinquefasciatus* is approximately 150 Hz below the mean female WBF.

Mating pairs of mosquitoes have shown that sexual recognition is made through an acoustic interaction, called frequency matching (Gibson and Russell 2006, Cator, Arthur et al. 2009, Warren, Gibson et al. 2009, Pennetier, Warren et al. 2010). Tethered *Toxorhynchites* converge their WBF within 8 Hz when presented with tones within 80 Hz of their own WBF or another mosquito at similar WBF (Gibson and Russell 2006). When presented with same sex WBF, both males and females would briefly converge their WBFs before they eventually diverged. Male-male pairs and female-female pairs of *Culex* actively avoid one another (Warren, Gibson et al. (2009) – supplementary material), while M and S form *Anopheles* opposite sex pairs only achieve 4-5% matching during recordings (compared to same types [25-38%]) (Pennetier, Warren et al. 2010). Low hybridisation in the *Anopheles* sub-species remains a mystery, however swarming visual discrimination (Diabaté, Dao et al. 2009) and difference in circadian activity (Sawadogo et al. 2013) do provide possible explanations. The hypothesis that mosquitoes utilise difference tones to detect conspecifics was applied to *Culex* (Warren, Gibson et al. 2009), *Aedes* (Cator, Arthur et al. 2009), *Anopheles* (Pennetier, Warren et al. 2010), but instead of an f2-f1 distortion signal identified in *Toxorhynchites*, harmonic convergence was described. These species, which demonstrate harmonic convergence, match the male's first harmonic and the females' second harmonic.

Frequency specific JO compound potentials are generated when an immobilised mosquito is stimulated with two pure tones, which represent the male and female WBF. There is an additional third frequency response, which represents the

difference between f1 and f2 (Figure 5.1). This is in fact the f2-f1 distortion product. The flagellum appears to have a stiffening, quadratic non-linearity (Lukashkin et al. 1999, Warren, Gibson et al. 2009) which allows the generation of difference tones, which in theory allows the facility to detect tones outside the hearing range of the JO. The harmonic convergence reported in Warren, Gibson et al. (2009) would require a 3f2 – 2f1 distortion product, which is completely absent during pure tone stimulation. The mosquito flagellum undergoes sinusoidal displacements to pure tones at the fundamental frequency of a pure tone and higher harmonics (Göpfert, Briegel et al. 1999), with the flagellum still able elicit vibrations as high as 3000 Hz (2000 Hz in Warren, Gibson et al. (2009) and 3000 Hz in Göpfert, Briegel et al. (1999)). Although the flagellum can vibrate at such frequencies, the JO low pass filters these mechanical vibrations such that the JO can only respond to frequencies much lower. It is unclear as to whether male mosquitoes can detect sounds higher than 1000 Hz, with threshold JO compound potentials reported in some cases (Cator, Arthur et al. 2009), and not in others (Warren, Gibson et al. 2009, Lapshin 2012). Here single pure tones did not generate JO potentials above 1001 Hz (Figure 3.2); which indicates that it is most likely that the generation of any distortion products occur well before the JO.

The WBF of a female mosquito is not a pure sine wave, and has multiple harmonic components itself (**Chapter two**, Warren, Gibson et al. (2009)), however it is actually the fundamental frequency which is the most important. Free flying male mosquitoes are able to create a consistent response to pure tones, without the natural harmonics found in free flying females (**Chapter two**). This finding is consistent with Wishart and Riordan (1959) as phonotaxis to a point source reduced by 19.2 % when removing the fundamental from the female WBF playbacks (20.1% success rate versus 0.9 % when fundamental removed).

There are three main arguments against mosquitoes using harmonic distortion as means of detecting potential mates; i) mosquitoes lack the functionality to generate the 3f2 – 2f1 distortion product in the JO; ii) the generation of a 3f2-2f1 distortion product, and the subsequent difference tone, is in an insensitive region of the JO; and iii) harmonic convergence requires the female to also detect and respond to

audition. If a male mosquito utilises f2-f1 distortion products in a male driven action instead, it not only gives the facility of detection, but also generates difference tones in the acoustic sweet spot of the JO.

It is hypothesised male and female mosquitoes undergo a mating ritual, which sees them match harmonics, perhaps as a test of fitness, which results in a mating copula (Cator, Arthur et al. 2009, Warren, Gibson et al. 2009). The results in this thesis indicate that mating is a male driven action, and that providing the sound falls within the attractive range of the JO (340-560 Hz), the male will approach the female at a high rate of repeatability (Figure 4.4). A measure of phonotaxis in free flight mosquitoes is not entirely novel (Wishart and Riordan 1959), but all experiments which have reported harmonisation between pairs has so far only been seen using tethered mosquitoes (Gibson and Russell 2006, Cator, Arthur et al. 2009, Warren, Gibson et al. 2009, Pennetier, Warren et al. 2010). WBF in tethered flight is erratic in all cases, whereas in the recordings here, a lot more stable to both stimulation from tethered females (Figure 4.1) and stimulation from pure tones (Figure 4.3). In tethered *Drosophila*, the total stroke amplitude and WBF is reduced and the time course of stroke deviation is distorted (Fry, Sayaman et al. 2005). If mosquitoes regulate their flight speed in the same way, it is likely that restricting the mosquito's movement will only serve to hinder their natural behaviour. The process of tethering could cause the mosquito to alter their wing beat, which in turn generate artificial behaviour not related with free flight. The tethered female does make fluctuations during flight, but this could be in accordance with male contact during RFM. In order to address this, it would be required to make these measurements with both free flying male and female, and determine if these fluctuations are a result of tethering, or it is a hallmark of their natural behaviour.

4.2 Temperature influences of free-flight behaviour

Tuning of the male JO and free-flight WBF increases in frequency as ambient temperature increases (**Chapter four**). WBF increases consistently with temperature in all flying insects studied so far with shifts of 9.4 $Hz \cdot 1^{o}C^{-1}$ in *Aedes aegypti*

(Tamarina, Zhantiev et al. 1979), 5.4 Hz·1^{o}C^{-1} in *Drosophila melanogaster* (Unwin et al. 1984), 2.9 Hz·1^{o}C^{-1} in *Musca domestica* (Unwin and Corbet 1984) and 0.6 - 0.7 Hz/^{o}C in *Periplaneta Americana* (Farnworth 1972). Frequency shifts increase linearly for all species up to 27^{o}C, however decrease between 27 - 32^{o}C. Beyond 35^{o}C the absolute WBF frequency begins to decrease. This is likely to be a reflection of decreases in internal thoracic temperature, via cuticular water loss (Farnworth 1972). The WBF of *Culex quienquefasciatus*, as reported in this thesis, increase at a rate of 13.8 Hz/ ^{o}C.

The rhythm of the WBF is dictated by a coupling of the muscle properties and the mechanical resonance of the wing-thorax system (Pringle 1967). The efficiency of flight is maximal when the optimal frequency of the flight muscles coincide with the resonant frequency of the wing-thorax system, and the most efficient muscle operating frequency is temperature dependant (Machin, Pringle et al. 1962). Unlike large insects such as bees, mosquitoes are unable to generate sufficient heat to raise the core temperature (Figure 6.2). In insects with small surface area such as mosquitoes and *Drosophila*, an increase in WBF has a net cooling effect, which increases the rates of convective cooling if the body is warmer than the air, and the evaporative cooling in dry air (Unwin and Corbet 1984). The influence of temperature on insect WBF is size dependent, as small hoverflies demonstrate the ability to self-cool during flight but warm up in larger hoverflies (Gilbert 1984).

JO tuning also increases with temperature, as *Aedes aegypti* hearing increases in frequency at a rate of 16.9 Hz/ ^{o}C in (Tamarina, Zhantiev et al. 1979), 14.1 Hz·1^{o}C^{-1} in *Culex quienquefasciatus* (Figure 6.5) and approximately 500 Hz·1^{o}C^{-1} in *Cicada* (Fonseca and Correia 2007). Although the resonance of flight systems of insects are temperature dependent, the tympanum of *Cicada* are not, and any changes in the tuning in the hearing organ is a result in changes the electrophysiological properties of the auditory neurons (Fonseca and Correia 2007). The mechanism which governs frequency tuning is attributed to changes in potassium channel kinetics. Tetraethylammonium (TEA) is an inhibitor that blocks potassium channels, and the introduction affects frequency selectivity in a manner similar to reduced temperature conditions (Fonseca and Correia 2007). BK channels are the rate limiting

factor in frequency tuning, regulated by membrane voltage and/or intracellular Ca^{2+} (Hodgkin and Huxley 1952).

Temperature also results in changes in behaviour with a shift of 5.5 Hz/ ^{o}C over 9 ^{o}C. It is well documented that the *Culex* genus are geographically segregated, with *Culex pipiens pipiens* located in temperate regions which can experience temperatures as low as 10 ^{o}C, and *Culex quinquefasciatus* which are found in tropical conditions with temperatures as high as 55 ^{o}C (Reiter 2001). In Argentina, *Culex pipiens* remain exclusively in the south, whereas *Culex quinquefasciatus* in the north, with limited hybridisation at the midpoint (Rosario – 4.7%). It is plausible to hypothesise that temperature plays its part in segregation of mosquito species, and that extreme temperature conditions to either temperate or tropical species could serve to compromise audition. *Culex quinquefasciatus* natural habitat at dusk has an average temperature of approximately 30 ^{o}C (Reiter 2001, Gokhale, Paingankar et al. 2013). When measuring gross potentials of the JO in temperate conditions (21 ^{o}C) the tuning of the JO is reduced to low frequencies, and absolute sensitivity lost up to one order of magnitude (Figure 6.5 – black curve). These findings present new questions; i) does a temperate conditions alter tropical mosquitoes ability to sensitively detect females during swarming? ii) Does the gradual increase in global temperatures allow for tropical mosquitoes to migrate further into temperate zones? iii) Does this increase the risk of tropical diseases becoming prevalent in temperate regions? It is projected by the Intergovernmental Panel on Climate Change (IPCC), based on current carbon emission levels that the global temperature will increase by an average 3^{o}C in the next 100 years. This predicts that in approximately 300 years' time, any pre-existing temperature barriers will no longer exist in the majority of temperature regions.

4.3 Suppression

The acoustic adaptation hypothesis stipulates that over time, acoustic signals evolved to be optimised to the habitats in which the species occur. The effects of this adaptation minimise the attenuation and distortion of nearby background noise (Morton 1975, Boncoraglio et al. 2007). The mosquito swarm is a noisy environment,

formed over visual markers predominantly by males. When a female approaches the swarm, the males detect the female flight-tones and a mating chase ensues (Roth 1948, Wishart and Riordan 1959, Charlwood and Jones 1979, Gibson 1985, Belton 1994). Male mosquitoes detect the near field component of sound through sinusoidal displacement of the flagellum, so any sound sources in close proximity could serve to influence or inhibit normal swarming behaviour.

In **Chapter five** it is shown that the presentation of a masking sound during acoustic stimulation alters the mosquito's behaviour (Figure 7.2). Acoustic masking is mediated by two non-mutually exclusive processes; either by competing and being more attractive than the female-like stimulus tone or by interfering with the males' ability to detect or locate the stimulus tone. RFM behaviour was directed to the masking speaker significantly more often than the stimulus speaker, however this did not account for all behavioural suppression (Figure 7.2). Auditory masking is likely to occur at the level of the antennae where the male and female flight-tones interact non-linearly to generate difference tones in the antennal vibrations (Warren, Gibson et al. 2009). The underlying mechanisms which mediate suppression are various, however there are three prominent theories. 1) The "line busy" mechanism in which the masker tone reduces the signal to noise ratio, 2) Adaptive masking, which reduces the excitatory response and 3) masker suppresses or inhibits the excitatory response elicited by the signal (Delgutte 1996). The last example has been investigated on several levels using two tone presentations, which closely replicates the experimental paradigm here.

In principle, male mosquitoes flying within a swarm should not serve to inhibit their ability to detect an approaching female as loud sounds above 600 Hz do not alter behaviour. However it does present the first evidence that male mosquitoes can be manipulated using sound, and in theory their natural mating process disrupted.

4.4 Further experiments

During the course of the thesis, I attempted to test several new avenues of research. This lead to potentially fruitful new research directions described below.

This thesis describes and quantifies the free flight and physiological behaviour of male mosquitoes, but it is well documented in the literature that a mating copula of most mosquito species is the result of a courtship between a male and female. In order to understand the relationship between a male and female in free flight, it is imperative to introduce the female to the experimental paradigm. The male demonstrates a consistent acoustic response and phonotaxis to a point source speaker without the presence of a female, however it is understood that the female also alters their WBF to harmonise with a male. Female mosquitoes also approach swarms of males but the cues that attract her to the swarm, including acoustic cues, have yet to be discovered. Free flight acoustic and visual recordings are important in discovering if female mosquitoes use acoustic cues in finding and interacting with males. The same techniques are required to help us understand the significance of frequency matching to discover if it really is a hallmark of natural behaviour, or perhaps an artefact caused by tethering.

Temperature influences free-flight WBF and JO tuning. The distortion product hypothesis indicates that the male mosquito utilises the difference frequency between his own WBF and that of a passing female to detect potential mates. In Chapter Four it is shown that the male WBF increases comparably with JO tuning and in accords with the literature (Tamarina, Zhantiev et al.), however what is fundamentally missing, is the effect of temperature on female WBF. It has been demonstrated in *Aedes aegypti* that the female WBF increases at ~7.2 $Hz \cdot 1^{o}C^{-1}$ (Villarreal et al. 2017), which is similar to that of males. It is important to discover the temperature dependence of female WBF and JO tuning in female *Culex* mosquitoes because any divergence from that in males could influence the chances of a male detecting a female and male-female interaction, when the male located the female.

Culex quinquefasciatus and *Culex pipiens pipiens* are tropical and temperate mosquitoes, respectively. As described in **Chapter four**, when the tropical species is introduced to temperate temperatures, male hearing is compromised. Hearing sensitivity is suppressed by up to two orders of magnitude, and tuning shifted to frequencies considered insensitive in detecting potential mates. Geographical segregation of tropical and temperate mosquito species could be influenced by

numerous factors, which include temperature. To understand the effects of temperature on mosquitoes further, a comparative study between *Culex quinquefasciatus* and *Culex pipiens pipiens* should be done. As low temperatures had a negative effect on the tropical species, then higher temperatures should serve to have a similar effect on the temperate mosquitoes in higher temperatures.

Acoustic suppression of DPs generated in the mosquito male JO is demonstrated in this thesis. The application of acoustic suppression the wild can subdue the formation of a mating copula, thus providing an alternative intervention to acoustic traps. The presentation of a masking tone suppresses the ability of a male mosquito to detect a stimulus tone. This now needs to be presented in a courtship scenario where groups of males/females are swarming, and measure the degree of interaction. This can be done by measuring the number of females that have been successfully inseminated by a male under normal conditions, and number of females inseminated under conditions where there is a masking speaker playing pure tones of various frequency.

Pollinators such as honeybees use electromagnetic cues to detect feeding sites and the hive, using the potential difference with flowers to promote pollen transfer (Clarke et al. 2013). Flying insects, such as the mosquito, also possess a positive electrical potential, which could provide information on feeding sites, but also provide the capacity for long distance detection. Early preliminary data using an electrostatic probe to measure the electrical field of free-moving tethered male mosquitoes indicates that the mosquito generates a very strong electromagnetic field. It has been long believed that sound plays an essential part to mosquito behaviour, but with cubic decay of particle velocity in air, limits the detection range to a few centimetres. The detection of an electrical field could provide a detection cue much stronger than acoustics, in particular the accumulation of a swarm, which could contain hundreds of mosquitoes at any one time.

Bibliography

Albert, J. T., et al. (2007). "Mechanical signatures of transducer gating in the *Drosophila* ear." Current Biology **17**(11): 1000-1006.

Aldersley, A., et al. (2016). "Quantitative analysis of harmonic convergence in mosquito auditory interactions." Journal of The Royal Society Interface **13**(117): 20151007.

Arthur, B. J., et al. (2010). "Neural responses to one-and two-tone stimuli in the hearing organ of the dengue vector mosquito." Journal of Experimental Biology **213**(8): 1376-1385.

Autrum, H. (1949). "Neue Versuche zum optischen Auflösungsvermögen fliegender Insekten." Cellular and Molecular Life Sciences **5**(7): 271-277.

Bailey, W. J. and G. K. Morris (1986). "Confusion of phonotaxis by masking sounds in the bushcricket *Conocephalus brevipennis* (*Tettigoniidae: Conocephalinae*)." Ethology **73**(1): 19-28.

Beach, R. (1980). "Physiological changes governing the onset of sexual receptivity in male mosquitoes." Journal of insect physiology **26**(4): 245249-247252.

Belton, P. (1974). An analysis of direction finding in male mosquitoes. Experimental analysis of insect behaviour, Springer**:** 139-148.

Belton, P. (1986). Sounds of insects in flight. Insect flight, Springer**:** 60-70.

Belton, P. (1994). "Attraction of male mosquitoes to sound." Journal of the American Mosquito Control Association **10**(2): 297-301.

Benelli, G. (2015). "Research in mosquito control: current challenges for a brighter future." Parasitology Research **114**(8): 2801-2805.

Benjamin, S. N. and W. E. Bradshaw (1994). "Body size and flight activity effects on male reproductive success in the pitcherplant mosquito (Diptera: *Culicidae*)." Annals of the Entomological Society of America **87**(3): 331-336.

Bennet-Clark, H. (1971). "Acoustics of insect song." Nature.

Bennet-Clark, H. (1984). "A particle velocity microphone for the song of small insects and other acoustic measurements." Journal of Experimental Biology **108**(1): 459-463.

Bennet-Clark, H. (1998). "Size and scale effects as constraints in insect sound communication." Philosophical Transactions of the Royal Society B: Biological Sciences **353**(1367): 407-419.

Boncoraglio, G. and N. Saino (2007). "Habitat structure and the evolution of bird song: a meta-analysis of the evidence for the acoustic adaptation hypothesis." Functional Ecology **21**(1): 134-142.

Boo, K. (1980). "Antennal sensory receptors of the male mosquito, *Anopheles stephensi*." Parasitology Research **61**(3): 249-264.

Boo, K. (1981). "Discontinuity between ciliary root processes and triple microtubules of distal basal body in mosquito sensory cilia." Korean Journal of Entomology **11**(1): 5-18.

Boo, K. S. and A. G. Richards (1975). "Fine structure of scolopidia in Johnston's organ of female *Aedes aegypti* compared with that of the male." Journal of insect physiology **21**(5): 1129-1139.

Bowen, M. (1991). "The sensory physiology of host-seeking behavior in mosquitoes." Annual review of entomology **36**(1): 139-158.

Boyan, G. (1981). "Two-tone suppression of an identified auditory neurone in the brain of the cricket *Gryllus bimaculatus* (*De Geer*)." Journal of Comparative Physiology A: Neuroethology, Sensory, Neural, and Behavioral Physiology **144**(1): 117-125.

Bradbury, J. W. and S. L. Vehrencamp (2011). "Principles of animal communication."

Brogdon, W. G. (1998). "Measurement of flight tone differentiates among members of the *Anopheles gambiae* species complex (Diptera: *Culicidae*)." Journal of Medical Entomology **35**(5): 681-684.

Brumm, H. and H. Slabbekoorn (2005). "Acoustic communication in noise." Advances in the Study of Behavior **35**: 151-209.

Carvalho, D. O., et al. (2014). "Two step male release strategy using transgenic mosquito lines to control transmission of vector-borne diseases." Acta tropica **132**: S170-S177.

Cator, L. J., et al. (2009). "Harmonic convergence in the love songs of the dengue vector mosquito." Science **323**(5917): 1077-1079.

Cator, L. J. and Z. Zanti (2016). "Size, sounds and sex: interactions between body size and harmonic convergence signals determine mating success in *Aedes aegypti*." Parasites & Vectors **9**(1): 622.

Charlwood, J. and M. Jones (1979). "Mating behaviour in the mosquito, *Anopheles gambiae* s. 1. close range and contact-behaviour." Physiological entomology **4**(2): 111-120.

Cheatham, M. A. and P. Dallos (1982). "Two-tone interactions in the cochlear microphonic." Hearing research **8**(1): 29-48.

Child, C. M. (1894). "Ein bisher wenig beachtetes antennales sinnesorgan der Insekten: mit besonderer Berücksichtigung der Culiciden und Chironomiden, W. Engelmann.

Church, N. S. (1959). "Heat loss and the body temperatures of flying insects." Journal of Experimental Biology **37**(1): 186-212.

Clarke, D., et al. (2013). "Detection and learning of floral electric fields by bumblebees." Science **340**(6128): 66-69.

Clements, A. (1999). "The Biology of Mosquitoes. Sensory Reception and Behavior, Vol. 2." CAB International Publication, London.

Clements, A. and F. Bennett (1968). "The structure and biology of a new species of *Mallophora Macq*.(Diptera, *Asilidae*) from Trinidad, WI." Bulletin of Entomological Research **58**(03): 455-465.

Clements, A. N. (1963). Physiology of mosquitoes, Pergamon Press, Oxford.

Coro, F. and M. Kössl (1998). "Distortion-product otoacoustic emissions from the tympanic organ in two noctuoid moths." Journal of Comparative Physiology A: Neuroethology, Sensory, Neural, and Behavioral Physiology **183**(4): 525-531.

David, C. T. (1982). "Compensation for height in the control of groundspeed by *Drosophila* in a new,'barber's pole'wind tunnel." Journal of Comparative Physiology A: Neuroethology, Sensory, Neural, and Behavioral Physiology **147**(4): 485-493.

Delgutte, B. (1996). Physiological models for basic auditory percepts. Auditory computation, Springer**:** 157-220.

Diabaté, A., et al. (2009). "Spatial swarm segregation and reproductive isolation between the molecular forms of *Anopheles gambiae*." Proceedings of the Royal Society of London B: Biological Sciences **276**(1676): 4215-4222.

Diabate, A. and F. Tripet (2015). "Targeting male mosquito mating behaviour for malaria control." Parasites & Vectors **8**(1): 347.

Downes, J. (1958). Assembly and mating in the biting *Nematocera*. Proceedings of the Tenth International Congress on Entomology.

Downes, J. (1969). "The swarming and mating flight of *Diptera*." Annual review of entomology **14**(1): 271-298.

Downes, J. A. (1961). Encyclopedia of Biology Reinhold, New York.

Eberl, D. F. and G. Boekhoff-Falk (2007). "Development of Johnston's organ in *Drosophila*." The International journal of developmental biology **51**(6-7): 679.

Eckhoff, P.A., (2011). "A malaria transmission-directed model of mosquito life cycle and ecology." Malaria journal, **10**(1), 303.

Ernstrom, G. G. and M. Chalfie (2002). "Genetics of sensory mechanotransduction." Annual review of genetics **36**(1): 411-453.

Farnworth, E. G. (1972). "Effects of ambient temperature and humidity on internal temperature and wing-beat frequency of *Periplaneta americana*." Journal of insect physiology **18**(2): 359-371.

Farris, H. E. and R. R. Hoy (2002). "Two-tone suppression in the cricket, *Eunemobius carolinus* (*Gryllidae, Nemobiinae*)." The Journal of the Acoustical Society of America **111**(3): 1475-1485.

Fonseca, P. and T. Correia (2007). "Effects of temperature on tuning of the auditory pathway in the *cicada Tettigetta josei* (Hemiptera, Tibicinidae)." Journal of Experimental Biology **210**(10): 1834-1845.

French, A. S. (1988). "Transduction mechanisms of mechanosensilla." Annual review of entomology **33**(1): 39-58.

Fry, S. N., et al. (2005). "The aerodynamics of hovering flight in *Drosophila*." Journal of Experimental Biology **208**(12): 2303-2318.

Fuchs, P., et al. (1990). "Calcium currents in hair cells isolated from the cochlea of the chick." The Journal of physiology **429**(1): 553-568.

Gentile, G., et al. (2001). "Attempts to molecularly distinguish cryptic taxa in *Anopheles gambiae ss*." Insect molecular biology **10**(1): 25-32.

Gibson, G. (1985). "Swarming behaviour of the mosquito *Culex pipiens quinquefasciatus*: a quantitative analysis." Physiological Entomology **10**(3): 283-296.

Gibson, G. and I. Russell (2006). "Flying in tune: sexual recognition in mosquitoes." Current Biology **16**(13): 1311-1316.

Gibson, N. (1945). "On the mating swarms of certain *Chironomidae* (*Diptera*)." Ecological Entomology **95**(6): 263-294.

Gilbert, F. S. (1984). "Thermoregulation and the structure of swarms in *Syrphus ribesii* (*Syrphidae*)." Oikos: 249-255.

Gokhale, M. D., et al. (2013). "Comparison of biological attributes of *Culex quinquefasciatus* (*Diptera: Culicidae*) populations from India." ISRN Entomology **2013**.

Gomes, W. and D. Vanmaekelbergh (1996). "Impedance spectroscopy at semiconductor electrodes: review and recent developments." Electrochimica acta **41**(7-8): 967-973.

Gong, J., et al. (2013). "NOMPC is likely a key component of *Drosophila*." European Journal of Neuroscience: 1-8.

Gong, Z., et al. (2004). "Two interdependent TRPV channel subunits, inactive and Nanchung, mediate hearing in *Drosophila*." The Journal of neuroscience **24**(41): 9059-9066.

Göpfert, M. C., et al. (2006). "Specification of auditory sensitivity by *Drosophila* TRP channels." Nature neuroscience **9**(8): 999-1000.

Gopfert, M. C., et al. (1999). "Mosquito hearing: sound-induced antennal vibrations in male and female *Aedes aegypti*." Journal of experimental biology **202**(20): 2727-2738.

Göpfert, M. C. and D. Robert (2000). "Nanometre–range acoustic sensitivity in male and female mosquitoes." Proceedings of the Royal Society of London B: Biological Sciences **267**(1442): 453-457.

Göpfert, M. C. and D. Robert (2001). "Active auditory mechanics in mosquitoes." Proceedings of the Royal Society of London B: Biological Sciences **268**(1465): 333-339.

Graber, V. (1882). "Die chordotonalen Sinnesorgane und das Gehor der Insekten." Arch. mikr. Anat. **20**: 506-640.

Gray, J. (1959). "Mechanical into electrical energy in certain mechanoreceptors." Progr. Biophys **9**: 285-324.

Hart, M. and P. B. a. R. Kuhn (2011). "The Risler Manuscript." European Mosquito Bulletin **29**: 103-113.

Hartberg, W. (1971). "Observations on the mating behaviour of *Aedes aegypti* in nature." Bulletin of the World Health Organization **45**(6): 847.

Heinrich, B (1974). "Thermoregulation in endothermic insects." Science **185**(4153): 747-756

Hodgkin, A. L. and A. F. Huxley (1952). "A quantitative description of membrane current and its application to conduction and excitation in nerve." The Journal of physiology **117**(4): 500-544.

Houghton, J. T. (1996). Climate change 1995: The science of climate change: contribution of working group I to the second assessment report of the Intergovernmental Panel on Climate Change, Cambridge University Press.

Howard, L. O. (1901). Mosquitoes, McClure, Phillips & Company.

Howard, L. O., et al. (1917). The Mosquitoes of North and Central America and the West Indies: Systematic description, Carnegie institution of Washington.

Jackson, J. C., et al. (2009). "Synchrony through twice-frequency forcing for sensitive and selective auditory processing." Proceedings of the National Academy of Sciences **106**(25): 10177-10182.

Johnston, C. (1855). "Original communications: auditory apparatus of the *Culex* mosquito." Journal of Cell Science **1**(10): 97-102.

Kahn, M. C., et al. (1945). "Recording of Sounds produced by certain Disease-carrying Mosquitoes." Science (Washington): 335-336.

Kahn, M. C. and W. Offenhauser Jr (1949). "The First Field Tests of Recorded Mosquito Sounds used for Mosquito Destruction1, 2." The American journal of tropical medicine and hygiene **1**(5): 811-825.

Kamikouchi, A., et al. (2009). "The neural basis of *Drosophila* gravity-sensing and hearing." Nature **458**(7235): 165-171.

Kemp, D. T. (1979). "Evidence of mechanical nonlinearity and frequency selective wave amplification in the cochlea." Archives of oto-rhino-laryngology **224**(1-2): 37-45.

Keppler, E. (1958). "Uber Das Richtungshoren Von Stechmucken." Zeitschrift Fur Naturforschung Part B-Chemie Biochemie Biophysik Biologie Und Verwandten Gebiete **13**(5): 280-284.

Kernan, M. J. (2007). "Mechanotransduction and auditory transduction in *Drosophila*." Pflügers Archiv-European Journal of Physiology **454**(5): 703-720.

Kim, J., et al. (2003). "A TRPV family ion channel required for hearing in *Drosophila*." Nature **424**(6944): 81-84.

Knab, F. (1906). "The swarming of *Culex pipiens*." Psyche: A Journal of Entomology **13**(5): 123-133.

Kössl, M. and G. Boyan (1998). "Otoacoustic emissions from a nonvertebrate ear." Naturwissenschaften **85**(3): 124-127.

Kostarakos, K. and H. Römer (2015). "Neural mechanisms for acoustic signal detection under strong masking in an insect." Journal of Neuroscience **35**(29): 10562-10571.

Landois, H. (1874). Thierstimmen, Herder.

Lapshin, D. (2012). "Mosquito bioacoustics: auditory processing in *Culex pipiens pipiens L*. Males (*Diptera, Culicidae*) during flight simulation." Entomological review **92**(6): 605-621.

Lee, J., et al. (2010). "*Drosophila* TRPN (= NOMPC) channel localizes to the distal end of mechanosensory cilia." PloS one **5**(6): 1-6.

Lee, N., et al. (2009). "A precedence effect resolves phantom sound source illusions in the parasitoid fly *Ormia ochracea*." Proceedings of the National Academy of Sciences **106**(15): 6357-6362.

Lees, R. S., et al. (2014). "Improving our knowledge of male mosquito biology in relation to genetic control programmes." Acta tropica **132**: S2-S11.

Legouix, J. P., et al. (1973). "Interference and two-tone inhibition." The Journal of the Acoustical Society of America **53**(2): 409-419.

Lehnert, B., et al. (2013). "Distinct Roles of TRP Channels in Auditory Transduction and Amplification in *Drosophila*." Neuron **77**(1): 115.

Lukashkin, A. N. and I. J. Russell (1999). "Analysis of the f 2− f 1 and 2 f 1− f 2 distortion components generated by the hair cell mechanoelectrical transducer: Dependence on the amplitudes of the primaries and feedback gain." The Journal of the Acoustical Society of America **106**(5): 2661-2668.

Lutz, F. E. (1924). Insect sounds, order of the Trustees, American Museum of Natural History.

Machin, K., et al. (1962). "The physiology of insect fibrillar muscle. IV. The effect of temperature on a beetle flight muscle." Proceedings of the Royal Society of London B: Biological Sciences **155**(961): 493-499.

Martin, P. and A. Hudspeth (2001). "Compressive nonlinearity in the hair bundle's active response to mechanical stimulation." Proceedings of the National Academy of Sciences **98**(25): 14386-14391.

Maxim, H. S. (1901). "Mosquitoes and musical notes." The Times **28**: 11.

Mayer, A. (1874). "Experiments on the supposed auditory apparatus of the mosquito." The American Naturalist **8**(10): 577-592.

McClelland, G. (1959). "Observations on the Mosquito, *Aëdes* (*Stegomyia*) *aegypti* (*L.*), in East Africa. I.—The Biting Cycle in an Outdoor Population at Entebbe, Uganda." Bulletin of Entomological Research **50**(02): 227-235.

McIver, S. (1971). "Comparative studies on the sense organs on the antennae and maxillary palps of selected male *culicine* mosquitoes." Canadian Journal of Zoology **49**(2): 235-239.

McIver, S. (1985). "Mechanoreception." Comprehensive insect physiology, biochemistry and pharmacology **6**: 71-132.

McIver, S. B. (1980). "Sensory aspects of mate-finding behavior in male mosquitoes (*Diptera: Culicidae*)." Journal of medical entomology **17**(1): 54-57.

McIver, S. B. (1982). "Sensilla of mosquitoes (*diptera: Culicidae*)." Journal of medical entomology **19**(5): 489-535.

McVean, A. (1991). "Some mechanical properties of the flagellar-pedicellar suspension in *Aedes aegypti (L.)*." Physiological entomology **16**(4): 435-438.

Mhatre, N. and D. Robert (2013). "A tympanal insect ear exploits a critical oscillator for active amplification and tuning." Current Biology **23**(19): 1952-1957.

Möckel, D., et al. (2007). "The generation of DPOAEs in the locust ear is contingent upon the sensory neurons." Journal of Comparative Physiology A **193**(8): 871-879.

Moran, D. T. and J. Carter Rowley (1975). "The fine structure of the cockroach subgenual organ." Tissue and Cell **7**(1): 91-105.

Moran, D. T., et al. (1977). "Evidence for active role of cilia in sensory transduction." Proceedings of the National Academy of Sciences **74**(2): 793-797.

Morton, E. S. (1975). "Ecological sources of selection on avian sounds." The American Naturalist **109**(965): 17-34.

Moulins, M. (1976). "Ultrastructure of chordotonal organs." Structure and function of proprioceptors in the invertebrates. Chapman and Hall, London: 387-426.

Mukabayire, O., et al. (2001). "Patterns of DNA sequence variation in chromosomally recognized taxa of *Anopheles gambiae*: evidence from rDNA and single-copy loci." Insect molecular biology **10**(1): 33-46.

Nielsen, E. T. and H. Greve (1950). "Studies on the swarming Habits of Mosquitos and other *Nematocera*." Bulletin of Entomological Research **41**(2): 227-258.

Nijhout, H. F. and H. G. Sheffield (1979). "Antennal hair erection in male mosquitoes: a new mechanical effector in insects." Science (New York, NY) **206**(4418): 595.

Nolen, T. and R. Hoy (1986). "Phonotaxis in flying crickets. II. Physiological mechanisms of two-tone suppression of the high frequency avoidance steering behavior by the calling song." Journal of comparative physiology. A, Sensory, neural, and behavioral physiology **159**(4): 441-456.

Ogawa, K.-i. and T. Kanda (1986). "Wingbeat frequencies of some *anopheline* mosquitoes of East Asia (*Diptera: Culicidae*)." Applied entomology and zoology **21**(3): 430-435.

Pennetier, C., et al. (2010). "“Singing on the wing” as a mechanism for species recognition in the malarial mosquito *Anopheles gambiae*." Current Biology **20**(2): 131-136.

Phuc, H. K., et al. (2007). "Late-acting dominant lethal genetic systems and mosquito control." BMC biology **5**(1): 11.

Pickles, J. O. (1988). An introduction to the physiology of hearing, Academic press London.

Pringle, J. (1967). "The contractile mechanism of insect fibrillar muscle." Progress in biophysics and molecular biology **17**: 1-12.

Reiskind, M. H. and A. A. Zarrabi (2012). "Is bigger really bigger? Differential responses to temperature in measures of body size of the mosquito, *Aedes albopictus*." Journal of insect physiology **58**(7): 911-917.

Reiter, P. (2001). "Climate change and mosquito-borne disease." Environmental health perspectives **109**(Supp 1): 141.

Risler, H. (1953). "Das Gehörorgan der Männchen von *Anopheles stephensi* Liston (Culicidae)." Zool. Jahrb. Abt. Anat. Ontog. Tiere **73**: 165-178.

Risler, H. (1955). "Das Gehörorgan der Männchen von *Culex pipiens L., Aedes aegypti* L. und *Anopheles stephensi Liston* (*Culicidae*), eine vergleichend morphologische Untersuchung." Zool. Jahrb. Anat. Ontog. Tiere **74**: 478-490.

Ritchie, M. G., et al. (2001). "Characterization of female preference functions for *Drosophila* montana courtship song and a test of the temperature coupling hypothesis." Evolution **55**(4): 721-727.

Robles, L. and M. A. Ruggero (2001). "Mechanics of the mammalian cochlea." Physiological reviews **81**(3): 1305-1352.

Roff, D. (1977). "Dispersal in *dipterans*: its costs and consequences." The Journal of Animal Ecology: 443-456.

Römer, H. (2013). Masking by noise in acoustic insects: problems and solutions. Animal communication and noise, Springer**:** 33-63.

Rosowski, J., et al. (1984). "Cochlear nonlinearities inferred from two-tone distortion products in the ear canal of the alligator lizard." Hearing research **13**(2): 141-158.

Roth, L. M. (1948). "A study of mosquito behavior. An experimental laboratory study of the sexual behavior of *Aedes aegypti* (*Linnaeus*)." The American Midland Naturalist **40**(2): 265-352.

Rowley, W. A. and C. L. Graham (1968). "The effect of temperature and relative humidity on the flight performance of female *Aedes aegypti*." Journal of insect physiology **14**(9): 1251-1257.

Sawadogo, S. P., et al. (2013). "Effects of age and size on *Anopheles gambiae ss* male mosquito mating success." Journal of medical entomology **50**(2): 285-293.

Schmidt, A. K. and R. Balakrishnan (2015). "Ecology of acoustic signalling and the problem of masking interference in insects." Journal of Comparative Physiology A **201**(1): 133-142.

Sellick, P. and I. Russell (1979). "Two-tone suppression in cochlear hair cells." Hearing research **1**(3): 227-236.

Simões, P. M., et al. (2016). "A role for acoustic distortion in novel rapid frequency modulation behaviour in free-flying male mosquitoes." Journal of Experimental Biology **219**(13): 2039-2047.

Smotherman, M. S. and P. M. Narins (1999). "Potassium currents in auditory hair cells of the frog basilar papilla." Hearing research **132**(1): 117-130.

Sukharev, S. and D. P. Corey (2004). "Mechanosensitive channels: multiplicity of families and gating paradigms." Sci. STKE **2004**(219): re4-re4.

Tamarina, N., et al. (1979). "Frequency characteristics of the flight sounds and of Johnson's organs in sympatric mosquitoes of the genus *Aedes* (*Culicidae*)." Parazitologiia **14**(5): 398-402.

Thurm, U., et al. (1983). "Cilia specialized for mechanoreception." J Submicrosc Cytol **15**(1): 151-155.

Tischner, H. (1955). "Gehörorgan und Fluggeräusch bei Stechmücken." Umschau Wissenschaft Technik **55**: 368-370.

Tischner, H. v. (1953). "Über den gehörsinn von stechmücken." Acustica **3**: 335-343.

Todi, S. V., et al. (2004). "Anatomical and molecular design of the *Drosophila* antenna as a flagellar auditory organ." Microscopy research and technique **63**(6): 388-399.

Torre, A. d., et al. (2001). "Molecular evidence of incipient speciation within *Anopheles gambiae ss* in West Africa." Insect molecular biology **10**(1): 9-18.

Unwin, D. and S. A. Corbet (1984). "Wingbeat frequency, temperature and body size in bees and flies." Physiological Entomology **9**(1): 115-121.

Van Dijk, P. and S. W. Meenderink (2006). Distortion product otoacoustic emissions in the amphibian ear. Auditory Mechanisms: Processes And Models: (With CD-ROM), World Scientific**:** 332-338.

Versteegh, C. P. and M. van der Heijden (2013). "The spatial buildup of compression and suppression in the mammalian cochlea." Journal of the Association for Research in Otolaryngology **14**(4): 523-545.

Villarreal, S. M., et al. (2017). "The Impact of Temperature and Body Size on Fundamental Flight Tone Variation in the Mosquito Vector *Aedes aegypti* (*Diptera: Culicidae*): Implications for Acoustic Lures." Journal of medical entomology: tjx079.

Walker, R. G., et al. (2000). "A *Drosophila* mechanosensory transduction channel." Science **287**(5461): 2229-2234.

Warren, B., et al. (2009). "Sex recognition through midflight mating duets in *Culex* mosquitoes is mediated by acoustic distortion." Current Biology **19**(6): 485-491.

Warren, B., et al. (2010). "The dynein–tubulin motor powers active oscillations and amplification in the hearing organ of the mosquito." Proceedings of the Royal Society of London B: Biological Sciences **277**(1688): 1761-1769.

Wekesa, J., et al. (1998). "Flight tone of field-collected populations of Anopheles gambiae and *An. arabiensis* (*Diptera: Culicidae*)." Physiological Entomology **23**(3): 289-294.

Whitehead, M., et al. (1996). "Visualization of the onset of distortion-product otoacoustic emissions, and measurement of their latency." The Journal of the Acoustical Society of America **100**(3): 1663-1679.

Wiederhold, M. L. (1976). "Mechanosensory transduction in" sensory" and" motile" cilia." Annual review of biophysics and bioengineering **5**(1): 39-62.

Wiley, R. H. (2006). "Signal detection and animal communication." Advances in the Study of Behavior **36**: 217-247.

Wishart, G. and D. Riordan (1959). "Flight responses to various sounds by adult males of *Aedes aegypti* (*L.*)(*Diptera*: *Culicidae*)." The Canadian Entomologist **91**(03): 181-191.

Wishart, G., et al. (1962). "Orientation of the males of *Aedes aegypti* (*L.*)(*Diptera*: *Culicidae*) to sound." The Canadian Entomologist **94**(06): 613-626.

Wolfrum, U. (1990). "Actin filaments: the main components of the scolopale in insect sensilla." Cell and Tissue Research **261**(1): 85-96.

Wolfrum, U. (1991). "Tropomyosin is co-localized with the actin filaments of the scolopale in insect sensilla." Cell and Tissue Research **265**(1): 11-17.

Wolfrum, U. (1997). "Cytoskeletal elements in insect sensilla." International Journal of Insect Morphology and Embryology **26**(3): 191-203.

Wondji, C., et al. (2005). "Species and populations of the *Anopheles gambiae* complex in Cameroon with special emphasis on chromosomal and molecular forms of *Anopheles gambiae ss*." Journal of medical entomology **42**(6): 998-1005.

Yack, J. E. (2004). "The structure and function of auditory chordotonal organs in insects." Microscopy research and technique **63**(6): 315-337.

Yuval, B., et al. (1993). "Effect of body size on swarming behavior and mating success of male *Anopheles freeborni* (*Diptera*: *Culicidae*)." Journal of insect behavior **6**(3): 333-342.